DEVELOPMENT OF BIOMIMETIC INTERFACES AND THEIR APPLICATIONS

by

Himabindu Nandivada

A dissertation submitted in partial fulfillment
of the requirements for the degree of
Doctor of Philosophy
(Chemical Engineering)
in The University of Michigan
2009

Doctoral Committee:

        Associate Professor Joerg Lahann (Chair)
        Professor Erdogan Gulari
        Professor Mark E. Meyerhoff
        Professor Michael J. Solomon

To my dearest mamma (grandmother),
Smt. Nandivada Anasuya

ACKNOWLEDGMENTS

First, I would like to express heartfelt gratitude to my research advisor Prof. Joerg Lahann for giving the opportunity to be part of his research group. His infectious enthusiasm, passion for science and his critical thinking inspire me to strive for the best. I hope we can continue this wonderful collaboration.

I would like to thank my committee members, Prof. Erdogan Gulari, Prof. Mark E. Meyerhoff and Prof. Michael J. Solomon for their helpful feedback on my dissertation. I am also grateful to my collaborators- Prof. Gary D. Smith and Prof. Paul H. Krebsbach.

I am grateful to Dr. Luis Villa-Diaz for patiently teaching me all the human embryonic stem cell culture techniques. It has been a long journey which has been frustrating at times but has led to exciting science.

I am thankful to my wonderful first labmates- Dr. David Peng, Dr. Kyung-Ho Roh and Dr. Hsien-Yeh Chen for their friendship. I would also like to thank all the Lahann group members- past and present, for all the wonderful experiences.

I am grateful to my circle of friends who made this an incredible journey- Vaishno, Sangati, Dhruv, Khamir, Allison, Rashmi, Julia, Malavika, Suparna, Linh, Yusuf, Kiran and all the ICMD peeps.

Last but not the least; I am indebted to my parents, Prof. N. N. Kishore and Mrs. N. Usha Devi, and my sisters, Vandana and Prabhava for their love and unwavering faith in me. This work would not be possible without their encouragement and support.

TABLE OF CONTENTS

CHAPTER 3. SPATIOSELECTIVE IMMOBILIZATION OF BIOMOLECULES ONTO VAPOR-BASED POLYMERS VIA CLICK CHEMISTRY...**47**

LIST OF FIGURES

LIST OF TABLES

ABSTRACT

This dissertation details strategies for the fabrication of sophisticated biofunctional materials and their use in biomedical and biotechnological application. These unique biointerfaces were designed by integrating biological entities with synthetic polymers and extensively characterized using surface analytical tools.

The first part of this dissertation focuses on the immobilization of specific moieties that render surfaces biomimetic. Synthesis of reactive polymers, poly(4-formyl-*p*-xylylene-co-*p*-xylylene) and poly(4-heptadecafluorononnonyl-*p*-xylylene-co-*p*-xylylene) was accomplished via chemical vapor deposition (CVD) polymerization. These reactive polymer coatings enabled the immobilization of proteins and oligosaccharides via chemoselective carbonyl-hydrazide coupling reaction. On the other hand, an alkyne-functionalized polymer coating, poly(4-ethynyl-*p*-xylylene-co-*p*-xylylene) was synthesized for the conjugation of proteins, saccharides and cell-adhesive oligopeptides via alkyne-azide "click" reaction, in a spatioselective manner. These platforms were further used for surface-directed adhesion of human endothelial cells. Another application of reactive polymers was directed towards the fabrication of polymer coatings, which mimic endothelial cells with respect to nitric oxide generation for cardiovascular stents. Photo-reactive polymer coatings were deposited using CVD polymerization and used to incorporate Cu(II) ligated cyclen (1,4,7,10-tetraazacyclododecane) onto the surface of a stent. These catalytic sites containing copper generated NO from endogenous S-nitrosothiols present in blood, and the measured NO

flux approached physiological ranges. These coatings attempt to solve the problems of restenosis and thrombosis associated with the placement of coronary artery stents.

In the second part of the dissertation, a chemically-defined polymer was fabricated, which supported long-term human embryonic stem (hES) cell cultures, for the first time, in the presence of several different culture media. Polymer, poly[2-(methacryloyloxy)ethyl dimethyl-(3-sulfopropyl)ammonium hydroxide] sustained the culture of hES cells for at least 25 passages in mouse fibroblast conditioned medium, at least 15 passages in commercially-available human cell conditioned medium and at least 10 passages in defined StemPro medium. Throughout the study, hES cells expressed undifferentiated cell markers, retained a normal karyotype and remained pluripotent. Development of a standardized culture matrix for hES cells represents a significant step towards future clinical applications of hES cells.

Taken together, these approaches offer novel solutions for target applications in tissue engineering, biomedical devices and microfluidics and further expand our toolbox of strategies for creating biologically-relevant surfaces.

CHAPTER 1

INTRODUCTION

1.1 Motivation and background

In the past few decades, there has been rapid development in the field of surface engineering, relating to the control of structure and properties of surfaces, which is of utmost importance for applications such as cell biology, tissue engineering, microfluidics, optics and electronics.[1-3] The main objectives of biomimetic surface engineering are (1) to modify the interfaces between biological and non-biological systems; (2) to gain valuable insight into the biological interactions at these interfaces; and (3) for the advancement of biomedical research.[1] The main advantage of surface modification strategies is the ability to influence biological interactions by changing the outermost surface, while still retaining the key physical properties of the material. If the surface modification is properly executed, the mechanical properties and functionality of the device will be unchanged, but the interface related biocompatibility will be improved, eliminating the need for redesigning the entire device or reevaluating the material.

Interactions between cells and biomaterials are governed by physicochemical properties of the biointerface and chemical cues provided by the ligands integrated on the surface.[4] Physicochemical parameters such as surface energy, surface topography, surface charge and chemical composition of the surface have a profound effect on biological response. Surface attributes (such as wettability, charge and surface reactivity) depend on the chemical and physical details of the molecular structure at the interface. At the same time, the ability to modify inorganic surfaces with organic molecules or biological

ligands is also a common requirement for a host of applications. The chemical signals provided by various biomolecules such as growth factors and cell-adhesive proteins influence the cellular behavior.

Biomolecule immobilization

A wide variety of biomolecules such as proteins and oligopeptides, sugars and polysaccharides, single and double-stranded oligonucleotides and DNA plasmids, simple lipids and phospholipids and a wide spectrum of recognition ligands and synthetic drug molecules, have been immobilized onto surfaces.[5] There are three major immobilization methods for biomolecules, namely physical adsorption, physical "entrapment" and covalent attachment.[5] Physical adsorption methods are generally based on van der Waals, electrostatic or other affinity forces. Biomolecules can also be immobilized through physical "entrapment" in hydrogels or dispersed in matrix systems. As compared to the physical methods, covalent immobilization enhances the stability of the biomolecule and prevents desorption.[5]

The major requirements for any bioconjugation strategy are that the biomolecules attached to the surface should be stable and the immobilization chemistry should preserve the conformation and accessibility of the ligands on the surface. The reaction chemistry for the conjugation should have fast kinetics and the linkage should be stable. A few examples of chemoselective reactive pairs (and type of bonds formed) commonly used in bioconjugation are carbonyl-hydrazide (hydrazone bond), carbonyl-aminooxy (oxime bond), and thiol-maleimide (thioether bond) reactions.[6] The conjugation of proteins to surfaces has been achieved through either the amine group (by reacting with the pentafluorophenol ester group) or by activating carboxylic acid groups with N-hydroxysuccinimide (NHS) in the presence of EDC.[6, 7] Specific biomolecules such as cell

adhesion peptides/proteins have been immobilized in order to control the cell-surface interactions. Hydrazide-containing reagents have been used for the conjugation of carbonyl-containing compounds where macromolecules containing carbonyl groups spontaneously react with hydrazide ligands to form hydrazone bonds.[6, 8] Thus, probes containing hydrazide functional groups can be used to label carbohydrates and the polysaccharide portion of cell surfaces. Recently, a series of cycloaddition reactions have received intense attention due to their extraordinary thermodynamic driving forces.[9] These cycloaddition reactions, often referred to as "click" reactions, are a set of reactions, which give stereoselective products, are insensitive to oxygen and water and are conducted in benign solvents. The most popular reaction of this group is the Huisgen 1,3-dipolar cycloaddition of azides and terminal alkynes to generate 1,2,3-triazoles.[10] The highly energetic azide and alkyne groups have a surprisingly narrow distribution of reactivity and are inert towards other functional groups.[11] This reaction has been used in bioconjugation strategies for microarrays, sensors, proteomics and in drug discovery.[12, 13]

Biomolecular patterning

A diverse array of techniques for the spatioselective immobilization of biomolecules at submicron and nanoscale have emerged.[4, 14, 15] The ability to design highly sophisticated and precise surfaces is essential for applications in biotechnology and medicine such as biosensors, tissue engineering and biomaterials.[16]

Biomolecular patterning requires highly specific conjugation of biomolecules in well-defined regions and spacing, while retaining native functionality of the biomolecules.[14] Furthermore, other regions of the substrate should demonstrate resistivity towards the biomolecules. Micro and nanopatterning techniques have been used to modulate cell shape, position, adhesive area and differentiation potential.[7, 17, 18] Several

strategies have been employed for the fabrication of micro- and nano-scale patterns such as photolithography, microcontact printing (soft lithography) and dip-pen nanolithography.[19, 20] These approaches have been used either directly to immobilize biomolecules or indirectly as templates for pattern creation.

Microcontact printing is a soft lithographic technique which has been used for patterning of biomolecules such as proteins,[7, 21, 22] peptides[15] and DNA[23]. Microcontact printing was first demonstrated for creating patterns of alkanethiols on gold.[24, 25] Briefly, a micropatterned Si master is used to create a patterned poly(dimethylsiloxane) (PDMS) stamp. Elastomeric PDMS stamp is inked with the desired solution and then brought into contact with the substrate to transfer the ink.

Reactive polymer coatings via chemical vapor deposition (CVD)

Success of any covalent bioimmobilization step depends on the availability of reactive functional groups on the surface. Over the past few years, vapor-based polymer coatings have emerged as a promising solution for surface modification due to their advanced processibility and excellent intrinsic biocompatibilty.[26, 27] Chemical vapor deposition (CVD) is a well established technique for the formation of inorganic layers, and it has been extended to generate thin conformal polymer coatings. The deposition itself is a room temperature process that does not require any catalyst, initiator or solvent and no byproducts are generated. Other advantages of this process include control of the composition and architecture of the films, high accuracy, and good adhesion to a wide variety of substrates (including biomedical and microfluidic devices). Functionalized poly(p-xylylenes) can be deposited via CVD polymerization to generate thin polymer films (5-100 nm) and, due to pre-defined chemical functionalities, provide a flexible solution to surface engineering challenges as they decouple surface design from bulk

properties. Hence, the technology comprises essentially a one-step coating procedure to generate functionalized surfaces without requiring any non-biological post-treatment on the deposited films.[28] The simplicity in providing a wide range of functional groups, the excellent adhesion to various substrates, and its applicability to devices with three-dimensional geometries are key advantages when compared to polymers deposited by solvent-based methods.

In the recent past, CVD polymerization of substituted [2,2]paracyclophanes has been instrumental in creating a wide array of functionalized poly(p-xylylenes) with a diverse class of functional groups, such as amines,[29, 30] esters,[31-33] ketones,[8, 34-36] and alcohols[37, 38] (Figure 1.1). The strategy used is based on the fact that the reactive functional groups on the polymer can be modulated based on the specific immobilization chemistry of the ligand. These surfaces bring the physical and mechanical advantages of the non-functional commercial polymer films together with the reactivity of the functional groups. Coronary stents which were coated with a functionalized CVD polymer and then used to immobilize the thrombin inhibitor r-hirudin showed a remarkable decrease in platelet activity.[39] CVD polymerization has also been used to synthesize polymeric coatings to immobilize proteins and antibodies inside microfluidic devices which can be further used for cell-based bioassays.[33] On the other hand, a novel photodefinable polymer has been prepared by CVD polymerization and used for the fabrication of hydrogel elements.[40, 41] This process has also been used to fabricate atom transfer radical polymerization (ATRP) initiator coatings,[42] and coatings which facilitate solvent-less bonding.[43] Furthermore, CVD has been extended for the fabrication of multi-functional polymer coatings with two or more functional groups to enable the immobilization of multiple ligands.[35, 44, 45]

1.2 Objectives of this work

This dissertation aims to develop strategies for the fabrication of biomimetic interfaces by integrating structural and recognition motifs, derived from biomolecules, with synthetic polymers. Biologically-active surfaces can be used for a variety of applications such as protein and oligosaccharide arrays, biomedical device coatings, and cell culture platforms.

Based on different targeted applications, the following issues were addressed:
- To develop strategies for spatioselective immobilization of biomolecules such as proteins, oligosaccharides and cell adhesive peptides.
- To design matrices specifically tailored for long-term human embryonic stem cell culture.
- To develop robust biomimetic polymer coatings applicable to implantable devices.

The approaches described in the following chapters will broaden the tool box of modern surface engineering.

1.3 Overview of the dissertation

Chapter 2 describes the covalently conjugation of biotin and saccharides onto carbonyl-functionalized polymers via hydrazone formation.

Chapter 3 describes the spatioselective immobilization of biomolecules on alkyne-derivatized vapor-based polymers via "click" chemistry.

Chapter 4 reports a culture platform for long-term culture of human embryonic stem cells.

Chapter 5 further extends the application of zwitterionic polymer (described in the previous chapter) towards fully-defined culture environments.

Chapter 6 details our work on the fabrication of nitric oxide generating coatings and application to cardiovascular stents.

Chapter 7 concludes the dissertation and describes potential future directions.

R$_1$	R$_2$	R$_3$	R$_4$
CHO	H	H	H
COCH$_3$	H	H	H
COC$_2$H$_5$	H	H	H
COCF$_3$	H	H	H
COC$_2$F$_5$	H	H	H
COPh	H	H	H
COPh	H	COPh	H
NH$_2$	H	H	H
NH$_2$	H	NH$_2$	H
CH$_2$NH$_2$	H	H	H
C≡CH	H	H	H
C≡CH	H	C≡CH	H

R$_1$	R$_2$	R$_3$	R$_4$
CH$_2$OH	H	H	H
CH$_2$OCH$_3$	H	H	H
CH$_2$OCOCH$_3$	H	H	H
COOCH$_3$	H	H	H
COOCH$_3$	COOCH$_3$	COOCH$_3$	COOCH$_3$
CH$_2$OCOPpf	H	H	H
CH$_2$OCOCF$_3$	H	H	H
Cl	H	H	H
Br	H	H	H
H	H	H	H

Figure 1.1: Schematic showing the chemical vapor deposition (CVD) polymerization of functionalized poly-*p*-xylylenes.[26]

1.5 References

1. Langer, R. & Tirrell, D.A. Designing materials for biology and medicine. *Nature* **428**, 487-492 (2004).
2. Hubbell, J.A. Bioactive biomaterials. *Curr. Opin. Biotechnol.* **10**, 123-129 (1999).
3. Ma, Z.W., Mao, Z.W. & Gao, C.Y. Surface modification and property analysis of biomedical polymers used for tissue engineering. *Colloids and Surfaces B-Biointerfaces* **60**, 137-157 (2007).
4. Engel, E., Michiardi, A., Navarro, M., Lacroix, D. & Planell, J.A. Nanotechnology in regenerative medicine: the materials side. *Trends in Biotechnology* **26**, 39-47 (2008).
5. Ratner, B.D., Hoffman, A.S., Schoen, F.J. & Lemons, J.E. Biomaterials Science: An Introduction to Materials in Medicine, Edn. 2nd. (Academic Press, 2004).
6. Hermanson, G.T. Bioconjugate Techniques, Edn. 1st. (Academic, San Diego, CA, 1996).
7. Kane, R.S., Takayama, S., Ostuni, E., Ingber, D.E. & Whitesides, G.M. Patterning proteins and cells using soft lithography. *Biomaterials* **20**, 2363-2376 (1999).
8. Nandivada, H., Chen, H.Y. & Lahann, J. Vapor-based synthesis of poly [(4-formyl-p-xylylene)-co-(p-xylylene)] and its use for biomimetic surface modifications. *Macromolecular Rapid Communications* **26**, 1794-1799 (2005).
9. Kolb, H.C., Finn, M.G. & Sharpless, K.B. Click chemistry: diverse chemical function from a few good reactions. *Angewandte Chemie, International Edition* **40**, 2004-2021 (2001).
10. Nandivada, H., Jiang, X.W. & Lahann, J. Click chemistry: Versatility and control in the hands of materials scientists. *Advanced Materials* **19**, 2197-2208 (2007).
11. Narayan, S. et al. "On water": Unique reactivity of organic compounds in aqueous suspension. *Angewandte Chemie-International Edition* **44**, 3275-3279 (2005).
12. Kolb, H.C. & Sharpless, K.B. The growing impact of click chemistry on drug discovery. *Drug Discovery Today* **8**, 1128-1137 (2003).
13. Devaraj, N.K. & Collman, J.P. Copper catalyzed azide-alkyne cycloadditions on solid surfaces: Applications and future directions. *QSAR Comb. Sci.* **26**, 1253-1260 (2007).
14. Mendes, P.M., Yeung, C.L. & Preece, J.A. Bio-nanopatterning of surfaces. *Nanoscale Research Letters* **2**, 373-384 (2007).
15. Christman, K.L., Enriquez-Rios, V.D. & Maynard, H.D. Nanopatterning proteins and peptides. *Soft Matter* **2**, 928-939 (2006).
16. Ito, Y. Covalently immobilized biosignal molecule materials for tissue engineering. *Soft Matter* **4**, 46-56 (2008).
17. Whitesides, G.M., Ostuni, E., Takayama, S., Jiang, X.Y. & Ingber, D.E. Soft lithography in biology and biochemistry. *Annual Review of Biomedical Engineering* **3**, 335-373 (2001).
18. Luo, W., Jones, S.R. & Yousaf, M.N. Geometric Control of Stem Cell Differentiation Rate on Surfaces. *Langmuir* **24**, 12129-12133 (2008).
19. Gates, B.D. et al. New approaches to nanofabrication: Molding, printing, and other techniques. *Chemical Reviews* **105**, 1171-1196 (2005).
20. Nie, Z.H. & Kumacheva, E. Patterning surfaces with functional polymers. *Nature Materials* **7**, 277-290 (2008).

21. Bernard, A., Renault, J.P., Michel, B., Bosshard, H.R. & Delamarche, E. Microcontact printing of proteins. *Advanced Materials* **12**, 1067-1070 (2000).

22. Rozkiewicz, D.I. et al. Covalent microcontact printing of proteins for cell patterning. *Chemistry-a European Journal* **12**, 6290-6297 (2006).

23. Gerding, J.D., Willard, D.M. & Van Orden, A. Single-feature inking and stamping: A versatile approach to molecular patterning. *Journal of the American Chemical Society* **127**, 1106-1107 (2005).

24. Kumar, A. & Whitesides, G.M. Features of gold having micrometer to centimeter dimensions can be formed through a combination of stamping with an elastomeric stamp and an alkanethiol ink followed by chemical etching. *Applied Physics Letters* **63**, 2002-2004 (1993).

25. Xia, Y.N. & Whitesides, G.M. Soft lithography. *Angewandte Chemie-International Edition* **37**, 551-575 (1998).

26. Lahann, J. Vapor-based polymer coatings for potential biomedical applications. *Polymer International* **55**, 1361-1370 (2006).

27. Lahann, J. Reactive polymer coatings for biomimetic surface engineering. *Chemical Engineering Communications* **193**, 1457-1468 (2006).

28. Lahann, J. & Langer, R. Novel poly(p-xylylenes): Thin films with tailored chemical and optical properties. *Macromolecules* **35**, 4380-4386 (2002).

29. Lahann, J., Choi, I.S., Lee, J., Jenson, K.F. & Langer, R. A new method toward microengineered surfaces based on reactive coating. *Angewandte Chemie-International Edition* **40**, 3166-+ (2001).

30. Lahann, J., Hocker, H. & Langer, R. Synthesis of amino[2.2]paracyclophanes - Beneficial monomers for bioactive coating of medical implant materials. *Angewandte Chemie-International Edition* **40**, 726-728 (2001).

31. Lahann, J., Klee, D. & Hocker, H. Chemical vapour deposition polymerization of substituted [2.2]paracyclophanes. *Macromolecular Rapid Communications* **19**, 441-444 (1998).

32. Lahann, J. et al. Reactive polymer coatings: A platform for patterning proteins and mammalian cells onto a broad range of materials. *Langmuir* **18**, 3632-3638 (2002).

33. Lahann, J. et al. Reactive polymer coatings: A first step toward surface engineering of microfluidic devices. *Analytical Chemistry* **75**, 2117-2122 (2003).

34. Chen, H.Y., Elkasabi, Y. & Lahann, J. Surface modification of confined microgeometries via vapor-deposited polymer coatings. *Journal of the American Chemical Society* **128**, 374-380 (2006).

35. Elkasabi, Y., Yoshida, M., Nandivada, H., Chen, H.Y. & Lahann, J. Towards multipotent coatings: Chemical vapor deposition and biofunctionalization of carbonyl-substituted copolymers. *Macromolecular Rapid Communications* **29**, 855-870 (2008).

36. Elkasabi, Y. et al. Partially Fluorinated Poly-p-xylylenes Synthesized by CVD Polymerization. *Chem. Vapor Depos.* **15**, 142-149 (2009).

37. Lahann, J. & Langer, R. Surface-initiated ring-opening polymerization of epsilon-caprolactone from a patterned poly(hydroxymethyl-p-xylylene). *Macromolecular Rapid Communications* **22**, 968-971 (2001).

38. Schurmann, K. et al. Biologic response to polymer-coated stents: In vitro analysis and results in an iliac artery sheep model. *Radiology* **230**, 151-162 (2004).

39. Lahann, J., Klee, D., Pluester, W. & Hoecker, H. Bioactive immobilization of r-hirudin on CVD-coated metallic implant devices. *Biomaterials* **22**, 817-826 (2001).

40. Suh, K.Y., Langer, R. & Lahann, J. A novel photoderinable reactive polymer coating and its use for microfabrication of hydrogel elements. *Advanced Materials* **16**, 1401-+ (2004).

41. Chen, H.Y. & Lahann, J. Fabrication of discontinuous surface patterns within microfluidic channels using photodefinable vapor-based polymer coatings. *Analytical Chemistry* **77**, 6909-6914 (2005).

42. Jiang, X.W., Chen, H.Y., Galvan, G., Yoshida, M. & Lahann, J. Vapor-based initiator coatings for atom transfer radical polymerization. *Adv. Funct. Mater.* **18**, 27-35 (2008).

43. Chen, H.Y., McClelland, A.A., Chen, Z. & Lahann, J. Solventless adhesive bonding using reactive polymer coatings. *Analytical Chemistry* **80**, 4119-4124 (2008).

44. Elkasabi, Y., Chen, H.Y. & Lahann, J. Multipotent polymer coatings based on chemical vapor deposition copolymerization. *Advanced Materials* **18**, 1521-+ (2006).

45. Elkasabi, Y. & Lahann, J. Vapor-based polymer gradients. *Macromolecular Rapid Communications* **30**, 57-63 (2009).

CHAPTER 2

BIOIMMOBILIZATION VIA VAPOR-BASED REACTIVE COATINGS

CONTAINING CARBONYL GROUPS

The material in this chapter has been adapted with minor modifications from the following published articles:

H. Nandivada, H.-Y. Chen, and J. Lahann, Vapor-based synthesis of poly[(4-formyl-*p*-xylylene)-co-(*p*-xylylene)] and its use for biomimetic surface modifications, Macromolecular Rapid Communications (2005) 26, 1794.

H. Nandivada, H-Y. Chen, Y. Elkasabi, J. Lahann, Reactive polymer coatings for biological applications, ACS Symposium Series no. 977, Chapter 17: Polymers for biomedical applications (2007).

Y. Elkasabi, M. Yoshida, H. Nandivada, H-Y. Chen, J. Lahann, Towards multipotent coatings: Chemical vapor deposition and biofunctionalization of carbonyl-substituted copolymers. Macromolecular Rapid Communications (2008) 29, 855-870.

Y. Elkasabi, H. Nandivada, H-Y. Chen, S. Bhaskar, J. D'Arcy, L. Bondarenko, J. Lahann, Vapor-based synthesis of partially fluorinated poly-*p*-xylylenes synthesized by chemical vapor deposition polymerization, Chemical Vapor Deposition (2009), 15 (4-6), 142-149.

Abstract

Several functionalized poly-*p*-xylyenes have been synthesized via CVD polymerization of substituted [2.2]paracyclophanes creating a wide range of different

reactive polymer coatings. This chapter describes the synthesis and characterization of an aldehyde-functionalized poly(*p*-xylylene), poly[(4-formyl-*p*-xylylene)-co-(*p*-xylylene)] and an ultrahydrophobic reactive perfluorinated polymer, poly(4-heptadecafluorononnonyl-*p*-xylylene-co-*p*-xylylene) via chemical vapor deposition (CVD) polymerization. Chemical composition of the resulting polymer thin films was confirmed by Fourier transform infrared (FTIR) spectroscopy and X-ray photoelectron spectroscopy (XPS). Furthermore, availability and reactivity of carbonyl groups on the surface of the polymers was studied using hydrazone formation.

2.1 Introduction

Engineering of material surfaces has emerged as a critical challenge in the development of a variety of biomedical devices.[1] Universally-applicable engineering protocols are required to design biological microenvironments for miniaturized systems, such as micro-total analysis systems (microTAS), microfabricated cell sorters, cell-based assays, microseparators for DNA, proteins, and polysaccharides.[2-7] In general, covalent linkage of biomolecules to a surface requires suitable chemical groups on the substrate that support chemoselective coupling reactions. Since most substrates of interest in the biomedical field do not bear reactive groups of appropriate types and densities, they must be introduced either in a proper surface functionalization step or via deposition of functionalized thin-film coatings. Recently, we established a surface modification technique based on the chemical vapor deposition (CVD) polymerization of substituted [2,2]paracyclophanes, to prepare a diverse class of functionalized poly(*p*-xylylenes) with a wide variety of functional groups such as amines, esters, and alcohols, which can be used for covalent binding of biomolecules.[8-14] This technique fulfills the need for a simple and broadly applicable surface modification system that creates stable platforms,

13

which present a variety of reactive functional groups. Commercially-available non-functionalized poly-p-xylylene or parylene coatings have been used in a variety of applications such as biomaterials, sensors, packaging, and in MEMS devices. Chemical vapor deposition provides a solvent-free environment, controllable polymer composition and architecture, good adhesion, and the ability to tailor surface properties within a wide range.[8, 15]

Although less common, the aldehyde group is a suitable candidate for surface modification because of its high specificity toward functional groups such as hydrazide, hydroxylamino, and thiosemicarbazide functionalities.[16-18] Aldehyde groups have already been generated on glass, silicon, and metal surfaces using multi-step silanization process or plasma polymerization of aldehyde-containing monomers.[19, 20] However, these substrate specific protocols result in poorly defined polymers or may involve the use of organic solvents and other chemicals which could potentially reduce the biological applicability of aldehyde-modified surfaces. Therefore, a substrate-independent procedure, such as CVD polymerization, is highly attractive for preparation of aldehyde-functionalized surfaces.

Surface wettability is another important attribute, which determines the suitability of surfaces for a range of different applications. In this respect, fluorinated polymers with low surface energy are particularly attractive due to their water-repellence, inertness, and low coefficient of friction.[21, 22] Fluorinated polymer films synthesized using CVD such as poly(octafluoro-*p*-xylylene) (also known as parylene-AF4) and poly(tetrafluoro-*p*-xylylene) (VT-4) have been demonstrated to exhibit excellent optical properties, low dielectric constants and high thermal stability.[23, 24] Despite these interesting properties, the coatings typically lacked reactive functional groups for further surface modification.

In order to incorporate the advantages of fluorinated polymers with the concept of reactive CVD coatings, fluorinated moieties can be attached to [2.2]paracyclophanes prior to CVD polymerization. In the past, several poly-*p*-xylylenes have been synthesized

with shorter fluorinated side chains resulting in relatively hydrophobic coatings.[8, 13, 25, 26] To further enhance this effect, we have now synthesized and CVD polymerized a [2.2]paracyclophane with a longer perfluorinated chain. Given the usefulness of non-functionalized as well as other perfluorinated PPX coatings for coating applications,[14, 23, 24, 27] widening the scope of CVD polymerization by applying this technique to reactive partially-fluorinated [2.2]paracyclophanes may significantly advance the field of low-surface energy coatings.

In this chapter, CVD polymerization of 4-formyl[2,2]paracyclophane (**1**) to yield an aldehyde-functionalized poly(*p*-xylylene), poly[(4-formyl-*p*-xylylene)-co-(*p*-xylylene)] (**2**) is described. Furthermore, ultrahydrophobic reactive perfluorinated polymer, poly(4-heptadecafluorononyl-*p*-xylylene-co-*p*-xylylene) (**4**) was synthesized by CVD polymerization of 4-heptadecafluorononyl[2.2]paracyclophane (**3**) which contained a carbonyl-functionalized derivative with an 8-carbon perfluorinated chain. Chemical composition of the resulting polymer thin films was confirmed by Fourier transform infrared (FTIR) spectroscopy and X-ray photoelectron spectroscopy (XPS). Furthermore, availability and reactivity of aldehyde groups on the surface of polymer **2** and **4** was established via specific chemical reaction with hydrazide functionalized ligands to yield hydrazone linkages and tethered biotin hydrazide and model sugars to these reactive surfaces.

2.2 Methods

Synthesis of 4-formyl[2.2]paracyclophane (1)

Synthesis of the precursor, 4-formyl[2.2]paracyclophane (**1**) has been well studied and characterized in the literature.[28] Precursor **1** was synthesized through the oxidation of

4-hydroxy[2.2]paracyclophane. The resulting product was characterized using ^{1}H NMR, ^{13}C NMR, FTIR spectroscopy, and Mass spectroscopy. The spectra compared well with the values given in the literature.[28]

^{1}H NMR (400 MHz, CDCl$_3$, TMS): δ = 2.91–3.30 (m, 7H), 4.07–4.13 (m, 1H), 6.36–6.39 (d-d, 1H), 6.42–6.44 (d-d, 1H), 6.48–6.51 (d, 1H), 6.55–6.60 (m, 2H), 6.72–6.74 (d, 1H), 7.01 (d, 1H), 9.94 (s, 1H). ^{13}C NMR (75 MHz, CDCl$_3$, TMS): δ = 33.58, 34.94, 35.10, 35.23, 132.12, 132.33, 132.88, 133.22, 136.08, 136.30, 136.55, 138.04, 139.40, 139.45, 140.61, 143.19, 191.90. FTIR (ATR): ν (cm^{-1}) = 873, 908, 1147, 1182, 1226, 1417, 1552, 1591, 1678, 1734, 2743, 2856, 2934. MS (70 eV): m/z = 36 (M$^+$), 132 (C$_8$H$_7$CHO$^+$), 104 (C$_8$H$_8^+$), 103 (C$_8$H$_7^+$), 77 (C$_6$H$_5^+$).

CVD Polymerization

Poly[(4-formyl-*p*-xylylene)-co-(*p*-xylylene)] (**2**) was obtained by the CVD polymerization of precursor **1** using a CVD installation consisting of a sublimation zone, pyrolysis zone, and deposition chamber. 50 mg of **1** was placed in the sublimation zone and substrate was fixed on the sample holder at 10 $^{\circ}$C. Compound **1** was slowly sublimed at a temperature of 100–120 $^{\circ}$C and at a reduced pressure of 0.54 mbar. Argon was used as carrier gas at a flow rate of 20 sccm. Under these conditions, precursor **1** was transported into the pyrolysis zone, which was heated at a temperature of 670 $^{\circ}$C. Finally, polymer film **2** was deposited on the substrate at 10 $^{\circ}$C.

Starting material, 4-heptadecafluorononyl[2.2]paracyclophane (**3**) was synthesized[31] and sublimed at 80-90 $^{\circ}$C and pyrolyzed at 620 $^{\circ}$C. Polymer poly(4-heptadecafluoronononyl-*p*-xylylene-co-*p*-xylylene) (**4**) was spontaneously formed on substrates kept at a temperature of 15 $^{\circ}$C

Polymer Characterization

FTIR spectroscopy was performed on a Nicolet 6700 spectrometer utilizing the grazing angle accessory (Smart SAGA) at a grazing angle of 85°. The elemental analysis of polymer **2** was conducted using XPS on a Perkin Elmer/PHI 5400 spectrometer. All spectra were calibrated with respect to non-functionalized aliphatic carbon with a binding energy of 285.0 eV. XPS data for polymer **4** were recorded on Axis Ultra X-ray photoelectron spectrometer (Kratos Analyticals, UK) equipped with a monochromatized Al K_{α} X-ray source. Lens mode was in hybrid, pass energy was set to 160.0 eV with an X-ray power of 150 kW, and aperture was 600 µm x 600 µm. Thickness measurements were recorded at a wavelength of 532 nm using an EP3-SW ellipsometry (Nanofilm Technologie GmbH, Germany). Nulling experiments were performed at an angle of incident of 60°, and an anisotropic Cauchy model was used to model the ellipsometric parameters psi and delta. Surface morphology was examined by scanning electron microscopy (Philips XL30 ESEM, high vacuum mode).

Polymer **2:** FTIR (grazing angle of 85°): ν (cm^{-1}) = 840, 903, 945, 1158, 1235, 1267, 1452, 1499, 1567, 1608, 1688, 2734, 2880, 2921. XPS (referenced to hydrocarbon at 285.0 eV): C_{1s}: 92.5% (theoretical: 94.4%); O_{1s}: 7.5% (theoretical: 5.6%).

Polymer **4**: FTIR (grazing angle 85°): ν (cm^{-1}) = 2934, 1714, 1568, 1498, 1458, 1416, 1370, 1330, 1251, 1222, 1154, 1061, 1005, 943, 880, 811. XPS (atomic ratios): F_{1s}/C_{1s}: 86.4 (calc. 85.6%), O_{1s}/C_{1s}: 5.9% (calc. 5.0%).

Contact angle measurements

A microsyringe was used to place a 5 µl droplet on the substrate and picture of the droplet was captured using a digital camera (Canon EOS 20D) after 5 sec. An image

processing software (ImageJ) was used to analyze the droplet images and calculate the contact angle.

Carbonyl-hydrazide reaction kinetics using NMR

Carbonyl-functionalized *p*-xylenes were synthesized following an approach slightly modified from synthetic procedures previously described for the corresponding [2.2]paracyclophanes (PCPs).[8, 29, 30] Model reactions of the carbonyl groups with hexanoic hydrazide were performed in an NMR tube and a sequence of ^{1}H NMR (Varian Inova, 400 MHz) spectra was collected in real-time. Prior to starting the reaction, a base ^{1}H NMR spectrum was taken as a reference. A slight excess of hexanoic hydrazide (1.1 equivalents) was dissolved in deuterated ethyl alcohol (Sigma Aldrich), and functionalized *p*-xylene was added. Next, acetic acid was added to initiate the reaction, and data acquisition was started immediately after the sample was placed in the NMR spectrometer. NMR spectra were acquired every 7 min for 2 h, and a final measurement was taken after 12 h.

Immobilization of biotinamidocaproyl hydrazide (5)

A polydimethylsiloxane (PDMS) stamp was created, as previously described in literature.[9] The PDMS stamp was treated for 30 min using a UV-ozone cleaner (Model no. 342, Jelight company Inc.) to render its surface hydrophilic. The oxidized stamp was then inked with a 10 mM solution of biotinamidocaproyl hydrazide (Pierce Biotechnology, IL) (**5**) in ethanol at a pH of 5–6 and stamped onto a surface coated with polymer **2**. The stamp was kept in contact with the substrate for 2 min and then patterned substrate was incubated for 2 h with rhodamine-labeled streptavidin (Pierce

Biotechnology, IL) (**6**) in an aqueous phosphate buffer PBS (pH 7.4, Sigma, MO) consisting of 0.1% (w/v) bovine serum albumin (Sigma, MO) and 0.02% (v/v) Tween 20 (Sigma, MO). Substrate was washed three times with the incubating buffer and rinsed with DI-water. Micropatterns on the substrate were visualized using a Nikon TE200 fluorescence microscope and confocal laser scanning microscope (CLSM) (Olympus FluoView 500, USA).

Patterning experiments with polymer **2**: PDMS stamp with diamond-shaped indentations (50 µm diagonal) with a center-center spacing of 75 µm.

Patterning experiments with polymer **4**: PDMS stamp with square-shaped indentations (400 µm on a side) with 50 µm gaps between square edges.

Particle patterning

After incubation with **5**, micropatterned surfaces were incubated with biotinylated biphasic PLGA microparticles for 2 h and washed extensively with PBS (pH 7.4). Particle-patterned surfaces were visualized using confocal laser scanning microscope (CLSM) (Olympus FluoView 500, USA).

Immobilization of 2-α-mannobiose (8)

The PDMS stamp used for microcontact printing consisted of alternating lines of 15 or 20 µm in width with a spacing of 30 µm. PDMS stamp was oxidized using a UV-ozone cleaner for 30 min and then inked with a 100 mM solution of adipic acid dihydrazide (**7**) in PBS consisting of 0.1% Tween 20 at a pH of 5–6. The stamp was kept in conformal contact with the substrate for 2 min and the substrate was washed repeatedly with PBS. Patterned substrate was then incubated for 3 h in a 10 mM solution of 2-α-

mannobiose (Sigma, MO) (**8**) in DMF at 60 °C. After washing the substrate with PBS,

patterned substrate was exposed, for 2 h, to a 100 mg/ml solution of rhodamine-

conjugated concanavalin-A (Molecular Probes, OR) (**9**) in PBS containing 1 mM $CaCl_2$

and 1 mM $MnCl_2$. After lectin incubation, the surface was washed with PBS. For

fluorescence microscopy, samples were examined with a Nikon TE200 microscope.

2.3 Results and discussion

Precursor synthesis and characterization

Precursor 4-formyl[2,2]paracyclophane (**1**) can be synthesized either using the

two-step synthesis from [2.2]paracyclophane or via oxidation of 4-

hydroxy[2,2]paracyclophane.[13, 28] Here, **1** was prepared in high yields via the latter route.

Data from mass spectroscopy compared well with **1** prepared according to the

[2.2]paracyclophane route.

Synthesis and characterization of polymer 2

The resulting dimer **1** was CVD polymerized to yield poly[(4-formyl-*p*-xylylene)-

co-(*p*-xylylene)] (**2**). For CVD polymerization (Figure 2.1), **1** was sublimed in the

sublimation chamber under a reduced pressure of 0.54 mbar at a temperature of 100–120

°C. Vaporized dimer **1** was then transported by argon gas into the pyrolysis zone, at a

temperature of 670 °C, where the methylene bridges were homolytically cleaved and

quinodimethanes were formed. These monomers were then adsorbed onto the substrate at

a temperature of 10 °C. Under these conditions, monomers underwent spontaneous

polymerization on the substrate. Elemental composition of polymer **2** was determined

using XPS (Table 2.1). From XPS survey spectrum and high-resolution spectra, a value of 92.5% for carbon and 7.5% for oxygen was found, compared to the theoretical composition of 94.4% for carbon and 5.6% for oxygen. Difference between the experimental and theoretical composition can be attributed to contamination during sample handling. High-resolution C1s spectrum of polymer **2** (Figure 2.2) showed that ratio between the α-carbon of formyl group (C–C=O) and arbonyl carbon (C=O) is 0.88, compared to calculated value of 1. Furthermore, signal at 291.2 eV indicated $\pi \rightarrow \pi^*$ transitions which are a characteristic feature of aromatic polymers and have been previously reported for poly(*p*-xylylenes).[8] Symmetric O_{1s} signal at 533.2 eV can be attributed to a single energy state for all the oxygen atoms in the polymer. Thus, XPS data confirmed the chemical structure of polymer **2** shown in Scheme 1. Strong carbonyl stretch at 1688 cm^{-1} in the FTIR spectrum also confirmed the presence of aldehyde group in polymer **2** after CVD polymerization. Further evidence of aldehyde group was provided by the characteristic band for aldehyde C–H stretching vibrations at 2734 cm^{-1}.

Polymer **2** exhibited good adhesion to a wide variety of substrates such as gold, silica, glass, and PDMS. Adhesion of polymer **2** was analyzed by pressing scotch tape onto a polymer-coated substrate and then peeling it off. Visual examination showed intactness of the film and FTIR spectrum confirmed presence of the polymer film (Figure 2.3). Polymer **2** was insoluble in aqueous solutions as well as in a variety of standard organic solvents such as ethanol, acetone, methanol, dichloromethane, chloroform, dimethylformamide, and toluene. Insolubility in organic solvents distinguishes these polymer films from paracyclophane as well as oligomers and low-molecular weight polymers and suggests that high molecular-weight polymers are formed under conditions of CVD polymerization described above.

Synthesis and characterization of polymer 4

Polymer coating **4** was synthesized by CVD polymerization of precursor under conditions typically used for poly-*p*-xylylenes (Figure 2.1). Owing to a long fluorinated side chain, precursor **3** possessed a higher molecular weight compared to other functionalized [2.2]paracyclophanes. Therefore, a sublimation temperature between 90-100 ^{o}C and lower optimum pyrolysis temperature of 630 ^{o}C were used. Characterization of polymer **4** using FTIR spectroscopy showed a strong peak at 1713 cm^{-1} indicating the carbonyl (C=O) stretch confirming presence of the functional group after CVD polymerization (Figure 2.4). Also, peaks at 1329, 1251, 1222, and 1154 cm^{-1} signified C-F vibrations. Experimental atomic ratios obtained from XPS were in good agreement with theoretical calculations (Table 2.2). Figure 2.5 shows survey and high-resolution C_{1s} XPS spectra for polymer **4**. In high-resolution C_{1s} spectrum, binding energy of 288.8 eV indicated the carbonyl carbon (C=O). Furthermore, ratio of C-F$_3$ to C-F$_2$ carbons equals 0.143, which agreed well with theoretical value of 0.149, indicating preservation of fluorinated ketone during CVD. Overall, high-resolution XPS spectrum reaffirmed the FTIR results.

Contact angle measurements of polymer **4** provided an insight into degree of hydrophobicity. Polymer **4** was compared to non-functionalized PPX and three fluorinated poly-*p*-xylylenes namely, poly(4,12-dibromo-1,1,9,9-tetrafluoro-*p*-xylylene) (TFPPX-Br$_2$) , poly(4-trifluoroacetyl-*p*-xylylene) (PPX-COCF$_3$) and poly(4-pentafluoropropionyl-*p*-xylylene) (PPX-COC$_2$F$_5$).[25, 31] Differences in position of functional group, functionalities and chain lengths influenced the contact angles (Figure 2.6). Greater degree of fluorination increased the contact angle.

Polymer **4** was deposited on a variety of different substrates such as gold, silicon, glass, and PDMS on which it showed good adhesion. To ascertain the adhesiveness of the polymer film, a piece of scotch tape was pressed onto the film and

peeled off.[30] Robustness of the film was examined visually (Figure 2.7) and FTIR was used for further confirmation. Moreover, polymer **4** was insoluble in aqueous solutions and several organic solvents such as ethanol, acetone, methanol, dichloromethane, chloroform, dimethylformamide, and toluene. This is an important property which differentiates the polymer from its precursor as well as other oligomers and low molecular weight polymers, thus indicating formation of a high-molecular weight polymer.

Study of carbonyl group reactivity

It is necessary to understand the relative chemical reactivity of different carbonyl groups towards target molecules (hydrazides). Ability to support chemical reactions on the surface of a substrate or a device is highly desirable for functionalized coatings. Availability and reactivity of carbonyl groups were studied using hydrazone formation. Hydrazones are formed via the conversion of aldehydes with hydrazines or hydrazides and is a widely used immobilization strategy.[18] In this context, reaction kinetics of different carbonyl functionalities was analyzed using in-situ ^{1}H NMR spectroscopy. Rather than reacting functionalized PCP monomers, corresponding functionalized *p*-xylenes were synthesized, because constrained ring system of the PCPs significantly alters their chemical reactivity and disqualifies them as model reactants for PPXs. Functionalized *p*-xylenes may be considered as the smallest repetition unit of the polymer coatings and, therefore, more closely resembles the PPX chain. By integrating two specific peaks on the NMR spectra, one characteristic of the reactants (–CH) and the other one indicating the product (–C–N–NH), percentage yield of the product was evaluated. Percentage yields were plotted as a function of time for the different reactions with functionalized *p*-xylene derivatives. Figure 2.8 shows kinetic curves fitted to the

experimental data. For most *p*-xylenes, NMR peaks characteristic of the product were evident within 15–20 min of initiating the reaction. NMR spectra for benzoyl-functionalized p-xylene showed no signals characteristic of the product over reaction durations as long as 15 h. Fluorinated carbonyl group was more reactive than non-fluorinated groups. Of the functional groups, $COCF_3$ was most reactive, followed by COC_2F_5, COC_2H_5, and COC_6H_5 in order of decreasing reactivity. Benzoyl (COC_6H_5) group yielded no detectable product within the evaluated reaction times.

Biotin immobilization via hydrazone formation

Using microcontact printing, the condensation reaction between aldehyde groups on the surface and a biotinyl hydrazide was performed at pH 5–6. For microcontact printing, biotinamidocaproyl hydrazide (**5**, structure shown in Figure 2.9) was inked onto an oxidized PDMS stamp and stamped onto the aldehyde substrate creating a pattern. We chose compound **5** as the prototype ligand owing to strong non-covalent interaction between biotin and streptavidin and streptavidin's ability to be used as a universal platform for further binding of biotinylated biomolecules.[9] After immobilization of compound **5**, biotin-binding was examined by utilizing rhodamine-labeled streptavidin (**6**) as the binding partner. Rhodamine-labeled streptavidin specifically bound to biotin-patterned surface (Figure 2.9) creating homogeneous and reproducible patterns on the reactive coating, thus showing that aldehyde groups on the surface are reactive and can be used as anchoring sites.

Ability to pattern surface of low surface energy coatings is an important requirement for surface engineering. Presence of a reactive keto group in the polymer provides an opportunity for surface modification, by using the reaction between keto group and hydrazide-containing ligands to form hydrazones.[30] Surface reaction between

polymer **4** and biotinyl hydrazide **5** was conducted using microcontact printing (Figure 2.10a). Biotin-patterned substrate was then visualized by incubating the substrate with rhodamine-labeled streptavidin (**6**) (Figure 2.10 b,c). Fluorescence was observed predominantly in the regions where the PDMS stamp was pressed onto the coating. This demonstrates availability of keto groups on the polymer surface towards surface reaction with hydrazide functionalized moieties.

Surface immobilization of saccharides

Specificity of hydrazides and hydrazines toward aldehydes and ketones also makes them superb binding agents for immobilization of saccharides.[18] Carbonyl-containing surfaces can be modified using dihydrazide homobifunctional linkers to form hydrazone bonds on one side and yielding alkyl hydrazide spacers on the other side, suitable for subsequent reaction with formyl-containing groups available in saccharides.[18] Adipic acid dihydrazide (**7**) was chosen as the linker due to its intermediate-length spacer arm, which leads to accessible reactive sites for further reaction. Using microcontact printing, substrate coated with polymer **2** was patterned with linker **7**, creating hydrazide-activated surfaces suitable for targeting saccharides (Figure 2.11). Hydrazide-modified polymer surface was further reacted with a disaccharide, 2-α-mannobiose (**8**). One mannose group reacted with hydrazide while leaving the other saccharide group free. Saccharide binding was investigated by applying a solution of rhodamine-labeled concanavalin A (**9**), a mannose-specific lectin, that recognizes free mannose units.[32] Patterned substrates were visualized using fluorescence microscopy (Figure 2.11). Rhodamine-labeled lectin specifically bound to disaccharide which was immobilized onto a substrate coated with polymer **2** and patterned with lines of linker **7**.

Combination of superhydrophobicity and reactivity

Superhydrophobicity of a surface is often created by the combination of low surface energy materials with a complex hierarchical surface architecture.[33] Superhydrophobic surfaces are described as surfaces with high contact angles (>150$^{\text{o}}$) and low contact angle hysteresis meaning water droplets easily roll off the surface.[34] For instance, superhydrophobicity of natural surfaces such as plant leaves is of great interest for studying the self-cleaning behavior.[34-36] Specifically, lotus leaves exhibit a phenomena called "lotus effect" where water droplets are almost spherical and roll off easily. Lotus leaves are covered with a waxy substance which has a contact angle of 103$^{\text{o}}$ by itself. The surface morphology of the leaves comprises of complicated microstructures which are further covered by nanostructures. Such a hierarchical structure traps air pockets inside imparting the surfaces the superhydrophobicity.[37]

Typically, superhydrophobic surfaces do not possess any reactivity and therefore cannot be used for further surface modifications. If perfluorinated coating **4** is applied to a substrate with rough topography, properties of a low surface energy reactive polymer coating will be enhanced and a reactive/superhydrophobic coating will be achieved. Reactive polymer coating **4** was deposited onto a poly(acrylamide) surface displaying a rough morphology, which was fabricated using electrohydrodynamic jetting.[38, 39] A layer of interconnected poly(acrylamide) particles was deposited onto a solid substrate using electrohydrodynamic jetting and then a uniform film of polymer **4** was coated onto these particles. Scanning electron micrographs (SEM) of the surface (with and without the CVD polymer layer) revealed that surface morphology consisted of a random distribution of particles with a diameter of 1-2 µm (Figures 2.12). In the past, electrohydrodynamic jetting has been used to enhance the surface roughness by creating a network of microparticles and nanofibers on flat substrates.[40, 41] Contact angle measurements showed that this combined film rendered a superhydrophobic character to the solid surface with a

contact angle of $> 153^o$ (Inset of figure 2.12b). This angle is much higher than contact angle of hydrophilic poly(acrylamide) surface ($\sim 15^o$ Inset of figure 2.12a) or a smooth surface coated with polymer film ($108.7^o \pm 2.3$). Moreover, water droplets freely rolled off the surface suggesting that surface has a very low hysteresis, one of the key characteristics of superhydrophobic surfaces. Finally, to demonstrate reactivity of the polymer, surface was reacted with compound **5** (as previously described) and incubated with Alexa Fluor 633 Streptavidin. Analysis with confocal scanning laser microscopy (CLSM) confirmed the reactivity of this superhydrophobic surface towards hydrazide-containing ligands (Figure 2.12c).

Interfacial roughness of the surface decreases the area of contact which in turn decreases the adhesive forces.[42] Superhydrophobic surfaces also greatly reduce protein adhesion due to water repellency of the surface which prevents protein solution penetration.[42] Superhydrophobic surfaces have also demonstrated anti cell adhesive properties which can be useful for clinical applications.

Particle patterning

In addition, interaction between streptavidin-patterned surfaces and biphasic PLGA particles, biotinylated on one compartment, was analyzed. Biotin and protein streptavidin interaction was used to create platforms for self-assembly due to widespread availability of biotin-functionalized biomolecules and high binding affinity between biotin and streptavidin ($K_a \sim 10^{13}$ M^{-1}). Furthermore, streptavidin is a tetrameric protein which can bind to four biotin molecules. After incubation of biotin-patterned surfaces with streptavidin, surfaces were incubated with biotinylated PLGA particles synthesized using electrohydrodynamic co-jetting process (Figure 2.13a). Analysis with CLSM confirmed the self-assembly of biotinylated particles onto streptavidin-patterned surfaces

(Figure 2.13b). High resolution confocal images showed an enhanced red signal indicating the specific orientation of the biphasic microparticles (Figure 2.13c).

2.4 Conclusions

In this chapter, the synthesis and characterization of a functionalized poly(*p*-xylylene), poly[(4-formyl-*p*-xylylene)- co-(*p*-xylylene)], using CVD polymerization was described. Usefulness of these polymer coatings for biomimetic surface modifications was also demonstrated. The underlying aldehyde-hydrazide coupling chemistry is an attractive bioconjugation approach, because it benefits from (1) rapid reaction kinetics and (2) relative inactivity of both the hydrazide and the carbonyl functionalities toward other biomolecules or biological functionalities, such as alcohols, acids, and thiols.[17, 18] The resulting surfaces may find potential applications for the surface engineering of biomaterials and microfluidic devices.

Furthermore, fluorinated [2.2]paracyclophane precursors with aromatic functionalization were polymerized to synthesize poly(4-heptadecafluoronononyl-*p*-xylylene-co-*p*-xylylene). Deposition of the polymer using CVD yielded coatings that were stable in a range of different organic solvents and aqueous solutions. Polymer was also shown to be reactive towards hydrazide-functionalized biotin, which then linked readily with fluorescently-labeled streptavidin. Finally, polymer coating was applied towards fabrication of superhydrophobic reactive coatings. This class of functionalized, fluorinated poly-*p*-xylylenes could be of great interest as low energy reactive vapor-based coatings for applications such as biomedical, automotive industries, anti-fouling coatings.

Figure 2.1: CVD polymerization of carbonyl-functionalized [2.2]paracyclophanes (**1** and **3**) yields the corresponding poly-*p*-xylylenes (**2** and **4**) respectively. Step I is the pyrolysis step and step II is the polymer deposition step.
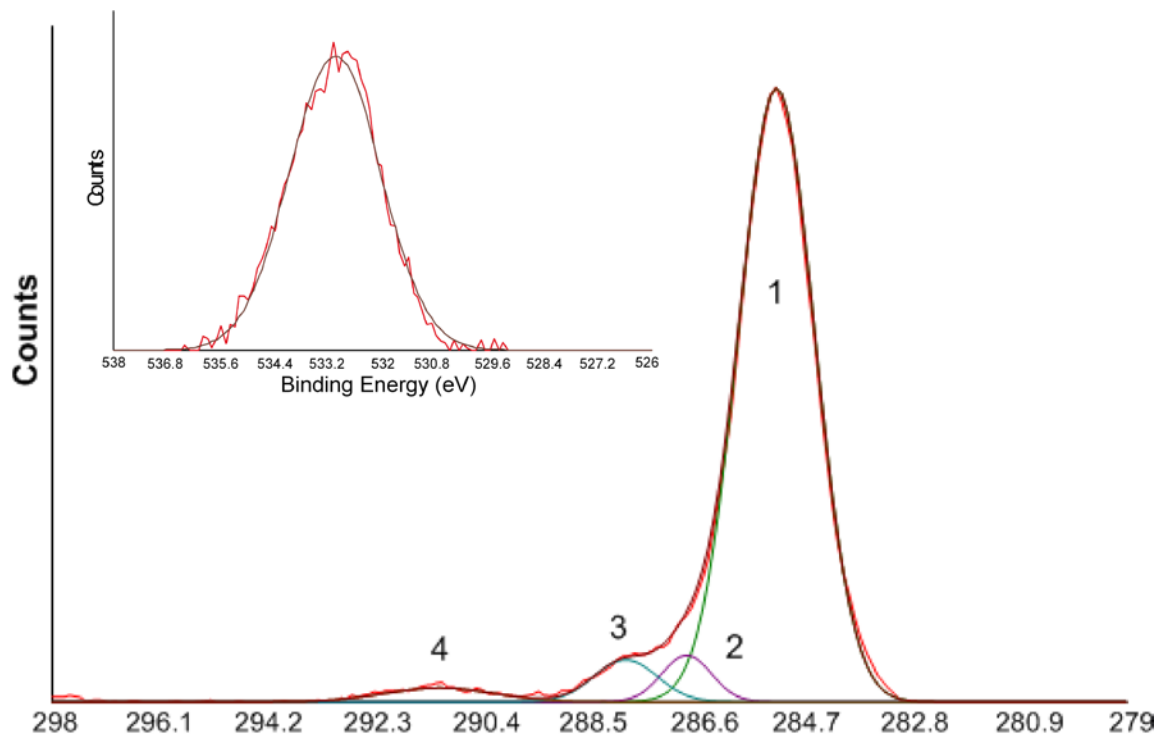
Figure 2.2: High-resolution C1s and O1s (inset) XPS spectra of aldehyde-functionalized polymer **2**.
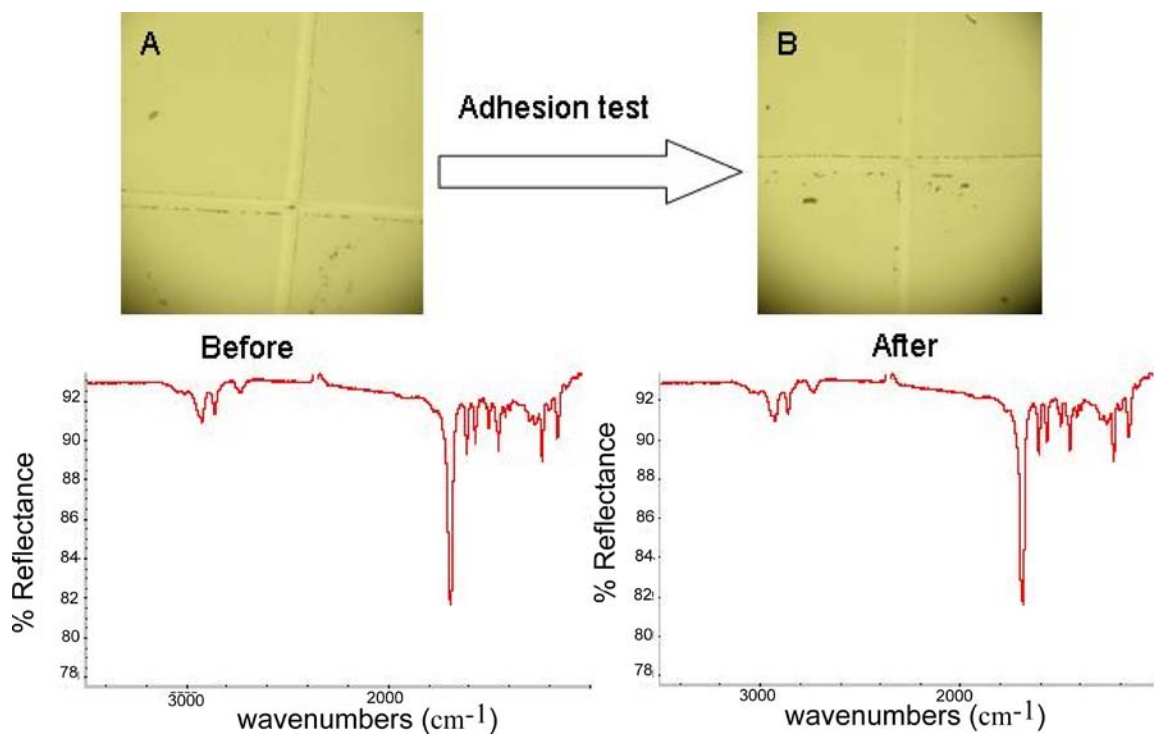
Figure 2.3: Testing the adhesion of polymer **2**. Polymer surface was first marked using a sharp object and then scotch tape was pressed onto the surface. Surface was observed before and after peeling off the tape. (A) Optical micrograph of the polymer surface before testing. (B) Optical micrograph of the film after testing showing intactness of the film. Corresponding IR spectra are also shown.
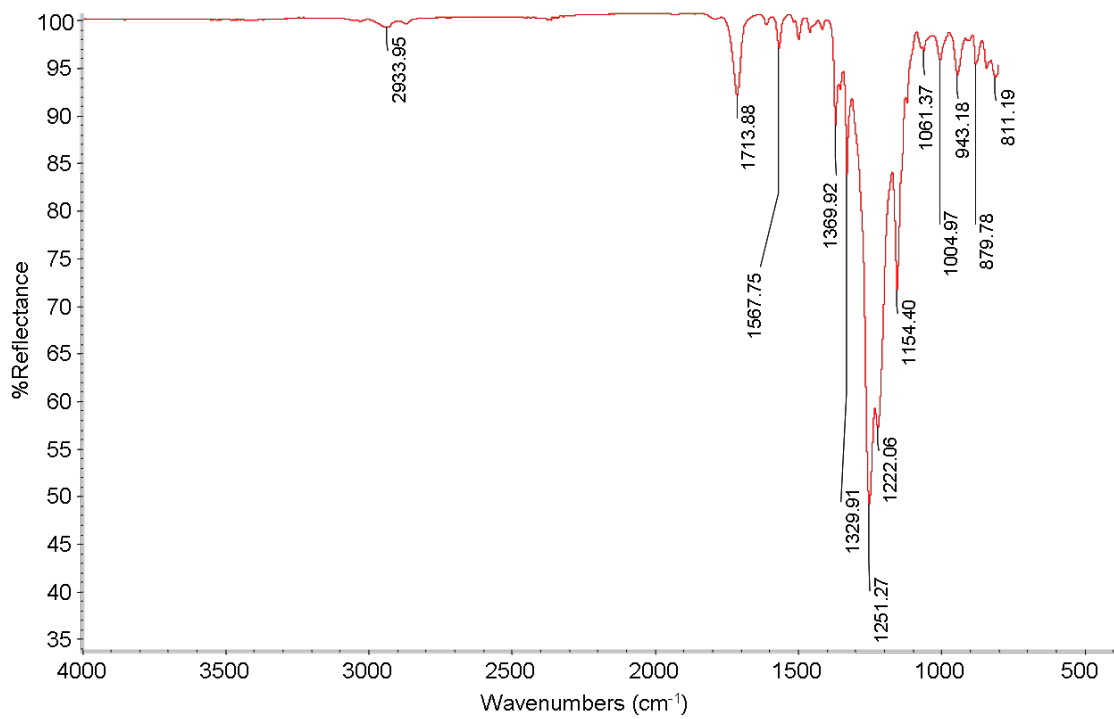
Figure 2.4: FTIR of polymer **4** deposited on a gold surface.
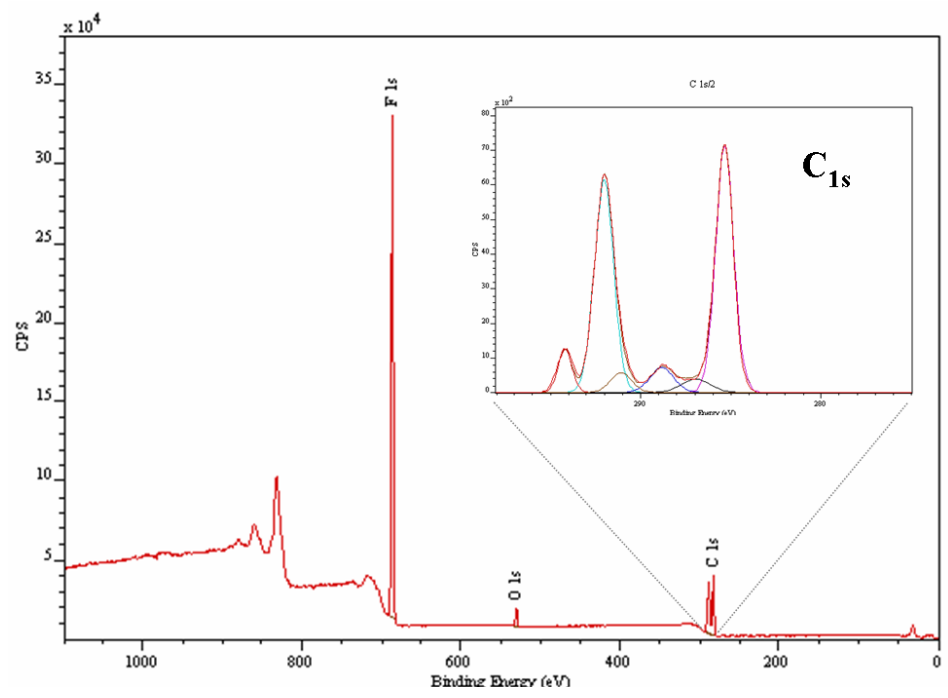
Figure 2.5: High resolution XPS of polymer **4**, inset shows the high-resolution C1s spectrum

33
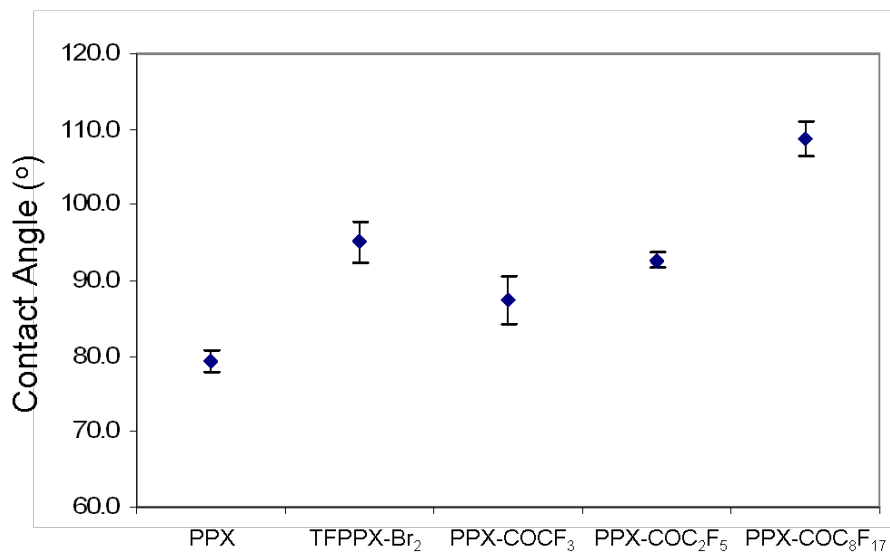
Figure 2.6: Comparing contact angles of non-functionalized PPX, TFPPX-Br$_2$, PPX-COCF3, PPX-COC2F5 and polymer **4**.
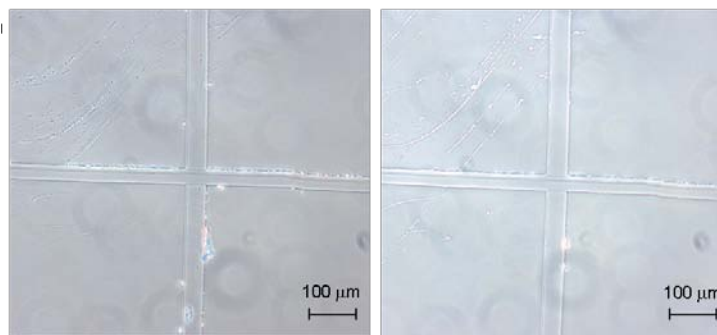
Figure 2.7: Testing the adhesion of polymer 4 using scotch-tape test. Optical micrographs before and after testing are shown on the left and right panels, respectively. IR spectra remained identical before and after testing
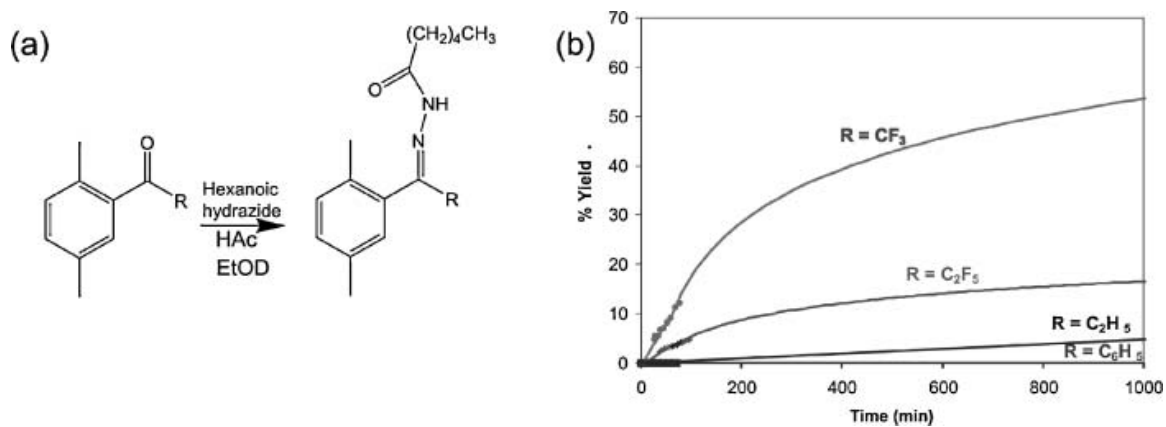
Figure 2.8: (a) Protocol used to determine reaction kinetics of different carbonyl-PPXs, using functionalized p-xylenes and hexanoic hydrazide as test molecules (b) Percentage yield of carbonyl reactions with respect to time, based upon ^{1}H NMR analysis of characteristic reactant and product peaks.
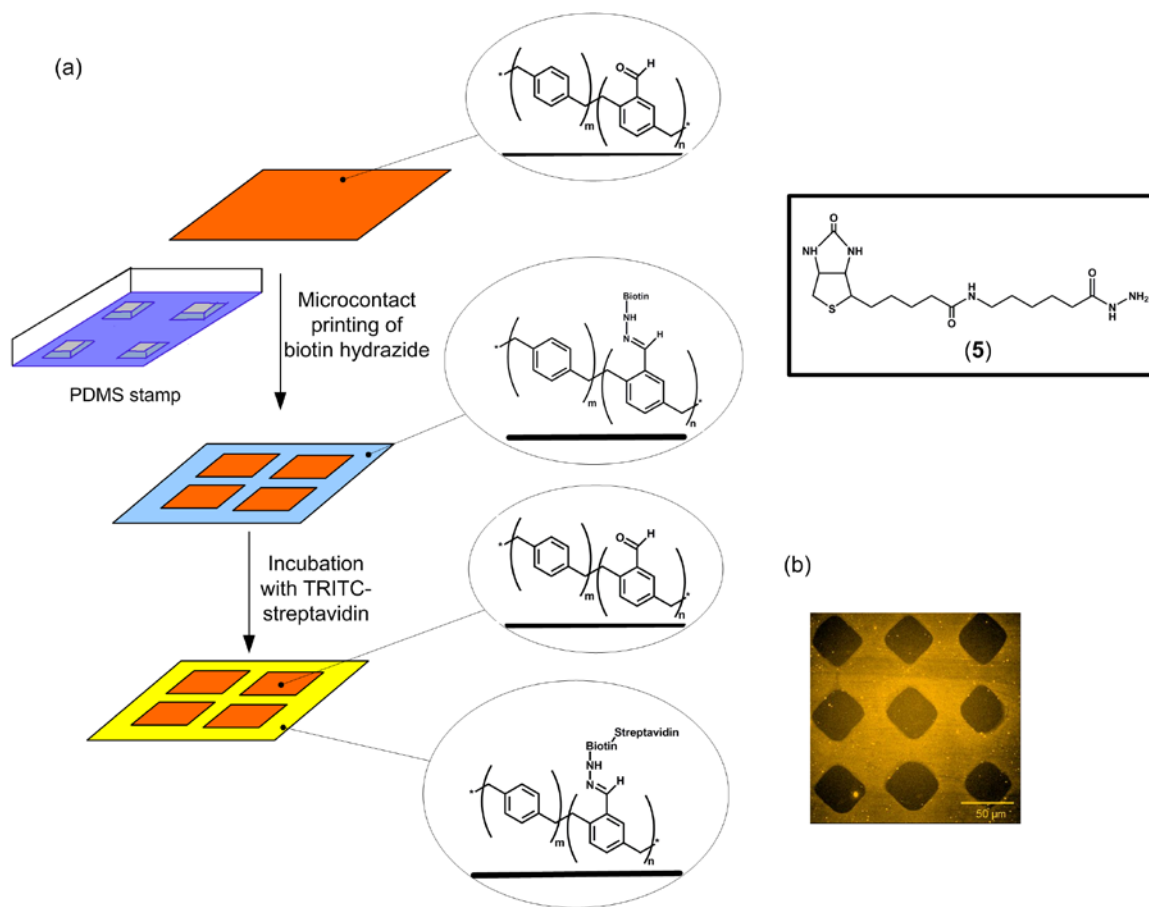
Figure 2.9: (a) Schematic description of the surface modification procedure used to modify polymer **2**; (b) a typical fluorescence micrograph of the surface showing rhodamine-labeled streptavidin (**6**) bound to ligand **5**, which was patterned onto polymer **2**.
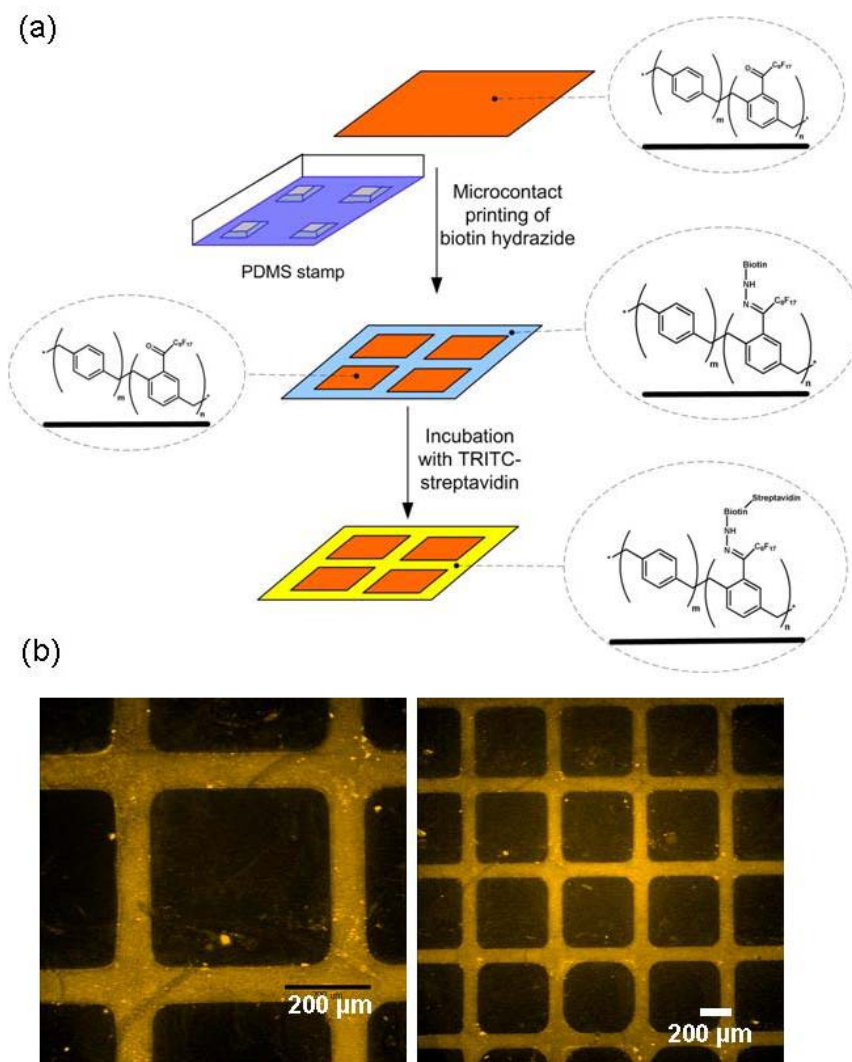
Figure 2.10: (a) Schematic of the microcontact printing process used to verify the reactivity of polymer **4** towards hydrazides. (b) Fluorescence micrographs of TRITC-labeled streptavidin (**6**) immobilized onto biotin hydrazide (**5**) patterned substrates.
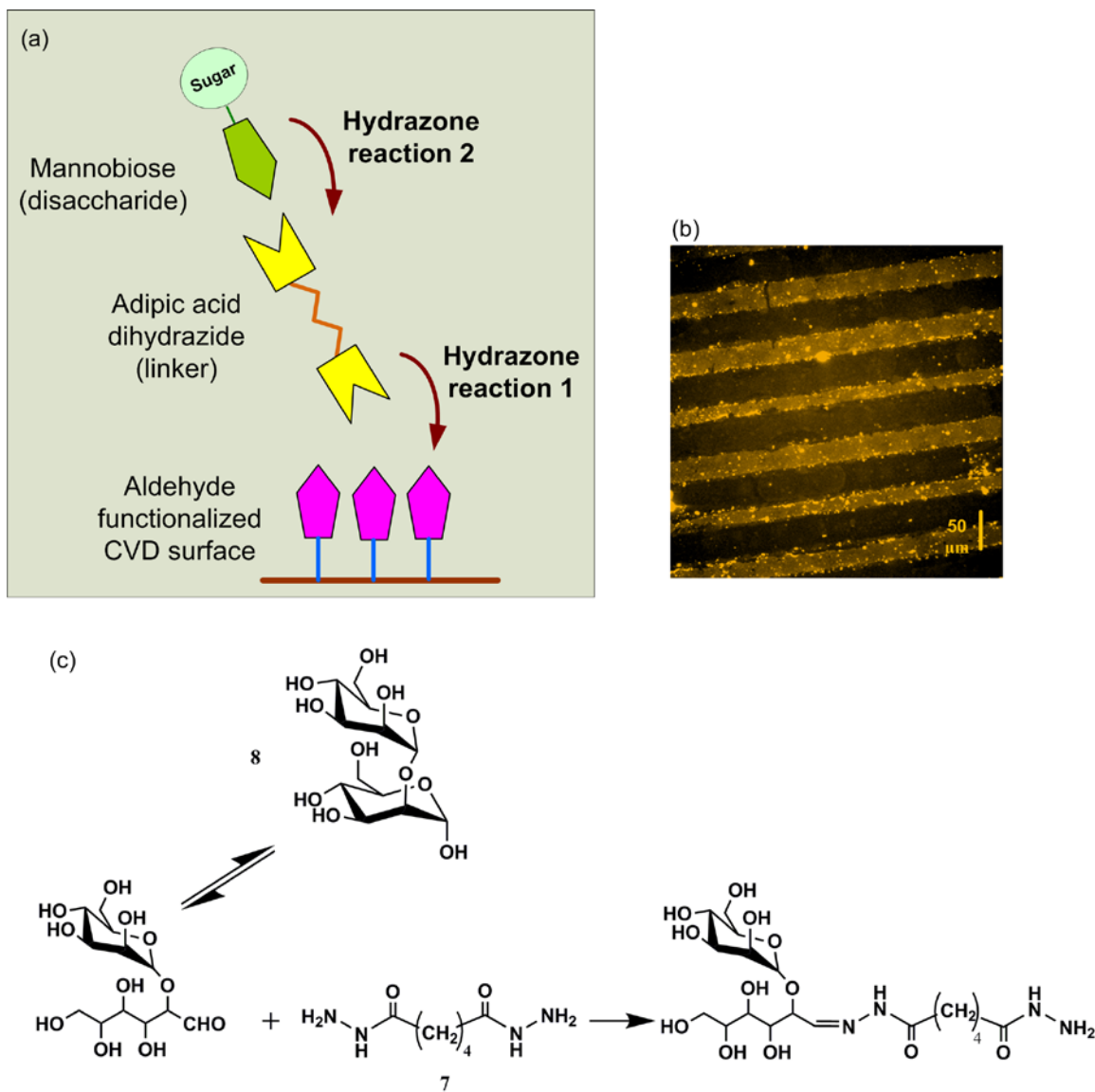
Figure 2.11: (a) Schematic depiction of the immobilization of oligosaccharides on polymer **2**; (b) corresponding fluorescence micrograph of the surface with rhodamine-labeled concanavalin-A (**9**) bound to **8** which is covalently linked to surfaces patterned with adipic acid dihydrazide linker **7**; line-profile with line widths of 20 mm (C-D, G-H) and 15 mm(A-B, E-F); (c) reaction between hydrazide containing linker **7** and disaccharide **8**.
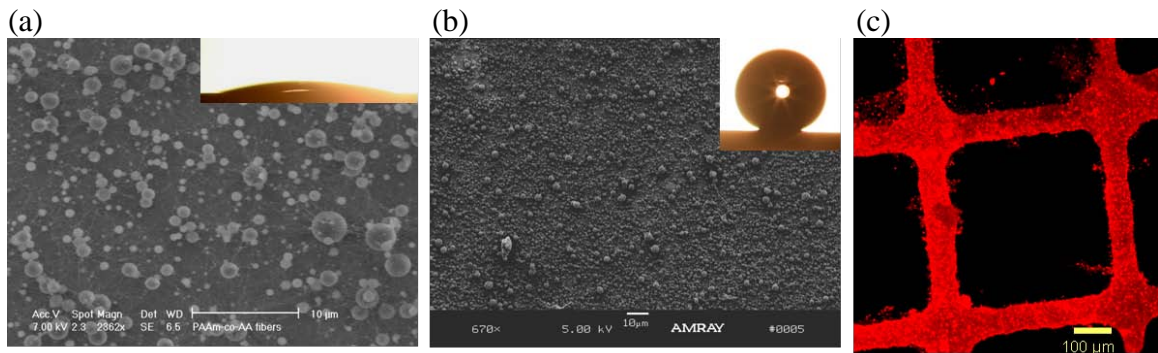
Figure 2.12: Scanning electron micrographs of the surface (a) before CVD coating (b) after CVD coating of polymer **4**. Insets show the corresponding water contact angles. (c) Confocal image showing binding of fluorescently-labeled streptavidin to biotinylated, micropatterned surfaces.
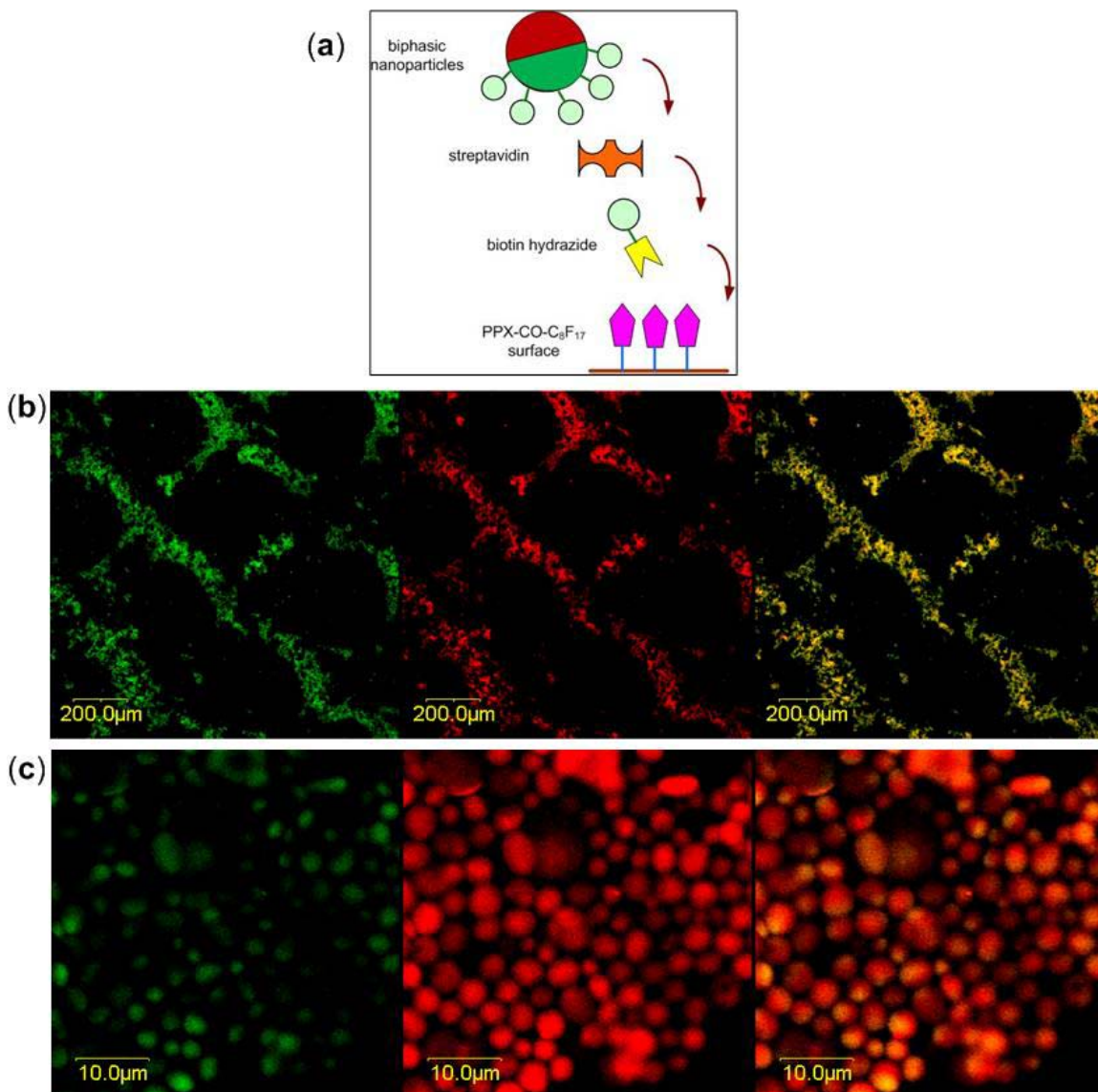
Figure 2.13: (a) Self-assembly of biotinylated biphasic microparticles on streptavidin-patterned polymer **4**. Biotinylated compartment contained green fluorescent dye and the other non-biotinylated compartment contained the green dye. (b) Confocal micrographs showing particles self-assembled onto micropatterned surfaces. (c) High resolution confocal images showing an enhanced red signal indicating the specific orientation of the biphasic microparticles.

Table 2.1: Chemical composition of polymer **2** determined using XPS

	$\underline{C}$-C	$\underline{C}$-C=O	$\underline{C}$=O	π-π*
BE (eV)	285.19	286.78	287.86	291.15
Position (in Figure 2.2)	1	2	3	4
Calculated (%)	88.2	5.9	5.9	-
Experimental (%)	87.7	4.4	5.0	2.9

Table 2.2: High resolution C1s XPS data for polymer **4**.

	Polymer **4**		
	BE (eV)	Expt. (%)	Calc. (%)
C-C	285.3	42.6	49.63
C-Br	--	--	--
C-C=O	286.9	3.7	5.04
C=O	288.8	5.7	5.04
C-F	--	--	--
π→π*	291.1	4.1	--
CF$_2$	292	38.2	35.25
CF$_3$	294.2	5.7	5.04

2.6 References

1. Langer, R. & Tirrell, D.A. Designing materials for biology and medicine. *Nature* **428**, 487-492 (2004).
2. Fu, A.Y., Spence, C., Scherer, A., Arnold, F.H. & Quake, S.R. A microfabricated fluorescence-activated cell sorter. *Nature Biotechnology* **17**, 1109-1111 (1999).
3. Li, P.C.H. & Harrison, D.J. Transport, manipulation, and reaction of biological cells on-chip using electrokinetic effects. *Analytical Chemistry* **69**, 1564-1568 (1997).
4. Effenhauser, C.S., Bruin, G.J.M., Paulus, A. & Ehrat, M. Integrated capillary electrophoresis on flexible silicone microdevices: Analysis of DNA restriction fragments and detection of single DNA molecules on microchips. *Analytical Chemistry* **69**, 3451-3457 (1997).
5. Mao, H.B., Yang, T.L. & Cremer, P.S. Design and characterization of immobilized enzymes in microfluidic systems. *Analytical Chemistry* **74**, 379-385 (2002).
6. Chen, S.H. et al. A disposable poly(methylmethacrylate)-based microfluidic module for protein identification by nanoelectrospray ionization-tandem mass spectrometry. *Electrophoresis* **22**, 3972-3977 (2001).
7. Monahan, J., Gewirth, A.A. & Nuzzo, R.G. Indirect fluorescence detection of simple sugars via high-pH electrophoresis in poly(dimethylsiloxane) microfluidic chips. *Electrophoresis* **23**, 2347-2354 (2002).
8. Lahann, J. & Langer, R. Novel poly(p-xylylenes): Thin films with tailored chemical and optical properties. *Macromolecules* **35**, 4380-4386 (2002).
9. Lahann, J., Choi, I.S., Lee, J., Jenson, K.F. & Langer, R. A new method toward microengineered surfaces based on reactive coating. *Angewandte Chemie-International Edition* **40**, 3166-+ (2001).
10. Lahann, J. et al. Reactive polymer coatings: A platform for patterning proteins and mammalian cells onto a broad range of materials. *Langmuir* **18**, 3632-3638 (2002).
11. Schurmann, K. et al. Biologic response to polymer-coated stents: In vitro analysis and results in an iliac artery sheep model. *Radiology* **230**, 151-162 (2004).
12. Lahann, J. & Langer, R. Surface-initiated ring-opening polymerization of epsilon-caprolactone from a patterned poly(hydroxymethyl-p-xylylene). *Macromolecular Rapid Communications* **22**, 968-971 (2001).
13. Lahann, J., Klee, D. & Hocker, H. Chemical vapour deposition polymerization of substituted [2.2]paracyclophanes. *Macromolecular Rapid Communications* **19**, 441-444 (1998).
14. Lahann, J. Vapor-based polymer coatings for potential biomedical applications. *Polymer International* **55**, 1361-1370 (2006).
15. Yoshida, M., Langer, R., Lendlein, A. & Lahann, J. From advanced biomedical coatings to multi-functionalized biomaterials. *Polymer Reviews* **46**, 347-375 (2006).

16. Gering, J.P., Quaroni, L. & Chumanov, G. Immobilization of antibodies on glass surfaces through sugar residues. *Journal of Colloid and Interface Science* **252**, 50-56 (2002).

17. Christman, K.L. & Maynard, H.D. Protein micropatterns using a pH-responsive polymer and light. *Langmuir* **21**, 8389-8393 (2005).

18. Hermanson, G.T. Bioconjugate Techniques, Edn. 1st. (Academic, San Diego, CA, 1996).

19. Yeo, W.S. & Mrksich, M. Electroactive substrates that reveal aldehyde groups for bio-immobilization. *Advanced Materials* **16**, 1352-+ (2004).

20. Gong, X., Dai, L., Griesser, H.J. & Mau, A.W.H. Surface immobilization of poly(ethylene oxide): Structure and properties. *J. Polym. Sci. Pt. B-Polym. Phys.* **38**, 2323-2332 (2000).

21. Imae, T. Fluorinated polymers. *Curr. Opin. Colloid Interface Sci.* **8**, 307-314 (2003).

22. Hutchings, L.R., Narrianen, A.P., Thompson, R.L., Clarke, N. & Ansari, L. Modifying and managing the surface properties of polymers. *Polymer International* **57**, 163-170 (2008).

23. Dolbier, W.R. & Beach, W.F. Parylene-AF4: a polymer with exceptional dielectric and thermal properties. *J. Fluor. Chem.* **122**, 97-104 (2003).

24. Senkevich, J.J. & Desu, S.B. Poly(tetrafluoro-p-xylylene), a low dielectric constant chemical vapor polymerized polymer. *Applied Physics Letters* **72**, 258-260 (1998).

25. Elkasabi, Y., Yoshida, M., Nandivada, H., Chen, H.Y. & Lahann, J. Towards multipotent coatings: Chemical vapor deposition and biofunctionalization of carbonyl-substituted copolymers. *Macromolecular Rapid Communications* **29**, 855-870 (2008).

26. Elkasabi, Y., Chen, H.Y. & Lahann, J. Multipotent polymer coatings based on chemical vapor deposition copolymerization. *Advanced Materials* **18**, 1521-+ (2006).

27. Lahann, J. Reactive polymer coatings for biomimetic surface engineering. *Chemical Engineering Communications* **193**, 1457-1468 (2006).

28. Brink, M. Improved synthesis of [2.2]paracyclophane and 4-formyl-[2.2]paracyclophane. *Synthesis*, 807-808 (1975).

29. Suh, K.Y., Langer, R. & Lahann, J. A novel photoderinable reactive polymer coating and its use for microfabrication of hydrogel elements. *Advanced Materials* **16**, 1401-+ (2004).

30. Nandivada, H., Chen, H.Y. & Lahann, J. Vapor-based synthesis of poly [(4-formyl-p-xylylene)-co-(p-xylylene)] and its use for biomimetic surface modifications. *Macromolecular Rapid Communications* **26**, 1794-1799 (2005).

31. Elkasabi, Y. et al. Partially fluorinated poly-p-xylylenes synthesized by CVD polymerization. *Chem. Vapor Depos.* **15**, 142-149 (2009).

32. Moothoo, D.N. & Naismith, J.H. A general method for co-crystallization of concanavalin A with carbohydrates. *Acta Crystallogr. Sect. D-Biol. Crystallogr.* **55**, 353-355 (1999).

33. Li, X.M., Reinhoudt, D. & Crego-Calama, M. What do we need for a superhydrophobic surface? A review on the recent progress in the preparation of superhydrophobic surfaces. *Chemical Society Reviews* **36**, 1350-1368 (2007).

34. Sun, T.L., Feng, L., Gao, X.F. & Jiang, L. Bioinspired surfaces with special wettability. *Accounts of Chemical Research* **38**, 644-652 (2005).

35. Feng, X.J. & Jiang, L. Design and creation of superwetting/antiwetting surfaces. *Advanced Materials* **18**, 3063-3078 (2006).

36. Feng, L. et al. Super-hydrophobic surfaces: from natural to artificial. *Advanced Materials (Weinheim, Germany)* **14**, 1857-1860 (2002).

37. Zhang, L., Zhou, Z.L., Cheng, B., DeSimone, J.M. & Samulski, E.T. Superhydrophobic behavior of a perfluoropolyether lotus-leaf-like topography. *Langmuir* **22**, 8576-8580 (2006).

38. Roh, K.H., Martin, D.C. & Lahann, J. Biphasic Janus particles with nanoscale anisotropy. *Nature Materials* **4**, 759-763 (2005).

39. Roh, K.H., Yoshida, M. & Lahann, J. Water-stable biphasic nanocolloids with potential use as anisotropic imaging probes. *Langmuir* **23**, 5683-5688 (2007).

40. Xia, F. & Jiang, L. Bio-inspired, smart, multiscale interfacial materials. *Advanced Materials* **20**, 2842-2858 (2008).

41. Acatay, K., Simsek, E., Ow-Yang, C. & Menceloglu, Y.Z. Tunable, superhydrophobically stable polymeric surfaces by electrospinning. *Section Title: Plastics Fabrication and Uses* **43**, 5210-5213 (2004).

42. Zhang, X., Shi, F., Niu, J., Jiang, Y.G. & Wang, Z.Q. Superhydrophobic surfaces: from structural control to functional application. *Journal of Materials Chemistry* **18**, 621-633 (2008).

CHAPTER 3

SPATIOSELECTIVE IMMOBILIZATION OF BIOMOLECULES ONTO VAPOR-BASED POLYMERS VIA CLICK CHEMISTRY

The material in this chapter has been adapted with minor modifications from the following published articles:

H. Nandivada, H.-Y. Chen, L. Bondarenko, J. Lahann, Reactive polymer coatings that "click", Angewandte Chemie International Edition (2006) 45, 20, 3360-3363.

H. Nandivada, X. Jiang, J. Lahann, Click chemistry: versatility and control in the hands of materials scientists, Advanced Materials (2007) 19, 2197-2208.

H. Nandivada, J. Lahann, Copper-catalyzed "click" chemistry for surface engineering; Chapter 12 in "Click Chemistry for Biotechnology and Materials Science"; J. Lahann, Ed.; Wiley NY (in press).

Abstract

Fabrication of biomimetic interfaces through covalent immobilization of biomolecules is a key challenge faced by materials scientists today. In this respect, copper-catalyzed alkyne-azide "click" chemistry has proved to be an invaluable tool, due to benign reaction conditions and functional group tolerance. Numerous strategies have been employed to incorporate the alkyne and azide functionalities onto the surface. Chemical vapor deposition polymerization is an attractive option which has been used to fabricate a wide range of chemical signatures for further surface modifications.

In this chapter, the use of copper-catalyzed "click" chemistry is discussed in the context of surface engineering. The synthesis and characterization of a vapor-based alkyne-functionalized polymer coating, poly(4-ethynyl-*p*-xylylene-co-*p*-xylylene) is described. Use of alkyne-functionalized polymer coating for spatially-controlled conjugation of azide-derivatized biomolecules such as biotin, saccharides and cell-adhesive peptides via "click" reaction is demonstrated. Furthermore, a surface capable of spatially directing endothelial cell attachment was fabricated using micropatterned peptide surfaces utilizing the "click" surface chemistry.

3.1 Introduction

Surface modification or functionalization via covalent coupling is one of the many strategies being explored by materials scientists. Surface functionalization reaction involves a solid surface interacting with the reactant in liquid or vapor phase and may involve complicated steric and kinetic effects. At the same time, most of the coupling reactions available for surface chemistry are limited by incomplete conversions, non-specificity, harsh reaction conditions and side reactions. In this respect, copper-catalyzed Huisgen's 1,3-dipolar cycloaddition between terminal alkyne and azide groups has proven to be an excellent choice due to its superior properties such as mild reaction conditions, high conversions, selectivity and reproducibility (Figure 3.1).[1-6] This reaction is compatible with a wide range of functional groups except for groups which disrupt the catalytic activity of copper.[7] The alkyne-azide "click" reaction demonstrates high reactivity in heterogeneous reaction systems, so it is useful for surface reactions. This also implies that solvent and catalyst system utilized during "click" reaction is quite important.[8]

"Click" active vapor-based polymers

Surface reaction on thin polymer films requires robust attachment of polymer films to the substrate and availability of reactive anchor groups for surface reactions. Chemical vapor deposition (CVD) polymerization has been used to fabricate functionalized coatings with good adhesion towards a wide variety of substrates.[9] This vapor-based process provides a solvent-free environment, good film adhesion and generates conformal coatings. The CVD process has been extended to create alkyne-derivatized polymer coatings. Im et al. synthesized an alkyne-functionalized polymer coating using an initiated-CVD (iCVD) process.[10] Using a single step approach, a commercially-available monomer, propargyl methacrylate, was polymerized to form poly(propargyl methacrylate). This polymer was also patterned using e-beam lithography to form nanometer patterns and the reactivity of the polymer was demonstrated by "click" reaction with azide-functionalized biotin.

Spatially-controlled "click" chemistry

The versatile "click" reaction is also compatible with microcontact printing which is a soft-lithographic process frequently employed to create micro or nanoscale patterns by depositing molecules on surfaces using a patterned stamp. More recently, Huisgen's click chemistry by microcontact printing was demonstrated on azide-functionalized SAMs.[11] Reinhoudt and coworkers first treated bromo-terminated SAMs with NaN$_3$ creating an azide-terminated monolayer. Then octadecyne was printed onto the monolayer using a PDMS stamp. The azide-functionalized surface was also reacted with fluorescently-labeled alkynes. This microcontact printing approach was conducted in the absence of the copper catalyst, because high local concentration of reagents in the vicinity of the stamp and the monolayer were believed to be sufficient for the completion

of the reaction. The authors suggest that one of the advantages of this strategy is the elimination of the copper catalysts, because copper in higher concentrations is typically considered cytotoxic and separation of the catalyst after click reaction can be cumbersome. This catalyst-free microcontact printing technique was further extended to pattern alkyne-containing oligonucleotides onto azide-modified glass slides.[12, 13] To create surface patterns, a layer of positively-charged dendrimers was first inked onto the PDMS stamp which promoted the binding of single-stranded DNA (ss-DNA) "ink" to the stamp surface. This stamp was then brought into contact with the azido-substrate without the presence of the catalyst and "click" reaction was initiated. Furthermore, covalently immobilized oligonucleotides were hybridized with their complementary strands. Alternatively, the strain-induced 1,3-dipolar cycloaddition of cyclic alkynes with azides has been recognized as a possibility to eliminate the copper catalyst and to potentially develop more biologically benign materials.[14]

"Click" chemistry for bioimmobilization

Immobilization of biomolecules on surfaces is of tremendous interest for a wide variety of applications such as biosensors, microarrays, bioactive implant surfaces and tissue engineering. Preservation of the biomolecular activity after the reaction is a key attribute for a successful bioconjugation reaction. This typically requires mild reaction conditions and absence of cross-reactivity between the functional groups present. By definition, "click" chemistry represents a collection of reactions with mild operating conditions, high yields and non-reactivity towards other functional groups. Due to their tolerance to a wide range of unprotected chemical groups, click reactions have been widely used to immobilize sugars, proteins, DNA, and even cells. Therefore, in this respect, alkyne-azide "click" reaction is attracting a lot of attention from materials and

surface scientists for bioconjugation, specifically due to the inactivity of alkyne and azide groups towards other functional groups present in biomolecules. Conjugation of molecules like carbohydrates, oligonucleotide probes, proteins and peptide sequences has been successfully demonstrated using "click" reaction on surfaces and will be discussed in further detail.

Several reports have described the immobilization of biotin on flat surfaces via "click" chemistry and have applied this chemistry to the highly specific albeit non-covalent biotin-streptavidin binding.[15, 16] For example, Lee *et al.* used "click" chemistry to functionalize polymeric nanobrushes with azide end-groups.[16] Ethylene glycol based polymer films were synthesized using surface-initiated ATRP onto initiator-containing SAMs. Subsequently the bromide-presenting polymer was reacted with sodium azide to introduce azide groups on the surface, which were then reacted with alkyne-containing biotin. This ethylene glycol based polymer film demonstrated non-biofouling characteristics combined with specific reactivity towards alkyne-functionalized ligands.

Glycan arrays provide an opportunity to study the complex protein-sugar interactions and enhance our understanding of the role of glycans present on cell surfaces.[17] Microarrays also allow the screening of multiple ligands simultaneously with minimal use of material. Copper-catalyzed "click" chemistry presents a robust strategy to covalently link saccharide molecules to a flat surface, thus mimicking the cell surface expressing these glycans.[18] Sugar-modified SAMs or glyco-SAMs have been used as glycan arrays because they provide better control over the density and orientation of the saccharide molecules and can be characterized after immobilization via surface analysis techniques. For example, Zhang *et al.* employed alkyne-azide "click" reactions to immobilize azide-functionalized sugars (mannose, lactose, α-galactose) on to alkyne-containing SAMs.[19] This method is much simpler than the direct assembly of pre-synthesized thiol-terminated sugar molecules, which require complex synthesis procedures. The unique platform displaying sugar-functionalized SAMs was further used

to study binding interactions between sugars and lectins by employing electrochemical characterization and surface plasmon resonance spectroscopy. This approach represents a label-free technique to elucidate real-time structure-activity information. Similarly, Kleinart et al. extended this study by synthesizing a series of functionalized thiol molecules and comparing the assembly of pre-formed glyco molecules with the previously described "click on SAM" approach.[20] Miura et al. studied the interactions between pathogenic protein Alzheimer amyloid-β (Aβ) and monosaccharide displaying silane-based monolayers which were created using Huisgen's 1,3-cycloaddition.[21] This study enabled the estimation of the core saccharide interacting structure of the Aβ protein.

"Click" conjugation has also been used to reversibly capture azide-modified saccharides on an alkyne-functionalized microtiter plate.[22, 23] A disulfide bridge was included in the linker to enable the cleavage and release of the captured oligosaccharide molecule for further characterization utilizing a reductive treatment with a thiol (dithiothreitol, DTT). Using this technique, a breast cancer antigen, Globo-H, was captured and analyzed after cleavage; thus demonstrating the utility of this method for biosensor applications.[23]

Copper-catalyzed Huisgen's 1,3-dipolar cycloaddition has also been used in conjunction with another reaction from the "click" family, namely the Diels-Alder reaction, for the immobilization of carbohydrates on solid surfaces.[15] Sun et al. synthesized a short heterobifunctional PEG linker with alkyne and cyclodiene terminal groups on either side. This linker was conjugated to maleimidocaproyl-functionalized substrates via Diels Alder reaction leaving the alkyne-terminal end for subsequent alkyne-azide "click" reaction with azide-functionalized ligands. This "dual-click" approach was used for the successful immobilization of biomolecules such as biotin, lactose and r-thrombomodulin. Success of the immobilization step was further confirmed using antibody-binding via surface plasmon resonance (SPR) spectroscopy.

Immobilization of saccharide molecules has also been achieved via microcontact printing of alkyne-functionalized carbohydrates onto azido SAMs.[12] Michel and Ravoo microcontact printed carbohydrate (mannose, glucose, galactose, and maltose) conjugates with alkyne functionality and used corresponding lectins to probe the sugars. Arrays provide important information regarding structure-function relationships, which may ultimately lead to better understanding of the immune responses.

Protein microarrays can be used to study protein-protein and protein-ligand interactions. Immobilized proteins are more robust than non-covalently bound proteins and also an enhanced sensitivity has been achieved.[24] However it is challenging to maintain the activity and conformation of the proteins during immobilization reactions. Some research groups have demonstrated the immobilization of proteins using copper-catalyzed "click" chemistry.[25, 26] Azide- or alkyne- modified proteins were covalently bound to alkynated or azidated glass slides via click chemistry.[26] Interestingly, it was observed that immobilization of the alkyne-functionalized protein on to an azide-presenting surface was more efficient than the other way around. This may indicate that alkyne groups were coupling with the copper ions during the reaction, thereby reducing the catalytic effects.

A fascinating approach for the fabrication of a density gradient of cell-adhesion peptides by "clicking" RGD azide-peptides onto an alkyne-gradient substrate has been reported by Gallant *et al*.[27] Briefly, variable UV-oxidation followed by a bifunctional linker was used to synthesize an alkyne-functionalized gradient. Subsequent reaction with a RGD azide-modified peptide resulted in a gradient of peptides, which was able to modulate smooth muscle cell attachment. The density of the immobilized moiety depends on the density of the functional group and the efficiency of the coupling chemistry.

This chapter focuses on the applicability of CVD polymerization for synthesizing alkyne-containing polymer coatings and subsequent spatially-directed Huisgen 1,3-dipolar cycloaddition on reactive polymer coating. This chapter also highlights the

53

utilization of "click" reaction for surface reactions with a specific focus on conjugation of biological ligands such as saccharides, proteins and cell-adhesion peptide sequences.

3.2 Methods

CVD polymerization and surface characterization

Precursors, di-ethynyl[2,2]paracyclophane (**2**) and 4-ethynyl[2,2]paracyclophane (**3**) were synthesized as previously described.[30] Di-ethynyl[2,2]paracyclophane (**2**) (50 mg) was sublimed at 90-110 ^{o}C and carried into the pyrolysis chamber by argon at a flow rate of 20 sccm. A pressure of 0.5 mbar was used. Depending on the pyrolysis temperature, the resulting polymer was different. Polymer **4** was deposited on the substrate at 15 ^{o}C.

4-ethynyl[2,2]paracyclophane (**3**) (50 mg) was sublimed at 90-110 ^{o}C and a reduced pressure of 0.5 mbar. Argon, at a flow rate of 20 sccm, was used as the carrier gas, which carried the precursors into the pyrolysis chamber at a temperature of 680 ^{o}C. Polymer poly(4-ethynyl-*p*-xylylene-co-*p*-xylylene) (**5**) was deposited on the substrate at 15 ^{o}C kept in the deposition chamber.

Fourier transform infrared spectroscopy (FTIR) was performed on a Nicolet 6700 spectrometer. X-ray photoelectron spectroscopy (XPS) was conducted using an Axis Ultra X-ray photoelectron spectrometer (Kratos Analyticals, UK) equipped with a monochromatized Al K_{α} X-ray source.

Polymer **4**: Case 1: Pyrolysis temperature of 650 ^{o}C. FTIR (grazing angle of 85°): ν (cm^{-1}) = 837, 1039, 1150, 1439, 1505, 1624, 1694, 1910, 2916, 3010, 3048. XPS (referenced to hydrocarbon at 285.0 eV): C (96.9%), O (3.1%); Case 2: Pyrolysis temperature of 550 ^{o}C. FTIR (grazing angle of 85°): ν (cm^{-1}) = 839.35, 877, 922, 1036,

1261, 1439, 1623, 1913, 2100, 2848, 2921, 3013, 3052, 3285. XPS (referenced to hydrocarbon at 285.0 eV): C (93.7%); O (6.3%).

Polymer **5**: FTIR (grazing angle of 85°): ν (cm^{-1}) = 833, 894, 1158, 1251, 1411, 1454, 1493, 1513, 1605, 1699, 1900, 2102, 2859, 2926, 3015, 3286. XPS (referenced to hydrocarbon at 285.0 eV): C (98.7%), O (1.3%); XPS signals: 285.6 eV (C1s); 291.7 eV (π-π*).

Height analysis data were recorded using an EP^3-SW imaging ellipsometer (Nanofilm AG, Germany) at a wavelength of 532 nm. Both, nulling (four zones) and mapping experiments were performed at an angle of incidence of 65°. Anisotropic Cauchy parameterization model was used for curve fitting. For the mapping mode, data was recorded by an imaging scanner with a lateral resolution of 1 μm with a field of view of about 100 μm x 500 μm.

Spatially-directed surface modification

Microcontact printing of biotinylated ligand (**6**) on polymer **5**: Patterned PDMS stamps were created as previously described.[28, 29] A thin layer of solution of ligand (**6**) (Photoprobe biotin, Vector labs, 10 μg/ml) and sodium ascorbate (1 mM) in a 2:1 mixture of water and tert-butyl alcohol was spread on **5** and the solvent was dried using N$_2$. The patterned PDMS stamp was oxidized for 20 min using UV-ozone cleaner (Jelight Co. Inc, Irvine, CA) and inked with CuSO$_4$ solution (1 mM in methanol) using a cotton swab. The stamp was then kept in contact with the polymer substrate for 12-18 h. After stamp removal, the patterned substrate was incubated with rhodamine-labeled streptavidin (50 μg/ml in aqueous phosphate buffer PBS containing 0.02% (v/v) Tween 20 and 0.1% (w/v) bovine serum albumin) for 1 h. Substrate was then repeatedly washed with the

incubating buffer, PBS and finally rinsed with DI-water. Fluorescence micrographs were captured using a Nikon TE200 fluorescence microscope.

A similar procedure was used for the immobilization of azido-saccharides1-azido-1-deoxy-β-D-glucopyranoside (**7**) and 1-azido-1-deoxy-β-D-galactopyranoside (**8**).

As described above, azido-peptide (**9**) (YIGSR-N$_3$ 20 µg/ml) was immobilized via microcontact printing. In this instance, the patterned stamp was kept in contact with the substrate for 3 h. After peptide patterning, this microcontact printing approach was repeated with an unpatterned flat PDMS stamp to immobilize PEG-N$_3$ (MW=5000, 50 µg/ml) on the remaining areas. Substrates were washed repeatedly with aqueous phosphate buffer PBS containing 0.02% (v/v) Tween 20, PBS and finally rinsed with DI-water.

Human endothelial cell culture

Cryopreserved human umbilical vein endothelial cells (HUVECs) were purchased from Lonza (Walkersville, MD) and cultured in complete Endothelial Growth Medium (EGM, Lonza) containing 2% fetal bovine serum. Cells were cultured in 75 cm^2 tissue culture-treated polystyrene flasks (Corning), maintained at 37 ^{o}C in a humidified atmosphere of 5% CO$_2$ and cell culture medium was replaced every other day until 80% confluency was attained. Cells were harvested from the flasks using 0.25% trypsin/ethylene-diaminetetraacetic acid solution (Sigma) and seeded on the substrates as needed.

For the cell patterning studies, peptide-patterned surfaces were rinsed with Dulbelcco's PBS (D-PBS) and placed in a multiwell plate. Cells were harvested from the flask and resuspended at a density of 1×10^4 cells/ml in Endothelial Basal Medium (EBM; Lonza) without serum and 1 ml was added to each well. They were allowed to adhere for

1 h without serum at 37 °C. Subsequently, this media was replaced with medium containing serum (EGM) and cells were maintained for 10 h. Substrates were washed with D-PBS, fixed with formaldehyde (4% v/v in D-PBS), permeabilized with TritonX-100 (0.1% v/v in D-PBS) and stained with rhodamine-conjugated phalloidin (Invitrogen). Samples were mounted with Prolong Gold containing DAPI (Invitrogen). Substrates were imaged using Olympus BX-51 fluorescence microscope (Microscopy and Image Analysis Laboratory, University of Michigan, Ann Arbor).

3.3 Results and discussion

CVD polymerization and surface characterization

Prior to polymer deposition using CVD polymerization, the starting materials di-ethynyl[2,2]paracyclophane (**2**) and ethynyl[2,2]paracyclophane (**3**) were prepared from the commercially available [2.2]paracyclophane (**1**), which was first converted to the respective di- and mono-formyl derivatives followed by Bestmann's acetylene synthesis.[30] Under the conditions of di-alkyne synthesis, pseudo-ortho and pseudo-meta derivatives have been reported as the major isomers,[30] but were not separated for subsequent CVD polymerization.

First, CVD polymerization of di-alkyne **2** was performed to yield poly(diethynyl-*p*-xylylene) (**4**) (Figure 3.2). For this purpose, **2** was sublimed at 90-110°C and a reduced pressure of 0.5 mbar. Reactants were then transported into pyrolysis chamber (at 650 °C) and then into deposition chamber (at 15 °C) where spontaneous formation of a polymer film was observed. However, FTIR spectrum of polymer films formed under these conditions did not show alkyne C-H stretch around 3200 cm^{-1}, indicating the absence of alkyne groups. Instead, several side products were formed, which were not further

characterized, but could potentially be due to an alkyne-vinylidine rearrangement.[31] Alteration of process conditions, (e.g., pyrolysis temperatures below 550 $^{\circ}$C), resulted in alkyne-functionalized polymers, with typical ellipsometric thicknesses of about 50 nm (for 50 mg of the precursor polymerized onto a 4 inch wafer). Nevertheless, these polymer films showed little reactivity, underwent thermal decomposition, and generally had quite poor stability towards organic solvents. Thus, they were not pursued further.

Unlike polymer **4**, CVD polymerization of mono-alkyne **3** produced poly(4-ethynyl-*p*-xylylene-co-*p*-xylylene) (**5**) without appreciable side reactions, even under typical CVD conditions (pressure of 0.5 mbar, sublimation, pyrolysis and substrate temperatures of 90-110 $^{\circ}$C, 680 $^{\circ}$C and 15 $^{\circ}$C, respectively) (Figure 3.2).[32] Moreover, FTIR spectrum of **5** revealed a strong alkyne C-H stretch at 3286 cm^{-1} and signal at 2100 cm^{-1} which can be attributed to C-C triple bond. Evidence from FTIR data was reaffirmed by X-ray photoelectron spectroscopy (XPS), which was used to quantify the surface elemental composition of **5**. Polymer **5** consists of about 98.7% carbon and 1.3 % oxygen. These traces of oxygen may be due to contaminations during CVD polymerization or subsequent sample handling. These data compared well with the theoretical composition of **5** (100 % carbon, hydrogen is not detected with XPS). Moreover, high resolution C1s spectrum of **5** further revealed a symmetric and narrow peak centered at 285.6 eV with a full width at half maximum (FWHM) of 1.13 eV. This can be associated with the presence of a single type of carbon, i.e. carbon that is bound to carbon or hydrogen.[33] The C1s peak spectrum further showed a smaller signal centered at 291.7 eV, which can be attributed to π-π* shake-up signal characteristic of aromatic π electrons and has been observed for similar polymer systems in the past.[34] Polymer **5** was found to have an thickness of 91.81±0.03 nm (for 50 mg of precursor) and was stable in aqueous solutions and organic solvents such as acetone, ethanol, methanol and chloroform. Probing the adhesiveness of **5** using the scotch tape test[35] showed that the film had good adhesion to a wide variety of substrates such as glass,

poly(dimethylsiloxane) (PDMS), silicon and gold. Moreover, the polymer showed a characteristic excitation peak at 380 nm and a characteristic emission peak at 450 nm. These peaks disappeared after heating the polymer to 150 °C for 3 h, presumably due to cross-linking of the polymer. To assess the thermal stability of polymer **5**, FTIR spectra of samples stored at 20 °C, 80 °C, 150 °C, and 250 °C were compared. The C-H stretch at 3283 cm^{-1} continuously decreased with increasing temperature and was absent in samples stored at 250 °C. Again, this suggests that the polymer has limited thermal stability, most likely due to crosslinking of the ethynyl groups.

Immobilization of azide-functionalized biotin

To assess whether reactive coating **5** can be used for heterogeneous click reactions, its reactivity against azides was studied. Specifically, Huisgen's 1,3-dipolar cycloaddition between **5** and an azide-containing biotin-based ligand (**6**) in the presence of copper(II) sulfate and sodium ascorbate was examined (Figure 3.3). As described for solvent-based systems, this irreversible fusion reaction occured in the presence of a copper(I) catalyst yielding five-membered heterocyclic triazoles.[4] Sodium ascorbate acts as a reductant, generating Cu(I) ions in situ from $CuSO_4$, which then function as the active catalyst of the cycloaddition.[4] Compound **6** was chosen as the representative ligand in this study, because biotin undergoes a strong non-covalent interaction with streptavidin, which in turn has been widely used for binding of a wide range of biotinylated biomolecules.[36]

To ensure spatial control during the cycloaddition reaction, a microcontact printing (µCP) approach was chosen. For this approach to be successful, the Cu(I) catalyst and azide reactant **6** had to be decoupled. This was achieved by microcontact printing only the Cu(I) catalyst onto a preadsorbed film of ligand **6**. In this two-step

process illustrated in Figure 3.4, a thin layer of **6** and sodium ascorbate was spread onto **5** and solvent was dried using N_2. Next, a patterned PDMS stamp was inked with a solution of $CuSO_4$ and kept in contact with the substrate for 12-18 h. Patterned substrate was incubated with an aqueous solution of rhodamine-labeled streptavidin. Fluorescence microscopy was used to assess the spatially-directed immobilization of **6** onto polymer **5**. Fluorescence micrographs shown in Figures 3.5a and 3.5c confirmed selective protein coupling in the regions where $CuSO_4$ solution was microcontact printed, thus proving the binding of **6** to polymer **5**. This supports the conclusion that alkyne groups on the polymer surface are reactive and can be effectively used as anchoring sites for surface modifications. The two-step approach (pre-adsorption + microcontact printing of catalyst) was found to be superior to concurrent microcontact printing of catalyst and azide. Furthermore, importance of catalytic activity of Cu(I) for heterogeneous click reaction was revealed. Regions without Cu(I) catalyst did not show fluorescence due to a lack of azide binding in the absence of the catalyst. To complement the fluorescence study, patterned surfaces were further analyzed by imaging ellipsometry in the mapping mode. Corresponding ellipsometric images shown in Figures 3.5b and 3.5d reveal protein patterns, together with the corresponding fluorescence patterns. Observed thickness differences of about 1-2 nm between biotinylated regions with streptavidin and non-biotinylated polymer regions are comparable with literature-reported thicknesses of protein monolayers.[37]

Immobilization of saccharides

To extend the applicability of alkyne-functionalized polymer **2** towards a robust platform for biomolecular immobilization, azide-functionalized saccharides were covalently coupled to polymer **5** (Figure 3.6). The procedure described above for

immobilization of ligand **6** was extended for the conjugation of azide-functionalized saccharides to alkyne-functionalized CVD polymer **5**. For this purpose, two azide-functionalized saccharides, 1-Azido-1-deoxy-β-D-glucopyranoside (**7**) and 1-Azido-1-deoxy-β-D-galactopyranoside (**8**) were immobilized on polymer **5** via microcontact printing. Briefly, a micro-structured elastomeric stamp was inked with copper catalyst and brought into contact with the polymer **5** which had a preadsorbed layer of the desired azido-saccharide solution.[38] Click reaction between azide-derivatized saccharides and alkyne groups on polymer **5** occurred only in regions where the stamp and substrate were in conformal contact. Subsequently, saccharide-binding was affirmed by incubating the micro-patterned substrates with the corresponding fluorescently-labeled lectins and analyzed using fluorescence microscopy. Azido-sugar **7** was probed with a glucose-binding lectin, fluorescein-conjugated concanavalin A (FITC-Con A) and rhodamine-labeled peanut agglutinin (TRITC-PNA), specific for β-galactose moieties, was used for compound **8**. Patterned substrates were visualized using fluorescence microscopy. Fluorescence micrographs reveal specific binding of FITC-ConA and TRITC-PNA to micro-patterns of **7** (Figure 3.7a) and **8** (Figure 3.7b), respectively, thus confirming the reactivity of alkyne-functionalized surface towards azide-functionalized saccharides.

Immobilization of cell-adhesion peptides and cell patterning

Ability to modulate cellular response by varying the surface properties is a key aspect of surface engineering.[39, 40] This can be achieved by immobilizing cell-adhesive proteins (mainly extracellular matrix proteins) or peptide sequences derived from these proteins.[40] Immobilizing of bioactive peptides triggers cellular responses such as adhesion, migration and cellular differentiation. Short peptide sequences typically convey the same bioactivity as the original protein while avoiding non-specific interactions.

These peptides also display an enhanced stability and can be used under conditions unsuitable for most biomolecules.

Moreover, laminin-derived peptide sequences have been shown to support adhesion of primary cells and also human embryonic stem cells.[41] Peptide sequence, YIGSR, present on β-chain of laminin molecule was chosen as the model peptide. Azide-functionalized YIGSR (**9**) was micropatterned on polymer **5** using microcontact printing (Figure 3.6). Inspection of the surface using imaging ellipsometry showed patterns with a height difference between the patterned and unpatterned areas of 0.1 nm (Figure 3.8a). Further the unpatterned regions of the surface were backfilled with PEG-azide to prevent non-specific binding effects.

Finally, to demonstrate activity of the immobilized peptide moieties towards mammalian cells, peptide **9** patterned substrates were tested with human endothelial cells (HUVECs) which represent a well-characterized cell culture system. Human endothelial cells were first cultured on peptide **9** patterned surfaces in serum-free conditions for 1 h. This enabled specific binding of endothelial cells to the surface via cell-adhesive peptide sequence **9** and prevented non-specific adhesion of cells due to the proteinaceous nature of serum. Serum-containing medium was then added to the culture system and human endothelial cells were allowed to grow on the peptide-patterned substrates for 10 h. After immunostaining with rhodamine-conjugated phalloidin (for actin) and DAPI (for nucleus), the surfaces were analyzed using fluorescence microscopy. It was observed that endothelial cells preferentially adhered to regions modified with azide-functionalized peptide **9** and minimal cell attachment was seen on the PEG-modified regions (Figure 3.8 b,c), hence, showing that peptide-patterned surfaces were able to direct the specific binding of endothelial cells on the surface.

3.4 Conclusions

In conclusion, alkyne-containing vapor-based polymer **5** showed remarkable reactivity towards azides via the chemoselective Huisgen's 1,3-dipolar cycloaddition. In contrast to the di-alkyne containing polymer **4**, reactive coating **5** showed excellent adhesion and stability. Alkyne-azide "click" reactions were successfully used for coupling of different azide functionalized biomolecules such as saccharides and peptides. The fact, that spatially-controlled cycloadditions can be conducted under mild reaction conditions, will enable the design of topologically differentiated biointerfaces. Key feature of this approach is the use of vapor-based coatings for spatially-controlled click-chemistry of biomolecules. Development of bioactive surfaces is an important step towards advanced biomaterials and biointerfaces. As a flexible bioconjugation platform, this regioselective immobilization strategy could be applicable in the design of biofunctional surfaces for diagnostics (e.g., microarrays), biosensors, and biomedical device coatings.
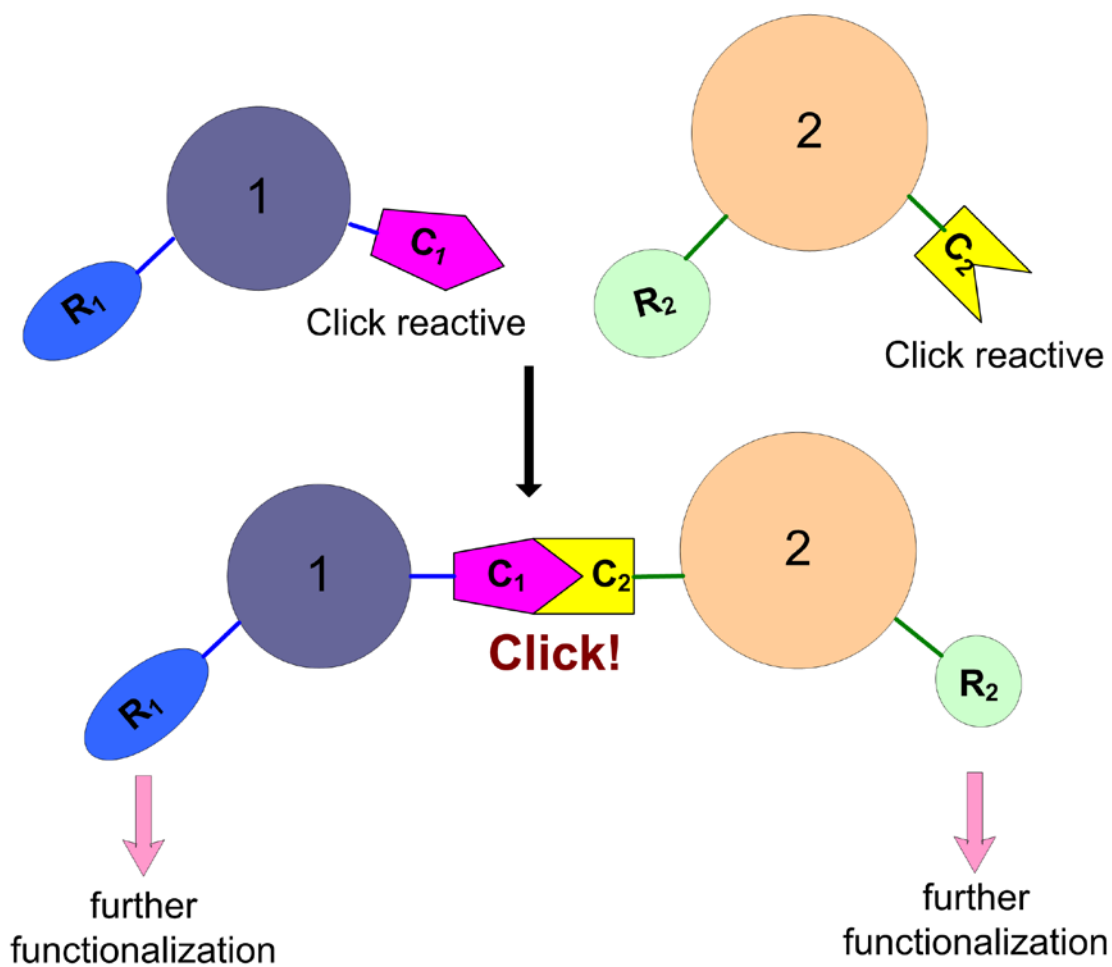
Figure 3.1: Multifunctional materials' design using "click chemistry",

2: $R^1 = C \equiv C\text{-}H$ $R^2 = C \equiv C\text{-}H$
3: $R^1 = C \equiv C\text{-}H$ $R^2 = H$

4: $R^1 = C \equiv C\text{-}H$ $R^2 = C \equiv C\text{-}H$
5: $R^1 = C \equiv C\text{-}H$ $R^2 = H$
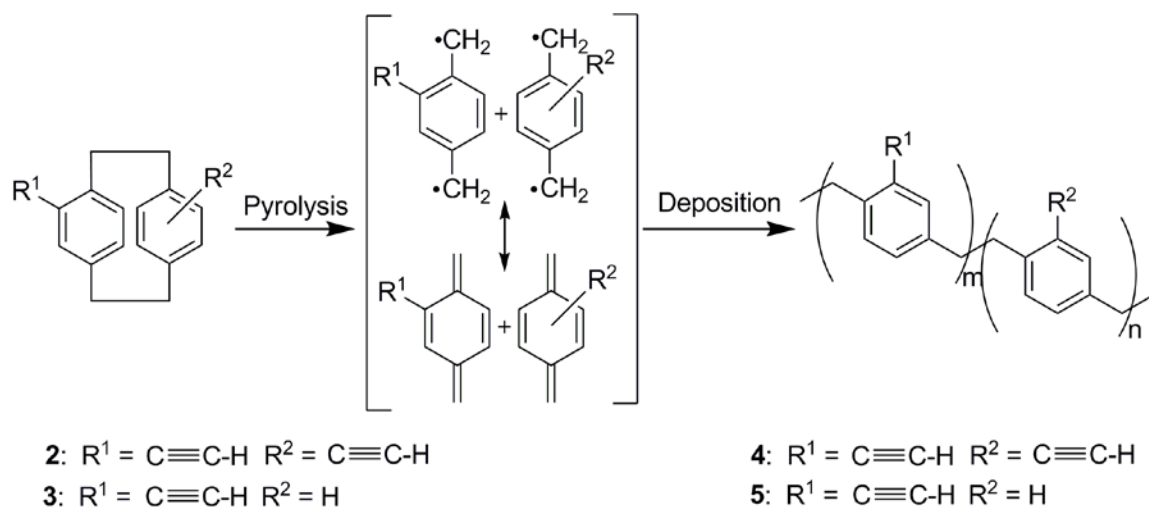
Figure 3.2: Synthesis of alkyne-containing polymers (**4**, **5**) via CVD polymerization of diethynyl-[2,2]paracyclophane (**2**) and 4-ethynyl-[2,2]paracyclophane (**3**).
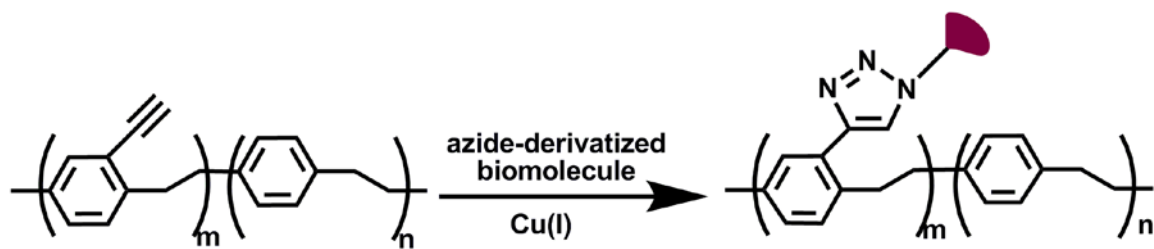
Figure 3.3: Huisgen 1,3-dipolar cycloaddition between azide-functionalized ligands (**6**, **7**, **8** and **9**) and the poly(4-ethynyl-*p*-xylylene-co-*p*-xylylene) (**5**).
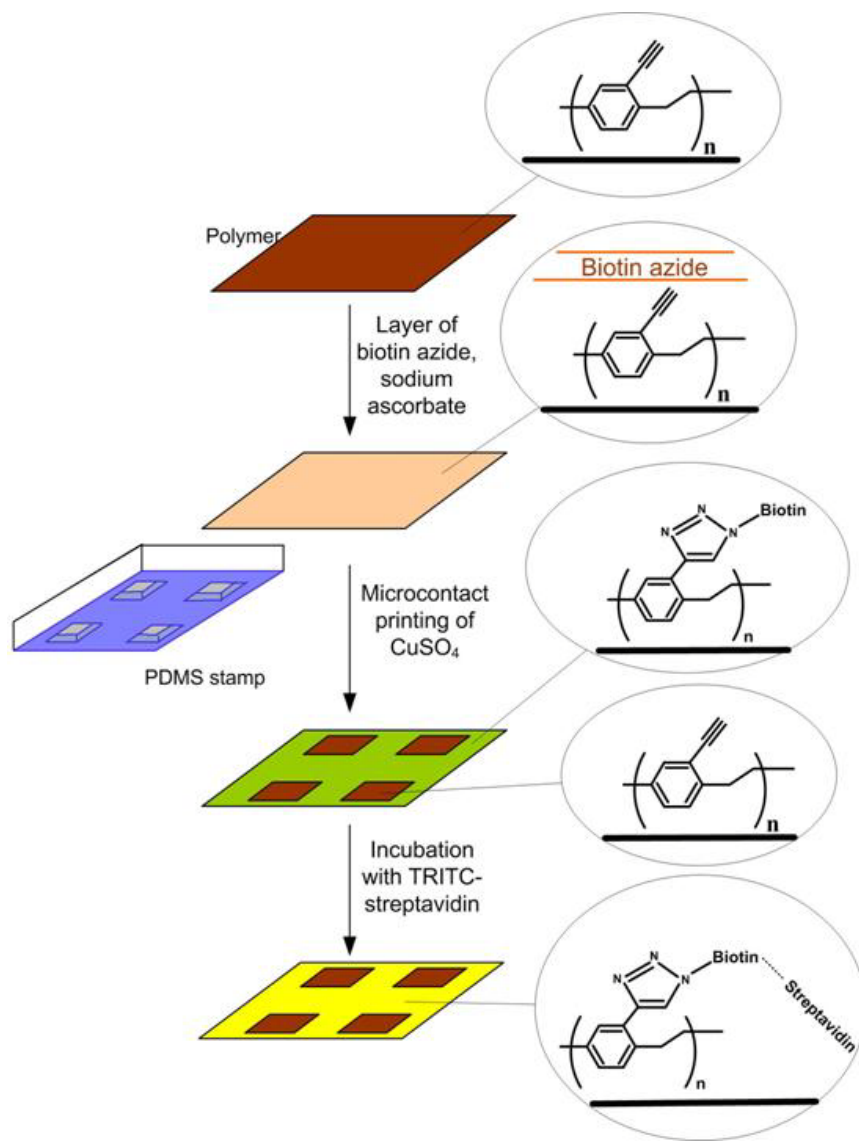
Figure 3.4: Immobilization of azide-containing ligand on the reactive polymer coating. The Cu(I) catalyst was microcontact printed on a preadsorbed layer of biotin-based azide-ligand (**6**) on the reactive polymer **5**.
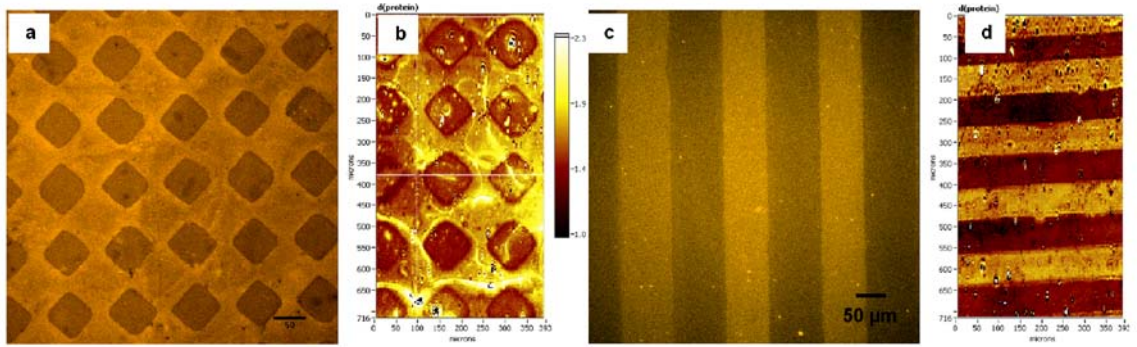
Figure 3.5: (a, c) Fluorescence micrographs showing the binding of TRITC-streptavidin to patterns of biotin azide formed by μCP, (b, d) Corresponding imaging ellipsometric images showing thickness maps of the patterned surfaces.
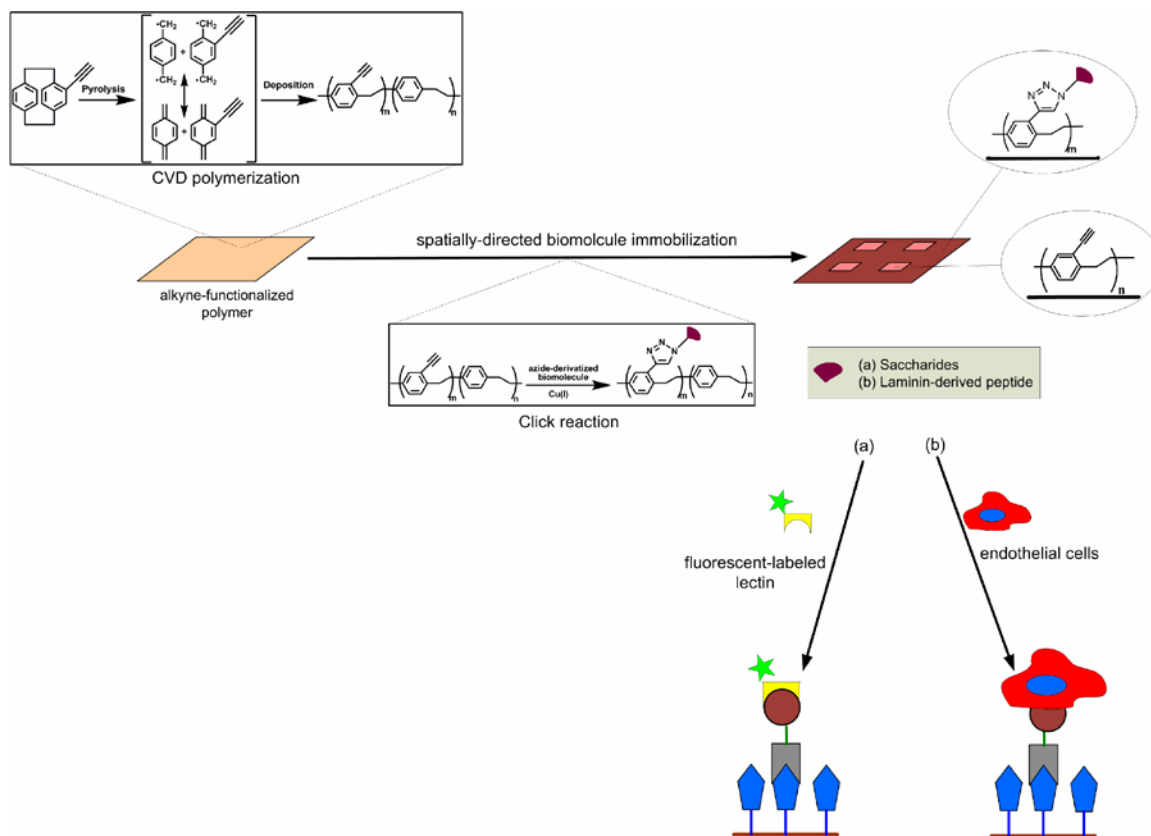
Figure 3.6. Illustration of the procedure for spatioselective clicking of biomolecules. (A) CVD polymerization. (B) Biomolecule immobilization using click reaction and microcontact printing. (C) (a) Using fluorescently-labeled lectins for saccharide patterned substrates (b) Human endothelial cell culture on peptide-patterned substrates.
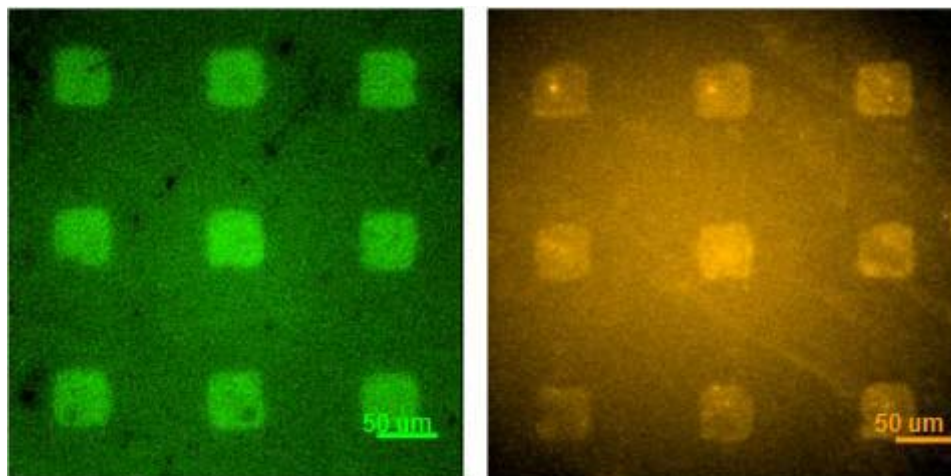
Figure 3.7: Fluorescence micrographs showing the immobilization of azide-functionalized saccharides on polymer **5** detected using fluorescently-labeled lectins: (a) FITC-ConA on sugar **7** and (b) TRITC-PNA on sugar **8**.
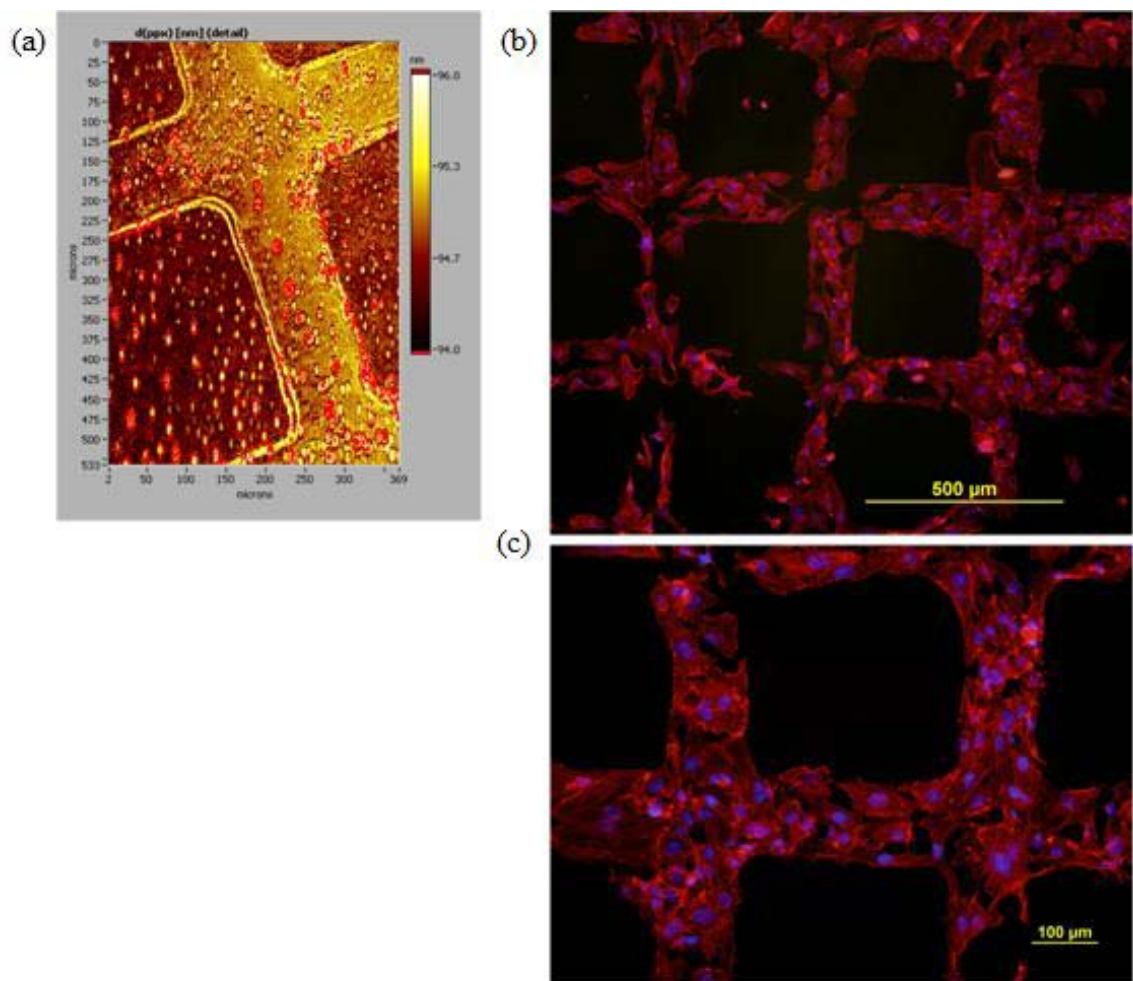
Figure 3.8: (a) Thickness map of peptide **9** patterned surface via imaging ellipsometry. (b, c) Fluorescence micrographs of endothelial cells attached to peptide **9** patterned surfaces. Red: actin cytoskeleton (rhodamine-phalloidin), blue: nucleus (DAPI).

3.6 References

1.   Kolb, H.C., Finn, M.G. & Sharpless, K.B. Click chemistry: Diverse chemical function from a few good reactions. *Angewandte Chemie, International Edition* **40**, 2004-2021 (2001).
2.   Meldal, M. Polymer "Clicking" by CuAAC reactions. *Macromol. Rapid Commun.* **29**, 1016-1051 (2008).
3.   Meldal, M. & Tornoe, C.W. Cu-catalyzed azide-alkyne cycloaddition. *Chemical Reviews* **108**, 2952-3015 (2008).
4.   Rostovtsev, V.V., Green, L.G., Fokin, V.V. & Sharpless, K.B. A stepwise Huisgen cycloaddition process: Copper(I)-catalyzed regioselective "ligation" of azides and terminal alkynes. *Angewandte Chemie-International Edition* **41**, 2596-+ (2002).
5.   Nandivada, H., Jiang, X.W. & Lahann, J. Click chemistry: Versatility and control in the hands of materials scientists. *Advanced Materials* **19**, 2197-2208 (2007).
6.   Devaraj, N.K. & Collman, J.P. Copper catalyzed azide-alkyne cycloadditions on solid surfaces: Applications and future directions. *QSAR Comb. Sci.* **26**, 1253-1260 (2007).
7.   Binder, W.H. & Sachsenhofer, R. Click chemistry in polymer and material science: An update. *Macromol. Rapid Commun.* **29**, 952-981 (2008).
8.   Binder, W.H. & Sachsenhofer, R. 'Click' chemistry in polymer and materials science. *Macromol. Rapid Commun.* **28**, 15-54 (2007).
9.   Yoshida, M., Langer, R., Lendlein, A. & Lahann, J. From advanced biomedical coatings to multi-functionalized biomaterials. *Polymer Reviews* **46**, 347-375 (2006).
10.   Im, S.G. et al. A Directly Patternable, Click-Active Polymer Film via Initiated Chemical Vapor Deposition. *Macromolecular Rapid Communications* **29**, 1648-1654 (2008).
11.   Rozkiewicz, D.I., Janczewski, D., Verboom, W., Ravoo, B.J. & Reinhoudt, D.N. \"Click\" chemistry by microcontact printing. *Angewandte Chemie, International Edition* **45**, 5292-5296 (2006).
12.   Michel, O. & Ravoo, B.J. Carbohydrate microarrays by microcontact "click" chemistry. *Langmuir* **24**, 12116-12118 (2008).
13.   Spruell, J.M. et al. Heterogeneous catalysis through microcontact printing. *Angewandte Chemie-International Edition* **47**, 9927-9932 (2008).
14.   Agard, N.J., Prescher, J.A. & Bertozzi, C.R. A strain-promoted [3+2] azide-alkyne cycloaddition for covalent modification of biomolecules in living systems. *Journal of the American Chemical Society* **126**, 15046-15047 (2004).
15.   Sun, X.L., Stabler, C.L., Cazalis, C.S. & Chaikof, E.L. Carbohydrate and protein immobilization onto solid surfaces by sequential Diels-Alder and azide-alkyne cycloadditions. *Bioconjugate Chemistry* **17**, 52-57 (2006).
16.   Lee, B.S. et al. Surface-initiated, atom transfer radical polymerization of oligo(ethylene glycol) methyl ether methacrylate and subsequent click chemistry for bioconjugation. *Biomacromolecules* **8**, 744-749 (2007).

17.   Hanson, S.R., Greenberg, W.A. & Wong, C.H. Probing glycans with the copper(I)-catalyzed [3+2] azide-alkyne cycloaddition. *QSAR Comb. Sci.* **26**, 1243-1252 (2007).

18.   Dedola, S., Nepogodiev, S.A. & Field, R.A. Recent applications of the Cu(I)-catalysed Huisgen azide-alkyne 1,3-dipolar cycloaddition reaction in carbohydrate chemistry. *Org Biomol Chem* **5**, 1006-1017 (2007).

19.   Zhang, Y. et al. Carbohydrate-protein interactions by "clicked" carbohydrate self-assembled monolayers. *Analytical Chemistry* **78**, 2001-2008 (2006).

20.   Kleinert, M., Winkler, T., Terfort, A. & Lindhorst, T.K. A modular approach for the construction and modification of glyco-SAMs utilizing 1,3-dipolar cycloaddition. *Org. Biomol. Chem.* **6**, 2118-2132 (2008).

21.   Miura, Y., Yamauchi, T., Sato, H. & Fukuda, T. The self-assembled monolayer of saccharide via click chemistry: Formation and protein recognition. *Thin Solid Films* **516**, 2443-2449 (2008).

22.   Fazio, F., Bryan, M.C., Blixt, O., Paulson, J.C. & Wong, C.-H. Synthesis of sugar arrays in microtiter plate. *Journal of the American Chemical Society* **124**, 14397-14402 (2002).

23.   Bryan, M.C. et al. Covalent display of oligosaccharide arrays in microtiter plates. *Journal of the American Chemical Society* **126**, 8640-8641 (2004).

24.   Camarero, J.A. Recent developments in the site-specific immobilization of proteins onto solid supports. *Biopolymers* **90**, 450-458 (2008).

25.   Gauchet, C., Labadie, G.R. & Poulter, C.D. Regio- and chemoselective covalent immobilization of proteins through unnatural amino acids. *Journal of the American Chemical Society* **128**, 9274-9275 (2006).

26.   Lin, P.C. et al. Site-specific protein modification through Cu-I-catalyzed 1,2,3-triazole formation and its implementation in protein microarray fabrication. *Angewandte Chemie-International Edition* **45**, 4286-4290 (2006).

27.   Gallant, N.D., Lavery, K.A., Amis, E.J. & Becker, M.L. Universal gradient substrates for "click" biofunctionalization. *Advanced Materials* **19**, 965-+ (2007).

28.   Lahann, J., Choi, I.S., Lee, J., Jenson, K.F. & Langer, R. A new method toward microengineered surfaces based on reactive coating. *Angewandte Chemie-International Edition* **40**, 3166-+ (2001).

29.   Lahann, J., Hocker, H. & Langer, R. Synthesis of amino[2.2]paracyclophanes - Beneficial monomers for bioactive coating of medical implant materials. *Angewandte Chemie-International Edition* **40**, 726-728 (2001).

30.   Bondarenko, L., Dix, I., Hinrichs, H. & Hopf, H. Cyclophanes. Part LII: Ethynyl[2.2]paracyclophanes - New building blocks for molecular scaffolding. *Synthesis*, 2751-2759 (2004).

31.   Gajewski, J.J. Hydrocarbon thermal isomerizations. (Elsevier Inc, San Diego; 2004).

32.   Lahann, J. & Langer, R. Novel poly(p-xylylenes): Thin films with tailored chemical and optical properties. *Macromolecules* **35**, 4380-4386 (2002).

33.   Polzonetti, G., Cianciusi, A.M., Furlani, A. & Russo, M.V. Photoelectron-spectroscopy study of FeCl3 doped polyphenylacetylene. *Synth. Met.* **28**, D413-D417 (1989).

34. Lahann, J. & Langer, R. Surface-initiated ring-opening polymerization of epsilon-caprolactone from a patterned poly(hydroxymethyl-p-xylylene). *Macromolecular Rapid Communications* **22**, 968-971 (2001).

35. Nandivada, H., Chen, H.Y. & Lahann, J. Vapor-based synthesis of poly [(4-formyl-p-xylylene)-co-(p-xylylene)] and its use for biomimetic surface modifications. *Macromolecular Rapid Communications* **26**, 1794-1799 (2005).

36. Lahann, J., Klee, D. & Hocker, H. Chemical vapour deposition polymerization of substituted [2.2]paracyclophanes. *Macromolecular Rapid Communications* **19**, 441-444 (1998).

37. Voros, J. The density and refractive index of adsorbing protein layers. *Biophys. J.* **87**, 553-561 (2004).

38. Nandivada, H., Chen, H.-Y., Bondarenko, L. & Lahann, J. Reactive polymer coatings that "click". *Angewandte Chemie, International Edition* **45**, 3360-3363 (2006).

39. Hammer, D.A. & Tirrell, M. Biological adhesion at interfaces. *Annu. Rev. Mater. Sci.* **26**, 651-691 (1996).

40. Garcia, A.J. in Polymers for regenerative medicine 171-190 (Springer-Verlag Berlin, Berlin; 2006).

41. Derda, R. et al. Defined substrates for human embryonic stem cell growth identified from surface arrays. *ACS Chemical Biology* **2**, 347-355 (2007).

CHAPTER 4

DEFINED SUBSTRATES FOR HUMAN EMBRYONIC STEM CELL CULTURE

The material in this chapter has been adapted with minor modifications from the following article:

L. G. Villa-Diaz*, H. Nandivada*, J. Ding, N. C. Nogueira-de-Souza, P. H. Krebsbach, K. S. O'Shea, J. Lahann, G. D Smith, Synthetic polymer coatings for long-term growth of human embryonic stem cells, (under review) [*co first authors].

Abstract

In this chapter, a synthetic polymer, poly[2-(methacryloyloxy)ethyl dimethyl-(3-sulfopropyl)ammonium hydroxide] (PMEDSAH), is identified which possesses the unique capability of supporting long-term culture of human embryonic stem cell cultures. This represents a considerable advance towards clinically-applicable cultures of human embryonic stem cell. Designing a fully-defined synthetic polymer coating that can maintain the undifferentiated state of hES cells in long-term cell culture, enables further investigation of the interrelationship between synthetic polymer matrices and hES cells.

4.1 Introduction

Human embryonic stem (hES) cells possess the unique properties of unlimited self-renewal and differentiation. hES cells are poised to play a prominent role in understanding of early development, in therapeutic applications and regenerative

75

medicine,[1, 2] which will fuel the need for culture systems that can provide clinical-grade hES cells.

Natural substrates for pluripotent stem cell culture

Owing to their sensitivity to environmental influences, undifferentiated hES cells can only be propagated for extended periods of time, when cultured on certain, naturally-derived cell substrates, such as mouse or human embryonic fibroblast cells (Figure 4.1(A)), Matrigel (derived from mouse sarcoma), laminin, hyaluronic acid, or fibronectin (Table 4.1).[1, 3-15] The naturally-derived substrates currently employed for hES cell propagation.have undefined composition, show batch-to-batch inconsistencies, and often contain contaminants, such as pathogens[16, 17]

Furthermore, feeder-independent cultures typically require the use of feeder-conditioned medium and high concentrations of basic fibroblast growth factor (bFGF).[5, 18] Matrigel is the most commonly used substrate for feeder-free hES cell culture in mouse embryonic fibroblast conditioned medium (MEF-CM).[5]

Synthetic substrates for pluripotent stem cell culture

Utilization of biomaterials for hES cell culture eliminates the need for direct coculture with supportive feeder layers and reduces contaminations introduced by naturally-derived substrates.[18] Synthetic culture matrices also improve the reproducibility of experimental outcomes. Furthermore, integration of biomolecules such as growth factors and cell-adhesive proteins into sophisticated biomaterials has also been used for controlled differentiation. However, to date, synthetic matrices have only sustained short-term hES cell propagation (Table 4.1).[19-22]

Synthetic matrices have been extensively used for murine ES cell cultures. An assessment of the propagation of murine embryonic stem cells on various poly(α-hydroxy esters) such as poly(D,L-lactide), poly(L-lactide), poly(glycolide) and poly(D,L-lactide-co-glycolide) (PLGA) revealed a significantly higher colonization rate on PLGA surfaces than the other poly(α-hydroxy esters).[23] PLGA surfaces were successful in colonization and maintenance of murine ES cells. In another study, murine ES cells were seeded on polymeric hydrogel slabs synthesized by blending hydroxyethyl methacrylate (HEMA) with ethylene dimethacrylate (EDMA) or 1-vinyl-2-pyrolidone (VP) with N,N'-divinylethyleneurea (DVEU) or EDMA.[24] Poor ES cell adhesion was observed on hydrophilic PVP surfaces. At shorter time periods, ES cells retained their undifferentiated state irrespective of the surface properties.

A synthetic matrix system composed of a semi-interpenetrating polymer network was reported for short-term self-renewal of hESCs.[25] This polymer hydrogel consisted of poly(N-isopropylacrylamide-co-acrylic acid) crosslinked with acrylated peptides and interpenetrated with cell adhesion moieties. hES cells cultured on this synthetic matrix adhered to the surface, remained viable and exhibited markers of undifferentiated hES cells. A combinatorial study showed the effects of laminin-derived peptides on hES cell proliferation and found that five out of 18 peptides tested supported short-term hES cell culture.[20] In addition, encapsulation of hES cells in hydrogel matrix of photoactive hyaluronic acid has also been shown to maintain undifferentiated state with preservation of karyotype and formation of embryoid bodies when maintained in MEF-CM; although this system relies on photopolymerization, DNA damage due to UV irradiation measured as expression of p53 was reported to be minimal.[26] Recently, a study assessing the ability of several biomaterials such as poly-L,D-lactide (PLDLA) and poly(desaminotyrosyl-tyrosine ethyl ester carbonate) (PDTEC), to support hES cell cultures, found that only undefined Matrigel was successful in sustaining long-term cultures.[22]

While these studies contributed toward a fundamental appreciation of the importance of the solid microenvironment, they failed to define the essential features of a successful cellular matrix in terms of undifferentiated growth and long-term proliferation of hES cells.

In this chapter, a fully-defined synthetic polymer coating, poly[2-(methacryloyloxy)ethyl dimethyl-(3-sulfopropyl)ammonium hydroxide] (PMEDSAH) is reported, which sustains long-term human embryonic stem (hES) cell growth. Introducing well-defined polymer-based hES cell culture matrices establishes a major step would facilitate important insights in developmental biology and hES cell-centered clinical therapies.

4.2 Material and Methods

Polymer synthesis

All polymer coatings were prepared on tissue culture polystyrene (TCPS) dishes (35 mm; Becton Dickinson and Co, Franklin Lakes, NJ). Graft-polymerization was carried out using a 0.25 M solution of methacrylate monomers (Sigma-Aldrich, MO) in a 4:1 mixture of water and ethanol.[27] The TCPS dishes were activated using a UV-ozone cleaner (Jelight Co. Inc, Irvine, CA) for 40 min. Surface-activated dishes were immersed into the monomer solution at 80 ^{o}C for 2.5 h. Polymer-coated dishes were allowed to cool to 50 ^{o}C and were rinsed with a warm saline solution (1% NaCl in water, at 50 ^{o}C). Polymer-coated dishes were then left overnight in saline solution at 50 ^{o}C. Dishes were cleaned by ultra-sonication in DI-water and dried under a stream of nitrogen gas. Polymer-coated dishes were stored at room temperature prior to cell culture. For FTIR

spectroscopy and ellipsometry, a gold-coated substrate coated with poly-*p*-xylylene was included in each graft-polymerization reactions.[28]

Characterization of polymer coatings

Elemental analysis of the polymer coatings was conducted using X-ray photoelectron spectroscopy (Axis Ultra XPS, Kratos Analyticals, UK) equipped with a monochromatized Al Kα X-ray source. Spectra were referenced to an unfunctionalized aliphatic carbon at 285.0 eV. Presence of polymer coatings was confirmed using Fourier transform infrared (FTIR) spectroscopy (Nicolet 6700 spectrometer) using the grazing angle accessory (SAGA) with a grazing angle of 85°. Coating thickness was recorded at a wavelength of 532 nm using EP^3-SW imaging ellipsometer (Nanofilm Technology GmbH, Germany). Four-zone nulling was performed at an angle of incidence of 70° and an anisotropic Cauchy parameterization model was used for curve fitting. Nanoindentation was performed by CSM instruments Inc (Needham, MA) using a CSM NanoHardness tester equipped with a conospherical diamond tip (with a radius of 20 µm) in the load-control mode. A typical nanoindentation experiment involved engaging the tip under loading rate of 1.00 mN/min, indenting to a maximum load of 0.5 mN, and then withdrawing the tip with the same rate as for the loading. For each hydrogel coating, load-displacement data was acquired for 5 indentations. Reduced modulus (E_r) was calculated using the unloading portions of these load-displacement curves according to a method developed by Gerberich et al.[29]

Preparation of polymer-coated dishes before cell culture

Before cell seeding, all polymer-coated dishes were sterilized with UV-light for overnight (12 h), washed twice with sterile phosphate buffer saline (PBS) and equilibrated with culture medium for at least 48 h at 37 ^{o}C in 5% CO_2 atmosphere.

Matrigel preparation

Matrigel (BD BioSciences, San Jose, CA) was diluted 1:20 in cold Dulbecco's modified Eagle's medium/F12 (DMEM/F12; GIBCO, Carlsbad, CA), applied to the dishes, and the coating was allowed to form overnight at 4 ^{o}C or for 2 h at room temperature.[30]

Cell culture media preparation

Culture medium for hES cells cultured on irradiated MEFs contained standard DMEM/F12 supplemented with 20% KnockOut serum replacement (GIBCO), 0.1 mM β-mercaptoethanol, 1 mM L-glutamine, 1% non-essential amino acids and 4 ng/ml human recombinant basic fibroblast growth factor (Invitrogen; Carlsbad, CA).

MEF-CM was prepared as described previously.[31] Irradiated MEFs (8x10^{6} cells) were seeded onto gelatin-coated culture dishes in medium composed of high glucose DMEM, 10% fetal bovine serum (FBS; GIBCO), 1% non-essential amino acids, and 200 mM L-glutamine. After 24 h, MEF culture medium was replaced with the hES cell culture medium described above (60 ml). This medium was left in contact with MEFs and was collected as MEF-CM after 24 h of conditioning. Media exchange was conducted daily and MEF-CM was collected for 3 days. The MEF-CM was frozen at -20

^{o}C and was supplemented with 0.1 mM β-mercaptoethanol, 2 mM L-glutamine, and 4 ng/ml bFGF before use.

Cell culture

Two federally-approved hES cell lines: BG01 (NIH code: BG01; BresaGen, Inc., Athens, GA), and H9 (NIH code: WA09; WiCell, Madison, WI) were used and cultured at 37 ^{o}C with 5% CO_2. Human ES cell colonies were observed every 48 h using a Leica stereomicroscope and differentiated cells were removed mechanically using a sterile "pulled-out" glass pipette. Cell culture medium was replaced every 48 h.

Cell culture media transition and passaging

Before mechanical harvesting of hES cells growing on MEFs, cell culture medium was replaced by MEF-CM. Cultures were passaged depending on size and density of colonies every 7-10 days. Undifferentiated hES cell colonies were then mechanically passaged by cutting small aggregates of cells using a sterile "pulled-out" glass pipette, when colonies are large, beginning to merge, and have centers that are dense and phase-bright compared to their edges. About 50-100 hES cell-aggregates were transferred to polymer- and Matrigel-coated dishes.

Cell-aggregate adhesion assay

Number of adhered colonies and number of floating embryoid bodies (EBs) were counted 48 h after cell seeding, to calculate the percentage of cell-aggregate adhesion using the following formula:

Cell-aggregate adhesion (%) = (number of adhered colonies)*(100)/(number of adhered colonies + number of EBs floating). Statistics were performed using an unpaired t-test.

Cell population-doubling time

Cell population-doubling time was calculated in terms of time required for the area of a colony to increase two-fold.[32] ImageJ software (http://rsb.nih.gov/ij) was used to measure area of the colonies. Colony area (n=10) was calculated at five time-points (for 5 days after cell seeding), and cell population-doubling time was determined by fitting an exponential function. Mean values were compared using an unpaired t-test.

Immunocytochemistry

Cells were fixed in 2% paraformaldehyde for 30 min at room temperature and then permeabilized with 0.1% Triton X-100 for 10 min. Primary antibodies were diluted in 1% normal donkey serum and incubated overnight at 4 ^{o}C and detected by respective secondary antibodies. Samples were imaged and captured using a Leica DM IRB inverted microscope with an Olympus DP-30 CCD camera. Throughout this study, hES cells were characterized every fifth passage by detection of the following hES cell markers: OCT3/4, SOX2, SSEA4, TRA-1-60 and TRA-1-81.

ImageJ software was used to count the number of OCT3/4 or SOX2 positive cells and number of cell nuclei present in each colony. Percentage of cells positive for each marker was calculated for colonies cultured on PMEDSAH- and Matrigel- coated plates. Unpaired t-test was used to calculate p values.

Cytogenetic analysis

Karyotype analysis was performed at Cell Line Genetics (Madison WI) applying standard protocols utilizing the GTL-banding method on at least 20 cells.

Evaluation of pluripotency

Undifferentiated H9 hES cells ($< 5x10^6$ cells) cultured on PMEDSAH and Matrigel in MEF-CM at passage 25 were injected subcutaneously into CB17 SCID mice (Charles River Laboratories, Wilmington, MA) to induce teratomas. When tumors became palpable, mice were euthanized; tumors were harvested, and processed for histological analysis at the Center for Organogenesis Morphology core (University of Michigan).

Pluripotency was also evaluated by EB formation from undifferentiated hES cells. Colonies were cultured in suspension in hES cell culture medium lacking bFGF to promote differentiation, for 10 days. Alternatively, hES cells were allowed to overgrow in MEF-CM without bFGF for 10 days.

Extraction and purification of total RNA

Cells were manually scraped from dishes and pelleted by centrifugation at 800 g. Pellets were then disrupted by vigorous pipetting in 1000 µl of Trizol Reagent (Invitrogen). Chloroform (200 µl) was added to this solution followed by centrifugation (~13,000 x g). Aqueous phase containing RNA was separated and additionally purified using the RNeasy Mini-Kit (Qiagen, Valencia, CA) following the manufacturer's RNA Clean-up protocol with the optional On-column DNAse treatment. RNA quality was

checked using RNA 6000 Nano assays performed on the Bioanalyzer 2100 Lab-on-a-Chip system (Agilent Technologies, Palo Alto, CA).

Reverse-transcription PCR (RT-PCR) analysis

Total RNA was reverse transcribed using SuperScript™ One-Step RT-PCR with platinum® Taq (Invitrogen). In a single reaction (50 µl), 1 µg of total RNA and 20 pmol of forward (f) and reverse (r) primers were used (Supplementary Table II online). The cDNA synthesis and pre-denaturation were carried out in the first cycle at 48 ºC for 45 min, followed by a second cycle at 94 ºC for 2 min. The PCR amplification was performed for 35 cycles at 94 ºC for 15 sec, 5 ºC for 30 sec, and 72 ºC for 1 min. The final extension cycle was run at 72 ºC for 8 min. Finally, 10 µl of PCR reaction products were loaded onto a 1.0% agarose gel and size-fractionated.

Microarray analysis

Total RNA (10 µg) from hES cells was hybridized to Affymetrix Human Genome U133 Plus 2.0 microarray (Affymetrix; Santa Clara, CA) following the manufacturer's instructions. Data analysis was performed using a Robust Multi-array average algorithm that converted the plot of perfect match probe intensities into an expression value for each gene.[33] Based on a variance of 0.05, probe-sets that did not appear to be differentially expressed in any sample were filtered and removed. Differentially expressed genes were detected by fitting a linear model to each probe-set and selecting those with a multiplicity-adjusted p-value (FDR) of 0.05 or less.[34, 35]

Quantitative Real-time PCR (qPCR) analysis

Total RNA was reverse-transcribed using MultiScribe™ Reverse Transcriptase System (Applied Biosystems; Foster city, CA). The ABI 7300 PCR and Detection System (Applied Biosystems) with SYBR® Green PCR Master Mix (Applied Biosystems) were used to conduct real-time PCR in triplicate for each sample. Primers used are listed in Supplementary Table II online. Human β-Actin was amplified as an internal standard. Relative quantification of NANOG, OCT3/4 and SOX2 gene expression was performed using the Comparative CT Method.[36]

4.3 Results and discussion

Synthetic polymer coatings could be exceptional candidates for hES cell matrix replacement strategies because of their highly reproducible fabrication and ease of use (Figure 4.1(B)).[37] However, actual implementation of these novel materials has been challenging[38] and no synthetic polymer coating has yet been used to support long-term culture of hES cells.[21]

Polymer synthesis and characterization

In this study, six polymer coatings were synthesized by surface-initiated graft-polymerization[27] onto tissue culture polystyrene and tested for their ability to promote attachment and proliferation of undifferentiated hES cells (Figure 4.2). Compared to alternate surface modification techniques, such as tethering of polymer chains onto the surface, this approach is known to result in higher surface densities.[39] Selected polymers shared an identical polymer backbone structure, but differed in their side chain chemistries. The polymers were: poly[2-hydroxyethyl methacrylate] (PHEMA),

poly[poly(ethylene glycol) methyl ether methacrylate] (PPEGMA), poly[3-sulfopropyl methacrylate] (PSPMA), poly[[2-(methacryloyloxy)ethyl]trimethylammonium chloride] (PMETAC), poly[carboxybetaine methacrylate] (PCBMA), poly[[3-(methacryloylamino)propyl]dimethyl(3-sulfopropyl)ammonium hydroxide] (PMAPDSAH) and PMEDSAH. This group of polymer coatings was compared to two solvent-cast poly(α-hydroxy esters), PLA and PLGA, as well as Matrigel-coated and unmodified TCPS dishes.

Chemical composition of the polymer coatings was confirmed using X-ray photoelectron spectroscopy (XPS) and Fourier transform infrared spectroscopy (FTIR). To assess differences in their mechanical properties, the coatings were further analyzed using nanoindentation.[40] This technique enables the measurement of the elastic moduli of ultrathin polymer coatings. Interestingly, nanoindentation experiments revealed that PMEDSAH coatings were significantly softer than other coatings included in this study as indicated by their reduced elastic modulus (Figure 4.2).[29, 41]

hES cell culture on polymers

H9 hES cells were mechanically harvested from cultures on mouse embryonic fibroblasts (MEF) and placed onto polymer-coated dishes and Matrigel in MEF-conditioned media (MEF-CM). While Matrigel supported adhesion and colony formation of more than 90% of hES cell-aggregates, no attachment was observed on PLA, PLGA and PCBMA. hES cells adhered, but spontaneously differentiated, during the first two passages on PMETAC, PSPMA, PHEMA, PPEGMA and unmodified TCPS dishes (Figure 4.2) and propagation of undifferentiated cells into subsequent passages was not possible. On the other hand, zwitterionic PMEDSAH supported attachment and proliferation of two hES cell lines (BG01 and H9). Furthermore, sulfobetaine-containing

86

polymer, PMAPDSAH also supported proliferation of H9 hES cells (Figure 4.2). PMAPDSAH-coated dishes supported the undifferentiated culture of H9 hES cells for 10 passages in MEF-CM.

Zwitterions are commonly found in nature in proteins, proteoglycans and in cellular surface lipids and in extracellular matrices, therefore zwitterionic materials may be biocompatible. More specifically, heparin sulfate which is present in cell surface membranes and extracellular matrix protein binds to a wide variety of protein ligands (such as growth factors) and regulates several signaling pathways (such as stem cell maintenance).[42-45] In addition, sulfation of certain natural or synthetic polymers has been shown to increase the specific binding of heparin-binding proteins such as growth factors, which in turn regulate cellular processes like differentiation and pluripotency.[46, 47]

Long-term hES cell culture and characterization

The cells monitored at regular intervals using karyotyping, expression of pluripotency markers and in vitro evaluation of pluripotency.[48] Throughout 25 passages, H9 hES cells seeded on PMEDSAH expressed characteristic hES cell markers, displayed a normal karyotype and retained pluripotency. H9 hES cells growing on PMEDSAH expressed characteristic pluripotent stem cell markers and transcription factors such as OCT3/4, SOX-2, SSEA-4, TRA-1-60 and TRA-1-81, which are associated with the undifferentiated state of hES cells (Figure 4.3(A)). After passage 3, 92±3% of the cells cultured on PMEDSAH coatings and 93±3% cells were positive for OCT3/4 and SOX-2 respectively. These results are comparable to results obtained with Matrigel-coated samples, which showed 92.1±3.1% OCT3/4 positive and 91.5±3.0% SOX-2 positive cells (Figure 4.3(B)). Furthermore, after passage 20, expression levels of undifferentiated and

pluripotent markers OCT3/4 (91±3%) and SOX2 (92±2%) were comparable to levels expressed by cells cultured on Matrigel.

Microarray analysis revealed similar expression levels of hES cell-specific genes in cells cultured on PMEDSAH and Matrigel. Further validation using qPCR revealed comparable RNA expression levels of NANOG, OCT3/4 and SOX2 (Figure 4.3(C)). Significantly, there were no differences in Wnt and TGF2 signaling pathways, which are important for the maintenance of hES cell pluripotency. No differences were found between hES cells cultured on PMEDSAH and Matrigel in expression of genes involved in cell-cell and cell-matrix adhesion.

Presence of a normal euploid karyotype is of paramount importance, because long-term cultures of mouse[49] and human[50-53] ES cells can develop aneuploidies, which would be detrimental to future biological utility and clinical applications of hES cells[54]. Standard GTL-banding analyses, at regular intervals throughout the study, revealed that hES cells cultured on PMEDSAH maintained a normal karyotype (Figure 4.3(D)).

Pluripotency of hES cells was assessed by overgrowing hES cells in a differentiation inducing medium followed by immunostaining with antibodies specific for β III tubulin (ectoderm), smooth-muscle actin (mesoderm) and α-fetoprotein (endoderm) to identify differentiated cells from the three germ layers (Figure 4.4(A)). Pluripotency was also validated *in vitro* by formation of embryoid bodies and detection of characteristic genes representative of the three embryonic germ layers: ectoderm (*KRT-18* and *NESTIN*), mesoderm (*FLT-1, BMP-4* and *VE-CADHERIN*) and endoderm (*AFP* and *GATA-4*) (Figure 4.4(B)).

Finally, pluripotency was evaluated by injecting undifferentiated hES cells into immunosuppressed mice to produce benign tumors called teratomas. Pluripotency of H9 hES cells was confirmed at passage 25 by trilineage differentiation in teratomas (Figure 4.4(C)).

These experiments indicate that hES cells cultured on PMEDSAH and Matrigel remain pluripotent both *in vitro* and *in vivo*, even after extended culture. Compared to animal-derived matrices, PMEDSAH is chemically defined, can be synthesized reproducibly (1,200 plates coated over a 4-year period), and has long-term stability. Moreover, long-term storage and UV-sterilization of polymer-coated dishes did not affect their ability to support hES cell growth and proliferation. In addition, hES cells cultured on PMEDSAH hydrogels were cryopreserved, thawed and successfully re-seeded onto fresh PMEDSAH-coated dishes. Under long-term culture conditions, hES cells supported by PMEDSAH coatings were phenotypically stable, expressed pluripotency markers, maintained a normal karyotype, and retained the capacity to differentiate both *in vivo* and *in vitro*.

4.4 Conclusions

The ability of PMEDSAH coatings to support hES cell culture in defined media has important implications for its application as a platform for stem cell expansion. Additional studies will be required to establish if the effect of PMEDSAH is due to an interplay between various physico-chemical properties of the polymer such as wettability, mechanical stiffness, surface topography and zeta potential. Unlike natural and recombinant matrices, PMEDSAH-coated dishes can be handled and stored with relative ease, and is an important step in defining the microenvironmental requirements of undifferentiated hES cell growth and directed differentiation. Future work will need to address the development of a fully defined microenvironment consisting of a fully defined matrix and compositionally-defined culture media.

4.5 Figures and Tables
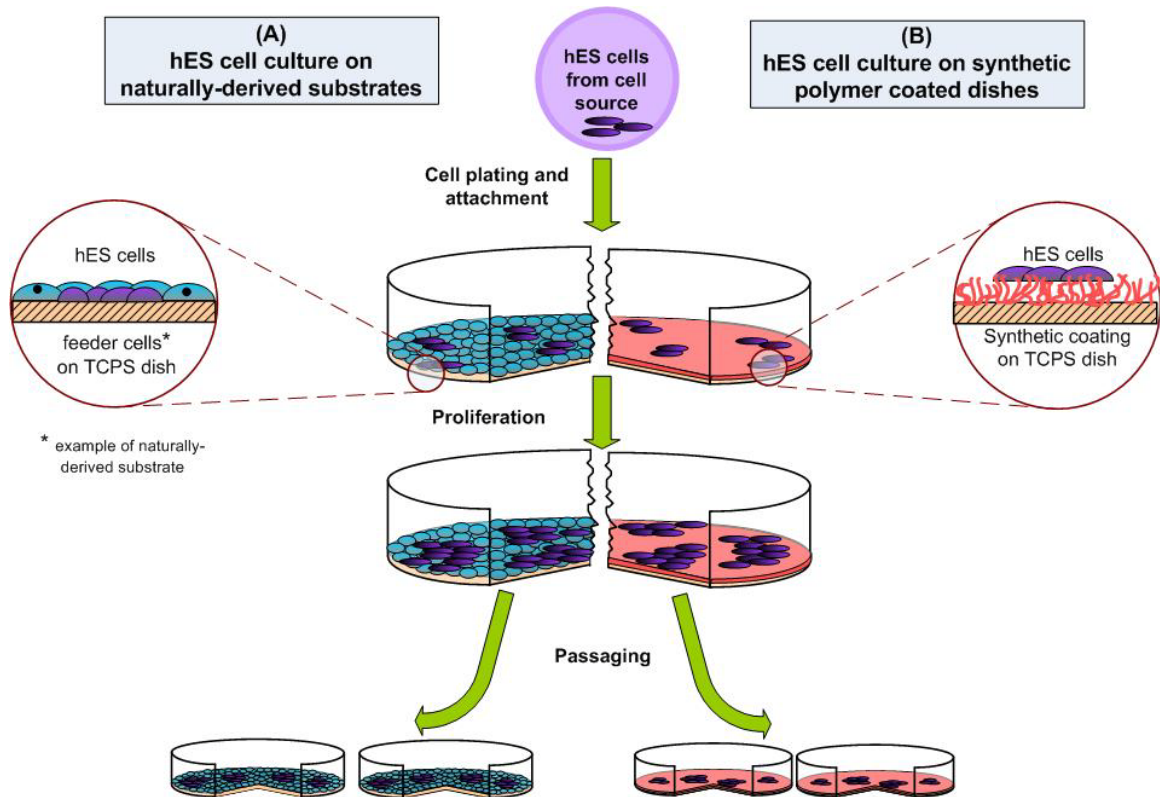
Figure 4.1: Long-term culture of human embryonic stem (hES) cells. (**A**) Traditionally, hES cell culture is performed on naturally-derived substrates. As an example, coculture with feeder cells is depicted here but other natural substrates including Matrigel, laminin and fibronectin have been used in the past. (**B**) An alternate approach based on synthetic polymer substrates is proposed in this chapter. Human ES cells cultured on these synthetic polymer substrates were compared to those growing on naturally-derived matrices. Specifically, hES cells showed normal euploid karyotype, consistently displayed markers of undifferentiated hES cells and had stable developmental potential forming cells of all three embryonic germ layers.
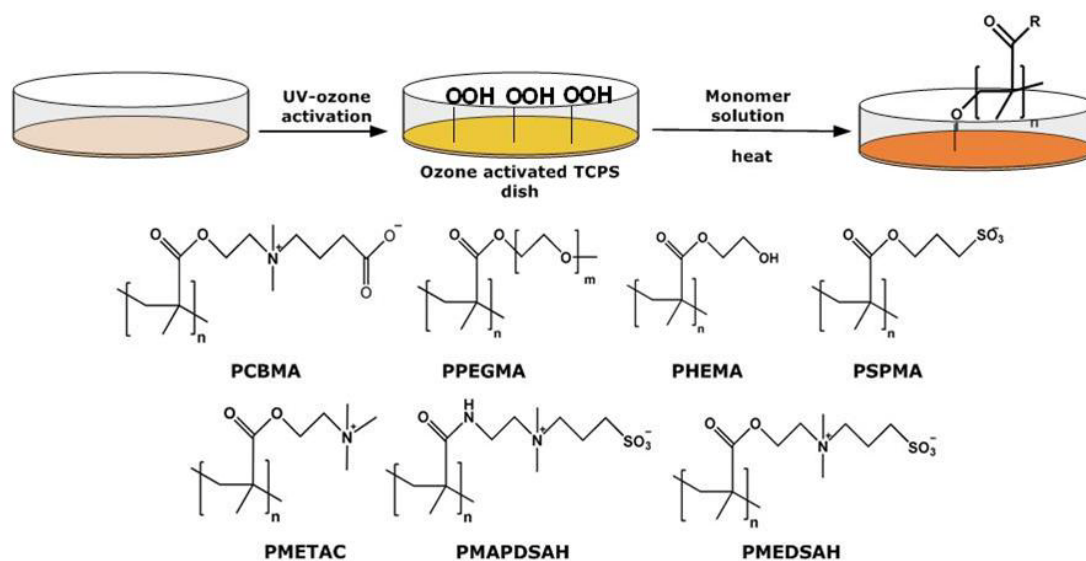
	PCBMA	PPEGMA	PHEMA	PSPMA	PMETAC	PMAPDSAH	PMEDSAH
Contact angle	71.6±4.8	63.3±3.1	56.0±3.7	50.2±4.1	40.5±5.7	60.1±6.4	17.1±1.1
Reduced elastic modulus (GPa)	3.3±0.1	3.9±0.1	3.0±0.5	3.0±0.1	3.3±0.1	3.3±0.2	2.5±0.1
Cell-aggregate adhesion (%)	0	5±1	12±1	14±2	8±1	50±1	15±1
Number of passages	0	1	2	2	2	10 (ongoing)	25

	PLGA	PLA	TCPS
Contact angle	80.1±3.4	85.6±1.9	90.2±4.6
Reduced elastic modulus (GPa)	–	–	3.5±0.1
Cell-aggregate adhesion (%)	0	0	8±2
Number of passages	0	0	0

Figure 4.2: Synthesis and characterization of polymer coatings. Schematic diagram showing surface-initiated graft-polymerization used to deposit different synthetic polymer coatings onto TCPS dishes. The TCPS surfaces were first activated by UV-ozone and then methacrylate-based monomer was polymerized from the surface. Tables list contact angle, reduced elastic modulus (GPa), initial hES cell-aggregate adhesion and number of passages achieved on each polymer coating. Polymers PLGA, PLA and PCBMA did not allow hES cell attachment. PPEGMA, PHEMA, PSPMA and PMETAC promoted initial adhesion, but did not allow extended cell culture. PMEDSAH and PMAPDSAH promoted undifferentiated growth and passaging of hES cells over several passages.
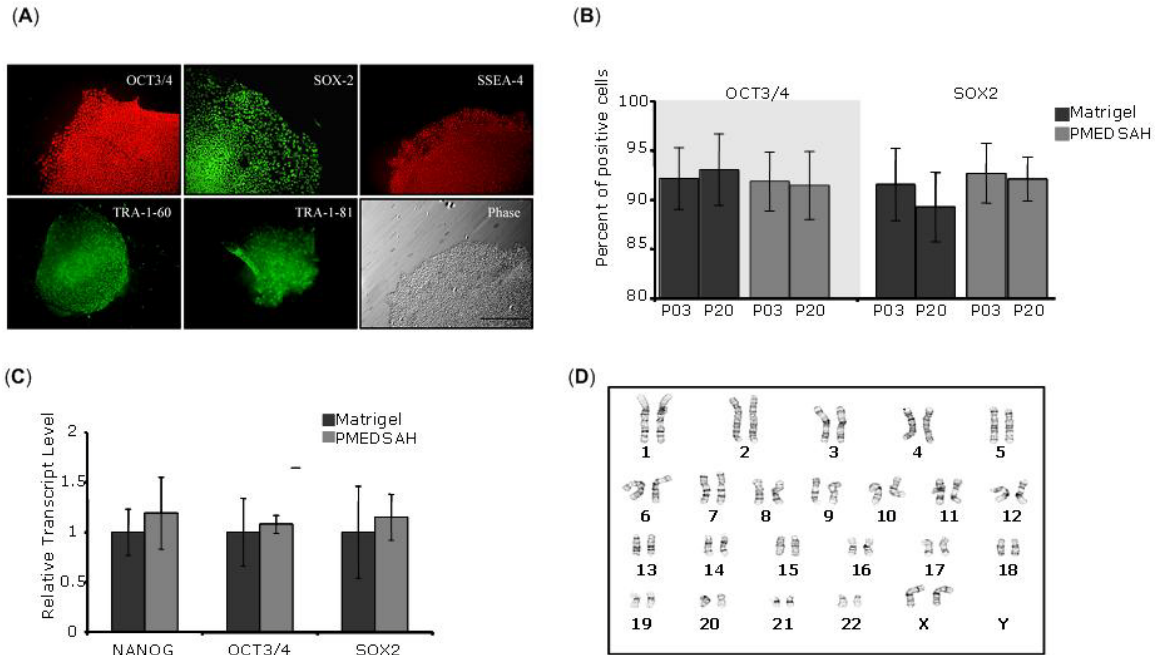
Figure 4.3: Characterization of hES cells cultured on PMEDSAH in MEF-CM. (A) Fluorescence micrographs of colonies of H9 cells cultured on PMEDSAH in MEF-CM showing expression of undifferentiated markers: OCT3/4, SOX2, SSEA-4 TRA-I-60 and TRA-I-81; and phase-contrast image. Scale bar is 500 μm. (B) Percentage (mean ± SEM) of hES cells positive for OCT3/4 and SOX2 at passage 3 (P03) and 20 (P20) growing on PMEDSAH compared to Matrigel. (C) Relative transcript levels of NANOG, OCT3/4 and SOX2 from hES cells cultured on PMEDSAH and Matrigel after analysis in RT-PCR. (D) Representative chromosomal spread of H9 cells cultured on PMEDSAH at passage 20 via standard GTL-banding analysis.
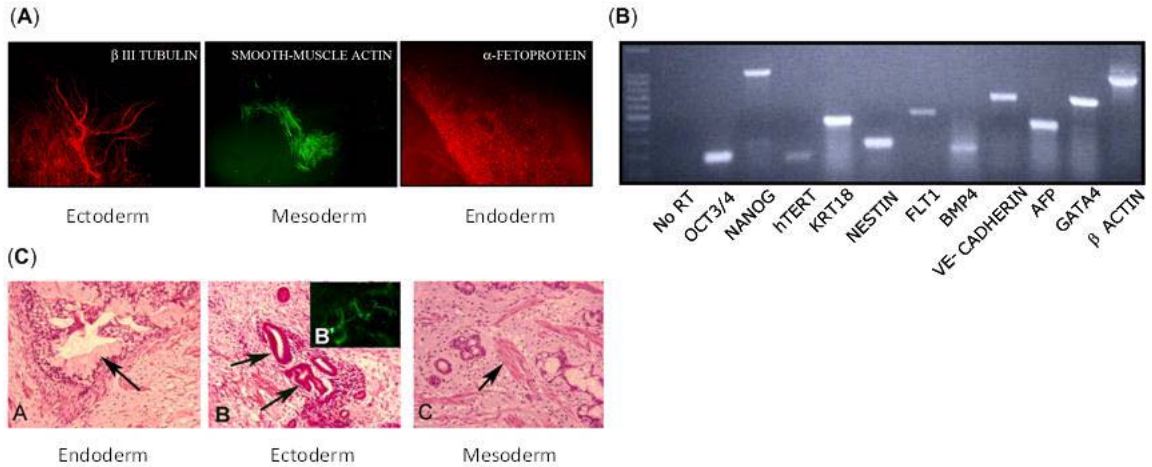
Figure 4.4: Characterization of hES cells cultured on PMEDSAH in MEF-CM. (A) Micrographs showing immunoreactivity for β-III tubulin (ectoderm), smooth muscle actin (mesoderm) and α-fetoprotein (endoderm) demonstrating pluripotent state of H9 cells. Scale bar in micrographs indicates 200 μm. (B) RT-PCR analysis of expression of markers of pluripotency (OCT3/4, NANOG, hTERT) from undifferentiated hES cell colonies and from ectoderm (KRT-18, NESTIN), mesoderm (BRACHURY, FLT-1, BMP-4, VE-CADHERIN) and endoderm (AFP, GATA-4) found in EBs. Negative control (Lane 1: no template) and positive control (β-ACTIN). (C) Pluripotency demonstrated *in vivo* by teratoma formation in immunosuppressed mice. H & E stained paraffin sections indicating endoderm (goblet-like cells: arrow A), ectoderm (neuroepithelial aggregates: arrows B; and cells expressing neuron-restricted protein β-III tubulin: arrow B') and mesodermal derivatives (cartilage, connective tissue and muscle: arrow C).

Table 4.1: Summary of substrates used for mouse and human ES cell culture from literature.[18]

Substrate type	Cell source	Substrate	Timeline of study
Feeder layer based	hESCs	Human foreskin fibroblasts	>70 passages
		Fetal skin cells	20 passages
		Fetal muscle cells	>50 passages
		Adult skin fibroblasts	>30 passages
		Adult muscle fibroblasts	>30 passages
		Commercially available fetal skin fibroblasts	>25 passages
		Adult fallopian tubal epithelial fibroblasts	>20 passages
		Adult marrow cells	13 passages
		Human adult uterine endometrial cells	90 passages
		Human adult breast parenchymal cells	50 passages
		Human embryonic fibroblasts	80 passages
		Human placental fibroblasts	>25 passages
		hESC-derived fibroblasts	44 passages 30–52 passages
Natural substrates	mESCs	LIF immobilized on gelatin	6 days
		Gelatin-coated polyamide nanofibers	3 days
	hESCs	Matrigel™	~130 passages
		Human serum	>27 passages
		Mouse embryonic fibroblasts ECM	>30 passages
		Hyaluronic acid	20 days
Synthetic substrates	mESCs	Hydroxyapatite polymers	48 h (time required for colonization)
		Poly(hydroxyethyl methacrylate)	4 days
		LIF-immobilized PET fibers	72–96 h
		Gelatin-immobilized PET fibers	15 days
	hESCs	Poly-(glycerolcosebacate)-acrylate	1 week
		Polyurethane microwells	>21 days
		Poly(N-isopropyl acrylamide-co-acrylic acid) SIPN	5 days

4.6 References

1. Thomson, J.A. et al. Embryonic stem cell lines derived from human blastocysts. *Science* **282**, 1145-1147 (1998).
2. Mimeault, M. & Batra, S.K. Concise review: Recent advances on the significance of stem cells in tissue regeneration and cancer therapies. *Stem Cells* **24**, 2319-2345 (2006).
3. Derda, R. et al. Defined substrates for human embryonic stem cell growth identified from surface arrays. *ACS Chemical Biology* **2**, 347-355 (2007).
4. Stojkovic, P. et al. An autogeneic feeder cell system that efficiently supports growth of undifferentiated human embryonic stem cells. *Stem Cells* **23**, 306-314 (2005).
5. Xu, C. et al. Feeder-free growth of undifferentiated human embryonic stem cells. *Nat Biotechnol* **19**, 971-974 (2001).
6. Amit, M., Shariki, C., Margulets, V. & Itskovitz-Eldor, J. Feeder layer- and serum-free culture of human embryonic stem cells. *Biol Reprod* **70**, 837-845 (2004).
7. Amit, M. et al. Human feeder layers for human embryonic stem cells. *Biol Reprod* **68**, 2150-2156 (2003).
8. Skottman, H. & Hovatta, O. Culture conditions for human embryonic stem cells. *Reproduction* **132**, 691-698 (2006).
9. Ellerstrom, C. et al. Derivation of a xeno-free human embryonic stem cell line. *Stem Cells* **24**, 2170-2176 (2006).
10. Cheon, S.H. et al. Defined feeder-free culture system of human embryonic stem cells. *Biology of Reproduction* **74**, 611 (2006).
11. Beattie, G.M. et al. Activin A maintains pluripotency of human embryonic stem cells in the absence of feeder layers. *Stem Cells* **23**, 489-495 (2005).
12. Draper, J.S., Moore, H.D., Ruban, L.N., Gokhale, P.J. & Andrews, P.W. Culture and characterization of human embryonic stem cells. *Stem Cells and Development* **13**, 325-336 (2004).
13. Chai, C. & Leong, K.W. Biomaterials approach to expand and direct differentiation of stem cells. *Molecular Therapy* **15**, 467-480 (2007).
14. Mallon, B.S., Park, K.Y., Chen, K.G., Hamilton, R.S. & McKay, R.D.G. Toward xeno-free culture of human embryonic stem cells. *International Journal Of Biochemistry & Cell Biology* **38**, 1063-1075 (2006).
15. Bigdeli, N. et al. Adaptation of human embryonic stem cells to feeder-free and matrix-free culture conditions directly on plastic surfaces. *Journal of Biotechnology* **133**, 146-153 (2008).
16. Ilic, D. Culture of human embryonic stem cells and the extracellular matrix micro environment. *Regenerative Medicine* **1**, 95-101 (2006).
17. Martin, M.J., Muotri, A., Gage, F. & Varki, A. Human embryonic stem cells express an immunogenic nonhuman sialic acid. *Nature Medicine* **11**, 228-232 (2005).

18. Abraham, S., Eroshenko, N. & Rao, R.R. Role of bioinspired polymers in determination of pluripotent stem cell fate. *Regenerative Medicine* **4**, 561-578 (2009).

19. Li, Y.J., Chung, E.H., Rodriguez, R.T., Firpo, M.T. & Healy, K.E. Hydrogels as artificial matrices for human embryonic stem cell self-renewal. *J Biomed Mater Res A* **79**, 1-5 (2006).

20. Derda, R., Li, L., Orner, B.P., Lewis, R.L., Thomson, J.A., Kiessling, L.L. Defined substrates for human embryonic stem cell growth identified from surfaces arrays. *ACS Chemical Biology* **2**, 347-355 (2007).

21. Anderson, D.G., Levenberg, S. & Langer, R. Nanoliter-scale synthesis of arrayed biomaterials and application to human embryonic stem cells. *Nature Biotechnology* **22**, 863-866 (2004).

22. Hakala, H. et al. Comparison of Biomaterials and Extracellular Matrices as a Culture Platform for Multiple, Independently Derived Human Embryonic Stem Cell Lines. *Tissue Eng. Part A* **15**, 1775-1785 (2009).

23. Harrison, J. et al. Colonization and maintenance of murine embryonic stem cells on poly(α-hydroxy ester). *Biomaterials* **25**, 4963-4970 (2004).

24. Kroupova, J., Horak, D., Pachernik, J., Dvorak, P. & Slouf, M. Functional polymer hydrogels for embryonic stem cell support. *J Biomed Mat Res* **76B**, 315-325 (2006).

25. Li, Y.J., Chung, E.H., Rodriguez, R.T., Firpo, M.T. & Healy, K.E. Hydrogels as artificial matrices for human embryonic stem cell self-renewal. *Journal of Biomedical Materials Research, Part A* **79A**, 1-5 (2006).

26. Gerecht, S. et al. Hyaluronic acid hydrogel for controlled self-renewal and differentiation of human embryonic stem cells. *Proceedings of the National Academy of Sciences of the United States of America* **104**, 11298-11303 (2007).

27. Wu, J.M. et al. A surface-modified sperm sorting device with long-term stability. *Biomedical Microdevices* **8**, 99-107 (2006).

28. Lahann, J. & Langer, R. Novel poly(p-xylylenes): Thin films with tailored chemical and optical properties. *Macromolecules* **35**, 4380-4386 (2002).

29. Gerberich, W.W. et al. Elastic loading and elastoplastic unloading from nanometer level indentations for modulus determinations. *J. Mater. Res.* **13**, 421-439 (1998).

30. Xu, C.H. et al. Feeder-free growth of undifferentiated human embryonic stem cells. *Nature Biotechnology* **19**, 971-974 (2001).

31. Villa-Diaz, L.G. et al. Analysis of the Factors That Limit the Ability of Feeder-Cells to Maintain the Undifferentiated State of Human Embryonic Stem Cells. *Stem Cells Dev* (2008).

32. Reubinoff, B.E., Pera, M.F., Vajta, G. & Trounson, A.O. Effective cryopreservation of human embryonic stem cells by the open pulled straw vitrification method. *Human reproduction (Oxford, England)* **16**, 2187-2194 (2001).

33. Irizarry, R.A. et al. Exploration, normalization, and summaries of high density oligonucleotide array probe level data. *Biostatistics* **4**, 249-264 (2003).

34. Smyth, G.K., Michaud, J. & Scott, H.S. Use of within-array replicate spots for assessing differential expression in microarray experiments. *Bioinformatics* **21**, 2067-2075 (2005).

35. Benjamini, Y. & Hochberg, Y. Controlling the false discovery rate - A practical and porwerful approach to multiple testing. *J. R. Stat. Soc. Ser. B-Methodol.* **57**, 289-300 (1995).

36. Schmittgen, T.D. & Livak, K.J. Analyzing real-time PCR data by the comparative C-T method. *Nat. Protoc.* **3**, 1101-1108 (2008).

37. Jagur-Grodzinski, J. Polymers for tissue engineering, medical devices, and regenerative medicine. Concise general review of recent studies. *Polymers for Advanced Technologies* **17**, 395-418 (2006).

38. Saha, K., Pollock, J.F., Schaffer, D.V. & Healy, K.E. Designing synthetic materials to control stem cell phenotype. *Current Opinion in Chemical Biology* **11**, 381-387 (2007).

39. Zhao, B. & Brittain, W.J. Polymer brushes: surface-immobilized macromolecules. *Progress in Polymer Science* **25**, 677-710 (2000).

40. Oyen, M.L. The materials science of bone: Lessons from nature for biomimetic materials synthesis. *Mrs Bulletin* **33**, 49-55 (2008).

41. Li, M., Carter, C.B. & Gerberich, W.W. Nanoindentation measurements of mechanical properties of polystyrene thin films. *Materials Research Society Symposium* **649**, 1-6 (2001).

42. Gesslbauer, B., Rek, A., Falsone, F., Rajkovic, E. & Kungl, A.J. Proteoglycanomics: tools to unravel the biological function of glycosaminoglycans. *Proteomics* **7**, 2870-2880 (2007).

43. Sasaki, N. et al. Heparan Sulfate Regulates Self-renewal and Pluripotency of Embryonic Stem Cells. *J. Biol. Chem.* **283**, 3594-3606 (2008).

44. Furue, M.K. et al. Heparin promotes the growth of human embryonic stem cells in a defined serum-free medium. *Proceedings of the National Academy of Sciences of the United States of America* **105**, 13409-13414 (2008).

45. Kreuger, J., Spillmann, D., Li, J.P. & Lindahl, U. Interactions between heparan sulfate and proteins: the concept of specificity. *J. Cell Biol.* **174**, 323-327 (2006).

46. Freeman, I., Kedem, A. & Cohen, S. The effect of sulfation of alginate hydrogels on the specific binding and controlled release of heparin-binding proteins. *Biomaterials* **29**, 3260-3268 (2008).

47. Barbucci, R. et al. Fibroblast cell behavior on bound and adsorbed fibronectin onto hyaluronan and sulfated hyaluronan substrates. *Biomacromolecules* **6**, 638-645 (2005).

48. Hoffman, L.M. & Carpenter, M.K. Characterization and culture of human embryonic stem cells. *Section Title: Biochemical Methods* **23**, 699-708 (2005).

49. Longo, L., Bygrave, A., Grosveld, F.G. & Pandolfi, P.P. The chromosome make-up of mouse embryonic stem cells is predictive of somatic and germ cell chimaerism. *Transgenic Res* **6**, 321-328 (1997).

50. Draper, J.S. et al. Recurrent gain of chromosomes 17q and 12 in cultured human embryonic stem cells. *Nature Biotechnology* **22**, 53-54 (2004).

51. Maitra, A. et al. Genomic alterations in cultured human embryonic stem cells. *Nat Genet* **37**, 1099-1103 (2005).

52. Brimble, S.N. et al. Karyotypic stability, genotyping, differentiation, feeder-free maintenance, and gene expression sampling in three human embryonic stem cell lines derived prior to August 9, 2001. *Stem Cells Dev* **13**, 585-597 (2004).

53. Imreh, M.P. et al. In vitro culture conditions favoring selection of chromosomal abnormalities in human ES cells. *J. Cell. Biochem.* **99**, 508-516 (2006).

54. Baker, D.E.C. et al. Adaptation to culture of human embryonic stem cells and oncogenesis in vivo. *Nature Biotechnology* **25**, 207-215 (2007).

CHAPTER 5

FULLY-DEFINED CULTURE SYSTEMS FOR HUMAN EMBRYONIC STEM CELLS

The material in this chapter has been adapted with minor modifications from the following article:

L. G. Villa-Diaz*, H. Nandivada*, J. Ding, N. C. Nogueira-de-Souza, P. H. Krebsbach, K. S. O'Shea, J. Lahann, G. D Smith, Synthetic polymer coatings for long-term growth of human embryonic stem cells, (under review) [*co first authors].

Abstract

Chemistry, charge, pH and topography of the microenvironment play a critical role in determining the behavior of human embryonic stem (hES) cells, thus triggering various developmental events, such as cell proliferation, differentiation, migration, and apoptosis.[1] However, a detailed understanding of the cellular microenvironment has been hampered by the lack of well-defined and biologically-functional cell culture matrices. In chapter 4, a compositionally-defined synthetic polymer coating, poly[2-(methacryloyloxy)ethyl dimethyl-(3-sulfopropyl)ammonium hydroxide] (PMEDSAH), was reported, which supported long-term culture of hES cells in mouse embryonic fibroblast conditioned medium (MEF-CM). Nevertheless, MEFs secrete unknown components into MEF-CM, which limit the utility of PMEDSAH for further clinical applications. Therefore, for a completely defined culture system, it is necessary to

demonstrate the applicability of PMEDSAH using clinically-compliant, commercially-available cell culture media.

Towards this goal, in this chapter, the efficacy of PMEDSAH was extended for hES cell growth in several different culture media including commercially-available defined media- mTeSR and StemPro. Further, a second zwitterionic polymer coating, poly[[3-(methacryloylamino)propyl]dimethyl(3-sulfopropyl)ammonium hydroxide] (PMAPDSAH; previously mentioned in chapter 4) was investigated for its ability to sustain long-term hES cell growth in different defined culture media.

5.1 Introduction

Several complex factors govern the interactions between cells and material surfaces.[2, 3] Firstly, cells have a non-rigid membrane which is heterogeneous with respect to charges and surface structures. In addition, cells are involved in actively secreting and transporting ions, proteins and other biological molecules, which results in the transformation or remodeling of the biomaterial surface.

Creation of platforms for culture of human embryonic stem (hES) cells requires a deeper understanding of the factors governing stem cell behavior. Recently, a range of physicochemical properties of the microenvironment have been reported to exert control over stem cell decisions.[4] Studies have shown that parameters such as geometry, topography, mechanical properties have a profound influence on the stem cell fate.[5-8] Manipulation of stem cells using materials, which can provide the necessary chemical cues based on chemistry, mechanics and molecular delivery, can advance the clinical applicability of stem cells.[9]

In chapter 4, a chemically-defined polymer PMEDSAH was described, which successfully supported the long-term proliferation of undifferentiated hES cell cultures.

The aforementioned polymer coating contains zwitterionic sulfobetaine side chains composed of a anionic sulfonate (SO_3^-) and positively-charged quarternary ammonium (N^+) group on each unit. These polyzwitterions are isoelectric at neutral pH with a typical dipole moment of 20-30 D.[10] The polymeric chains have been shown to undergo strong reversible intra- and inter-chain interactions depending on the molecular weight of the polymer.[11]

Development of defined hES cell culture media

Interactions with unknown components in the media can potentially contribute to differentiated cellular phenotype and add variability to the culture environment. In this respect, considerable research is being done towards understanding the role of various components in the hES cell culture medium and creating better defined media.[12, 13]

Traditionally, "feeder-free" cultures of hES cells require the use of feeder-conditioned medium and absence of this medium leads to spontaneous differentiation of the hES cells.[9]

Significant progress has been made in the development of defined hES cell media,[14, 15] however, long-term culture still requires use of recombinant extracellular matrix proteins[16] or animal-derived matrices,[17] which have raised substantial concerns because they are sources of variability[18] and xenogeneic contamination.[19]

Derivation and propagation of hES cells was first demonstrated in defined medium (TeSR1),[14] which was subsequently modified by replacing some of the recombinant components with FDA-approved naturally-derived components and mTeSR1 medium was formulated.[20] Complete mTeSR1 medium (STEMCELL Technologies, Vancouver, BC), which contains recombinant human bFGF and bovine serum albumin, has been formulated for use with Matrigel-coated surfaces. This defined

medium has been successfully used for extended feeder-free culture of hES cells and induced pluripotent stem (iPS) cells.

Recently, several other commercially-available proprietary media, which claim clinical suitability, have become available. StemPro hESC SFM (Invitrogen, Carlsbad, CA), a reportedly fully-defined, serum-free and feeder-free medium, has been shown to support a number of hES cell lines.[15, 21] The components used to create the medium are cGMP-manufactured providing a consistent environment for hES cell culture. However this medium also requires culture in the presence of Geltrex (reduced growth factor basement membrane matrix purified from Engelbreth-Holm-Swarm tumor; similar to Matrigel).

In an effort to exclude animal-derived components from the culture media, several products are being marketed which consist of either human derived components or human feeder cells. HEScGRO (Milipore, Billerica, MA) is a serum-free and animal component-free medium which has been shown to maintain various hES cell lines in the pluripotent state. However, use of mitotically-inactivated human feeder cell layers is recommended for successful hES cell culture in this medium. More recently, a serum-free medium conditioned with a proprietary human cell type (GlobalStem Inc., Rockville, MD) has been developed for culture of undifferentiated and pluripotent hES cells.

Since long-term culture in the presence of the aforementioned defined media requires the use of naturally-derived matrices, development of a synthetic polymer matrix that can support hES cell expansion in defined media is important. This will enhance the knowledge of factors that regulate stem cell growth and differentiation, furthering the use of hES cells in biotechnology, and enable potential clinical applications. In this chapter, the application of zwitterionic polymer PMEDSAH (described in chapter 4) was extended towards fully-defined culture environments.

5.2 Methods

Polymer synthesis

Polymer coatings were prepared on tissue culture polystyrene (TCPS) dishes (35 mm; Becton Dickinson and Co, Franklin Lakes, NJ). Graft-polymerization was carried out using a 0.25 M solution of methacrylate monomers (Sigma-Aldrich, MO) in a 4:1 mixture of water and ethanol.[22] The TCPS dishes were activated using a UV-ozone cleaner (Jelight Co. Inc, Irvine, CA) for 40 min. Surface-activated dishes were immersed into the monomer solution at 80 $^{\circ}$C for 2.5 h. Polymer-coated dishes were allowed to cool to 50 $^{\circ}$C and were rinsed with a warm saline solution (1% NaCl in water, at 50 $^{\circ}$C). Polymer-coated dishes were then left overnight in saline solution at 50 $^{\circ}$C. Dishes were cleaned by ultra-sonication in DI-water and dried under a stream of nitrogen gas. Polymer-coated dishes were stored at room temperature prior to cell culture. For FTIR spectroscopy and elllipsometry, a gold-coated substrate coated with poly-*p*-xylylene was included in each graft-polymerization reactions.[23]

Characterization of polymer coatings

Elemental analysis of the polymer coatings was conducted using X-ray photoelectron spectroscopy (Axis Ultra XPS, Kratos Analyticals, UK) equipped with a monochromatized Al Kα X-ray source. Spectra were referenced to an unfunctionalized aliphatic carbon at 285.0 eV. Presence of polymer coatings was confirmed using Fourier transform infrared (FTIR) spectroscopy (Nicolet 6700 spectrometer) using the grazing angle accessory (SAGA) with a grazing angle of 85°. Coating thickness was recorded at a wavelength of 532 nm using EP^3-SW imaging ellipsometer (Nanofilm Technology GmbH, Germany). Four-zone nulling was performed at an angle of incidence of 70° and

an anisotropic Cauchy parameterization model was used for curve fitting. Nanoindentation was performed by CSM instruments Inc (Needham, MA) using a CSM NanoHardness tester equipped with a conospherical diamond tip (with a radius of 20 µm) in the load-control mode. A typical nanoindentation experiment involved engaging the tip under loading rate of 1.00 mN/min, indenting to a maximum load of 0.5 mN, and then withdrawing the tip with the same rate as for the loading. For each hydrogel coating, load-displacement data was acquired for 5 indentations. Reduced modulus (Er) was calculated using the unloading portions of these load-displacement curves according to a method developed by Gerberich et al.[24]

Enzyme linked immunosorbent assay (ELISA) for bFGF binding

ELISA kit for bFGF (Raybiotech Inc., Norcross, GA) was used to study differences in bFGF binding to PMEDSAH- and PMAPDSAH- coated surfaces. ELISA assay was performed on each polymer in triplicates. Defined medium, mTeSR (1 ml) was added to each dish and incubated overnight at 37 ^{o}C. The dishes were washed with the wash buffer (provided in the kit) twice to remove unbound bFGF and incubated with biotinylated anti-human FGF (500 µl) for 45 min. The dishes were washed twice with the wash buffer and incubated with HRP-streptavidin (500 µl) for 45 min. After two washing cycles, TMB substrate solution (250 µl) was added for 30 min for development of color which is proportional to the amount of bFGF bound to the surface. Finally, a stop solution was added which changed the color from blue to yellow and the intensity of color was measured at 450 nm using a microplate reader (BioTek). Uncoated TCPS dishes were used as control substrates

Preparation of polymer-coated dishes before cell culture

Before cell seeding, all polymer-coated dishes were sterilized with UV-light for overnight (12 h), washed twice with sterile phosphate buffer saline (PBS) and equilibrated with culture medium for at least 48 h at 37 ^{o}C in 5% CO_2 atmosphere.

Cell culture media preparation

Culture medium for hES cells cultured on irradiated MEFs contained standard DMEM/F12 supplemented with 20% KnockOut serum replacement (GIBCO), 0.1 mM β-mercaptoethanol, 1 mM L-glutamine, 1% non-essential amino acids and 4 ng/ml human recombinant basic fibroblast growth factor (Invitrogen; Carlsbad, CA).

MEF-CM was prepared as described previously.[25] Irradiated MEFs ($8x10^6$ cells) were seeded onto gelatin-coated culture dishes in medium composed of high glucose DMEM, 10% fetal bovine serum (FBS; GIBCO), 1% non-essential amino acids, and 200 mM L-glutamine. After 24 h, MEF culture medium was replaced with the hES cell culture medium described above (60 ml). This medium was left in contact with MEFs and was collected as MEF-CM after 24 h of conditioning. Media exchange was conducted daily and MEF-CM was collected for 3 days. The MEF-CM was frozen at -20 ^{o}C and was supplemented with 0.1 mM β-mercaptoethanol, 2 mM L-glutamine, and 4 ng/ml bFGF before use.

Human-cell-conditioned-medium (hCCM, GlobalStem, Inc., Rockville, MD), mTeSR^{TM}1 (STEMCELL Technologies, Vancouver, BC) and StemPro®hESC SFM (Invitrogen, Carlsbad, CA) were prepared according to manufacturers' protocols, with the exception that defined medium, StemPro was prepared with DMEM/F12 plus L-glutamine and 15 mM HEPES (GIBCO). Media were pre-equilibrated at 37 ^{o}C in 5% CO_2 atmosphere before use.

Media were pre-equilibrated at 37 $^{\circ}$C in 5% CO_2 atmosphere before use.

Cell culture

Federally-approved hES cell line H9 (NIH code: WA09; WiCell, Madison, WI) was used and cultured at 37 $^{\circ}$C with 5% CO_2. Human ES cell colonies were observed every 48 h using a Leica stereomicroscope and differentiated cells were removed mechanically using a sterile "pulled-out" glass pipette. Cell culture medium was replaced every 48 h.

Cell culture media transition and passaging

Before mechanical harvesting of hES cells growing on MEFs, cell culture medium was replaced by either MEF-CM or hCCM. Similarly, a transition to defined media was performed. Cultures were passaged depending on size and density of colonies every 7-10 days. Undifferentiated hES cell colonies were then mechanically passaged by cutting small aggregates of cells using a sterile "pulled-out" glass pipette. About 50-100 hES cell-aggregates were transferred to polymer-coated dishes.

Cell-aggregate adhesion assay

Number of adhered colonies and number of floating embryoid bodies (EBs) were counted 48 h after cell seeding, to calculate the percentage of cell-aggregate adhesion using the following formula:

Cell-aggregate adhesion (%) = (number of adhered colonies)*(100)/(number of adhered colonies + number of EBs floating). Statistics were performed using an unpaired t-test.

Cell population-doubling time

Cell population-doubling time was calculated in terms of time required for the area of a colony to increase two-fold.[26] ImageJ software (http://rsb.nih.gov/ij) was used to measure area of the colonies. Colony area (n=10) was calculated at five time-points (for 5 days after cell seeding), and cell population-doubling time was determined by fitting an exponential function. Mean values were compared using an unpaired t-test.

Immunocytochemistry

Cells were fixed in 2% paraformaldehyde for 30 min at room temperature and then permeabilized with 0.1% Triton X-100 for 10 min. Primary antibodies were diluted in 1% normal donkey serum and incubated overnight at 4 ^{o}C and detected by respective secondary antibodies. Samples were imaged and captured using a Leica DM IRB inverted microscope with an Olympus DP-30 CCD camera. Throughout this study, hES cells were characterized every fifth passage by detection of the following hES cell markers: OCT3/4, SOX2, SSEA4, TRA-1-60 and TRA-1-81.

ImageJ software was used to count the number of OCT3/4 or SOX2 positive cells and number of cell nuclei present in each colony. Percentage of cells positive for each marker was calculated for colonies cultured on PMEDSAH- and Matrigel- coated plates. Unpaired t-test was used to calculate p values.

Cytogenetic analysis

Karyotype analysis was performed at Cell Line Genetics (Madison WI) applying standard protocols utilizing the GTL-banding method on at least 20 cells.

Evaluation of pluripotency

Undifferentiated H9 hES cells ($< 5x10^6$ cells) cultured on PMEDSAH and Matrigel in MEF-CM at passage 25 were injected subcutaneously into CB17 SCID mice (Charles River Laboratories, Wilmington, MA) to induce teratomas. When tumors became palpable, mice were euthanized; tumors were harvested, and processed for histological analysis at the Center for Organogenesis Morphology core (University of Michigan).

Pluripotency was also evaluated by EB formation from undifferentiated hES cells. Colonies were cultured in suspension in hES cell culture medium lacking bFGF to promote differentiation, for 10 days. Alternatively, hES cells were allowed to overgrow in MEF-CM without bFGF for 10 days.

Extraction and purification of total RNA

Cells were manually scraped from dishes and pelleted by centrifugation at 800 g. Pellets were then disrupted by vigorous pipetting in 1000 µl of Trizol Reagent (Invitrogen). Chloroform (200 µl) was added to this solution followed by centrifugation (~13,000 x g). Aqueous phase containing RNA was separated and additionally purified using the RNeasy Mini-Kit (Qiagen, Valencia, CA) following the manufacturer's RNA Clean-up protocol with the optional On-column DNAse treatment. RNA quality was

checked using RNA 6000 Nano assays performed on the Bioanalyzer 2100 Lab-on-a-Chip system (Agilent Technologies, Palo Alto, CA).

Reverse-transcription PCR (RT-PCR) analysis

Total RNA was reverse transcripted using SuperScript™ One-Step RT-PCR with platinum® Taq (Invitrogen). In a single reaction (50 μl), 1 μg of total RNA and 20 pmol of forward (f) and reverse (r) primers were used (Supplementary Table II online). The cDNA synthesis and pre-denaturation were carried out in the first cycle at 48 ºC for 45 min, followed by a second cycle at 94 ºC for 2 min. The PCR amplification was performed for 35 cycles at 94 ºC for 15 sec, 5 ºC for 30 sec, and 72 ºC for 1 min. The final extension cycle was run at 72 ºC for 8 min. Finally, 10 μl of PCR reaction products were loaded onto a 1.0% agarose gel and size-fractionated.

5.3 Results and discussion

Physicochemical parameters such as surface topography, surface energy, surface charge and chemical composition of the surface have a profound effect on cellular response.[27] The development of a standardized, controllable and sustainable culture matrix for hES cell populations constitutes an important step to elucidate basic stem cell function and may contribute towards future biotechnological and medical applications of hES cells.

Polymer synthesis and characterization

PMEDSAH and PMAPDSAH were synthesized by surface-initiated graft-polymerization directly onto tissue culture polystyrene (TCPS) dishes.[22]

Chemical composition of the polymer coatings was confirmed using Fourier transform infrared spectroscopy (FTIR) and X-ray photoelectron spectroscopy (XPS).

Distinct IR bands at 1732.9 cm^{-1}, 1485 cm^{-1} and 1208.4 cm^{-1} indicated presence of carbonyl, quaternary ammonium and sulfonate groups respectively and clearly identified the PMEDSAH coatings. To further confirm evidence from FTIR studies, the elemental composition of PMEDSAH was quantified by means of XPS. Presence of characteristic signals associated with nitrogen, sulfur and oxygen at 402.0 eV, 168.0 eV and 532.0 eV, respectively as well as the relative composition of these elements showed good agreement with the expected chemical composition of PMEDSAH. In addition, the high resolution C1s XPS spectrum of PMEDSAH revealed characteristic signals associated with hydrocarbon ($\underline{C}$-H/C) at 285.0 eV, ammonium-bond carbon ($-\underline{C}$-N$^+$(CH$_3$)$_2$-) at 286.4 eV, and ester carbon ($-\underline{C}$OO-) at 288.9 eV (Figure 5.1). Taken together, FT-IR and XPS analyses not only established the chemical composition of PMEDSAH coating, but also provided strong evidence for the presence of sulfonate and ammonium groups at the surface

Elemental analysis of PMAPDSAH using XPS revealed the presence of characteristic signals associated with carbon (285 eV), nitrogen (402 eV), oxygen (532 eV) and sulfur (168 eV for S 2p) and the relative composition of these elements showed good agreement with the theoretical composition of the polymer (Table 5.1). In addition, from the XPS survey spectrum of PMAPDSAH, the ratio of nitrogen to sulfur was calculated to be 1.7 which compared well with the theoretical value of 2 and differs from that calculated for PMEDSAH (N:S = 1).

Contact angle measurements showed that the contact angle of PMAPDSAH was 60.1±6.4^{o} compared to 17.1±1.1^{o} for PMEDSAH-coated dishes and 90.2±4.6^{o} for uncoated TCPS (Table 5.2). Thus, PMAPDSAH-coated surfaces were more hydrophobic compared to PMEDSAH but slightly more hydrophilic than the uncoated TCPS surfaces.

Nanoindentation measurements revealed that PMAPDSAH coatings had a higher elastic modulus of 3.3±0.2 GPa than that for PMEDSAH (2.5±0.1 GPa), further highlighting the differences between the two polymers (Table 5.2).

Enzyme linked immunosorbent assay (ELISA) for bFGF binding

It has been demonstrated that basic fibroblast growth factor (bFGF) is essential for the culture of undifferentiated hES cells, especially in feeder-free culture environments.[28, 29] In addition, bFGF rapidly degrades under standard cell culture conditions and requires specific stabilization.[30, 31] In the past, it has been observed that mouse embryonic fibroblast conditioned medium (MEF-CM) can stabilize about 75% of exogenous bFGF, while unconditioned medium requires a higher initial concentration of bFGF to offset the bFGF degradation.[31] Proteomic analysis of MEF-CM showed that the bFGF stabilization effect in MEF-CM was due to heparin sulfate proteoglycans secreted by the MEFs.[31] This stabilization can be achieved through the addition of exogenous stabilization factors such heparin sulfate proteoglycans or structural motifs attached to the surface which mimic the effect of heparin.

To better understand the underlying mechanisms governing the behavior of hES cells towards the two zwitterionic polymers, binding of bFGF was studied using an enzyme linked immunosorbent assay (ELISA). The polymer-coated and uncoated dishes were incubated with mTeSR medium (overnight at 37 ^{o}C) and bFGF ELISA was performed. The assay revealed that there was 2-fold higher binding of bFGF to the

111

zwitterionic polymer-coated surfaces compared to uncoated TCPS surfaces (Figure 5.2).
This finding leads to the hypothesis that the zwitterionic sulfobetaine coatings may be
involved in mediating an increased binding of FGF to the surface, thus stabilizing the
growth factor longer during culture.

hES cell culture on PMEDSAH in xeno-free conditions

Towards a clinically-compliant hES cell culture system consisting of the synthetic
matrix and a xeno-free medium, BG01 and H9 hES cells were grown on PMEDSAH-
coated dishes in the presence of a commercially-available human-cell-conditioned-
medium (hCCM). After 15 passages, BG01 and H9 cells showed similar cell population-
doubling times, expressed hES cell markers, retained normal karyotypes and remained
pluripotent (Figure 5.3). Interestingly, a significant increase in H9 hES cell-aggregate
adhesion was observed on PMEDSAH using hCCM (86±6%) compared to MEF-CM
(15±1%; Figure 5.4(A)). Cell-aggregate adhesion was also significantly higher for H9
cells in hCCM than for BG01 cells cultured under the same conditions (47±5%; Figure
5.3(C)) suggesting that there may be important biological differences between cell lines
in their expression of adhesion receptors.

hES cell culture in defined conditions

PMEDSAH was examined for its ability to support hES cell cultures in two
serum-free defined media (StemPro and mTeSR).[14, 15, 17, 21] StemPro medium was able to
support 10 passages of H9 hES cells (Figure 5.4) However, BG01 hES cells could not be
passaged beyond 3 passages in StemPro. After 10 passages of H9 cells in StemPro
medium, cell population-doubling times, expression of undifferentiated and pluripotent

markers, and normal karyotypes were confirmed (Figure 5.4(A,B)). Moreover, H9 cells maintained the ability to differentiate into endoderm, mesoderm and ectoderm (Figure 5.4(C,D)). On the other hand, hES cells grown in mTeSR could not be sustained on PMEDSAH.

Further, PMAPDSAH was investigated for its ability to sustain hES cell culture in defined media. Unlike PMEDSAH, H9 cells were grown on PMAPDSAH in mTeSR for 5 passages. Furthermore, PMAPDSAH also supported the proliferation of H9 hES cells in StemPro medium for 5 passages. Under both conditions, the cells expressed standard undifferentiated and pluripotent hES cell markers (Figure 5.5).

5.4 Conclusions

The work presented in this chapter represents a significant step towards a fully defined, reproducible culture system for hES cell expansion. Moving forward, this defined polymer coating provides us a platform to study the underlying mechanisms governing cell-biomaterial interactions, by removing all the variable factors previously present in the system. In addition, growth in fully-defined culture conditions has also allowed us to identify previously unsuspected differences between hES cell lines. This system represents a unique defined cellular microenvironment- chemically-defined substrate combined with a defined cell culture medium.

5.5 Figures and Tables

(A)

(B)

Element	% experimental	% theoretical
Carbon	72.7	61.1
Nitrogen	3.2	5.6
Oxygen	20.9	27.8
Sulfur	3.2	5.6

XPS Peak position	Component peaks	% experimental	% theoretical
284.9	hydrocarbon (C–C–C)	45.9	54.5
286.3	ammonium carbon (-C-N$^+$(CH$_3$)$_2$-); ether (-C-O); carbon next to ester (-C-COO-)	44.8	36.4
289.0	ester carbon (-COO)	9.9	9.1
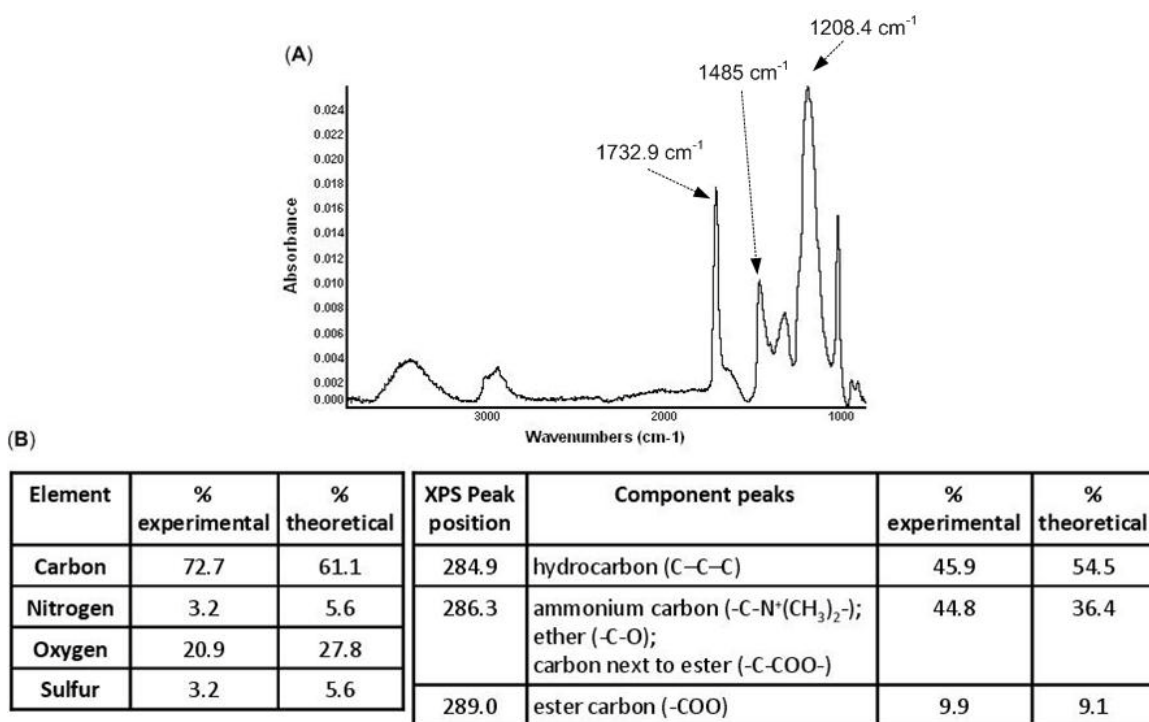
Figure 5.1: Surface characterization of PMEDSAH. (A) Fourier transform infrared (FTIR) spectrum of PMEDSAH coating showing distinct bands at 1732.9 cm^{-1}, 1485 cm^{-1} and 1208.4 cm^{-1} which indicated the presence of carbonyl, quaternary ammonium and sulfonate groups, respectively. (B) Table lists elemental composition of PMEDSAH attained using X-ray photoelectron spectroscopy (XPS). Relative composition of these elements was in agreement with the expected chemical composition of PMEDSAH. Second table lists characteristic signals from high resolution C$_{1s}$ XPS spectrum of PMEDSAH. Signals associated with different chemical environments of carbon present in the polymer chain and the corresponding concentrations are given. These values correlate well with the theoretical values calculated based on the chemical structure of the polymer.
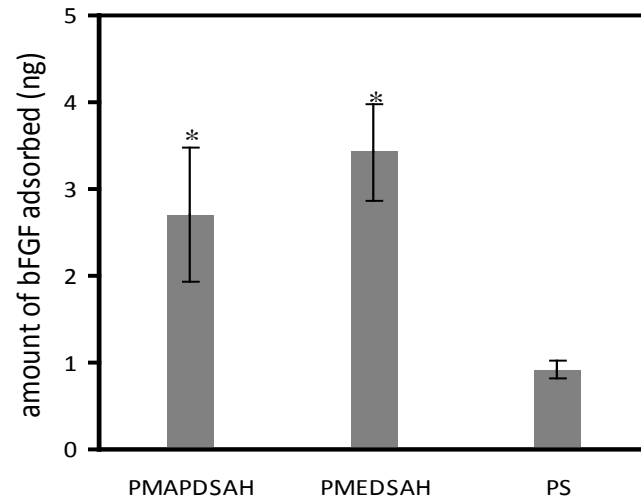
Figure 5.2: Amou[nt]...[PMAPDSAH and PMEDS]AH-coated dishes compared to uncoated TCPS dishes detected by bFGF ELISA (*p<0.05).
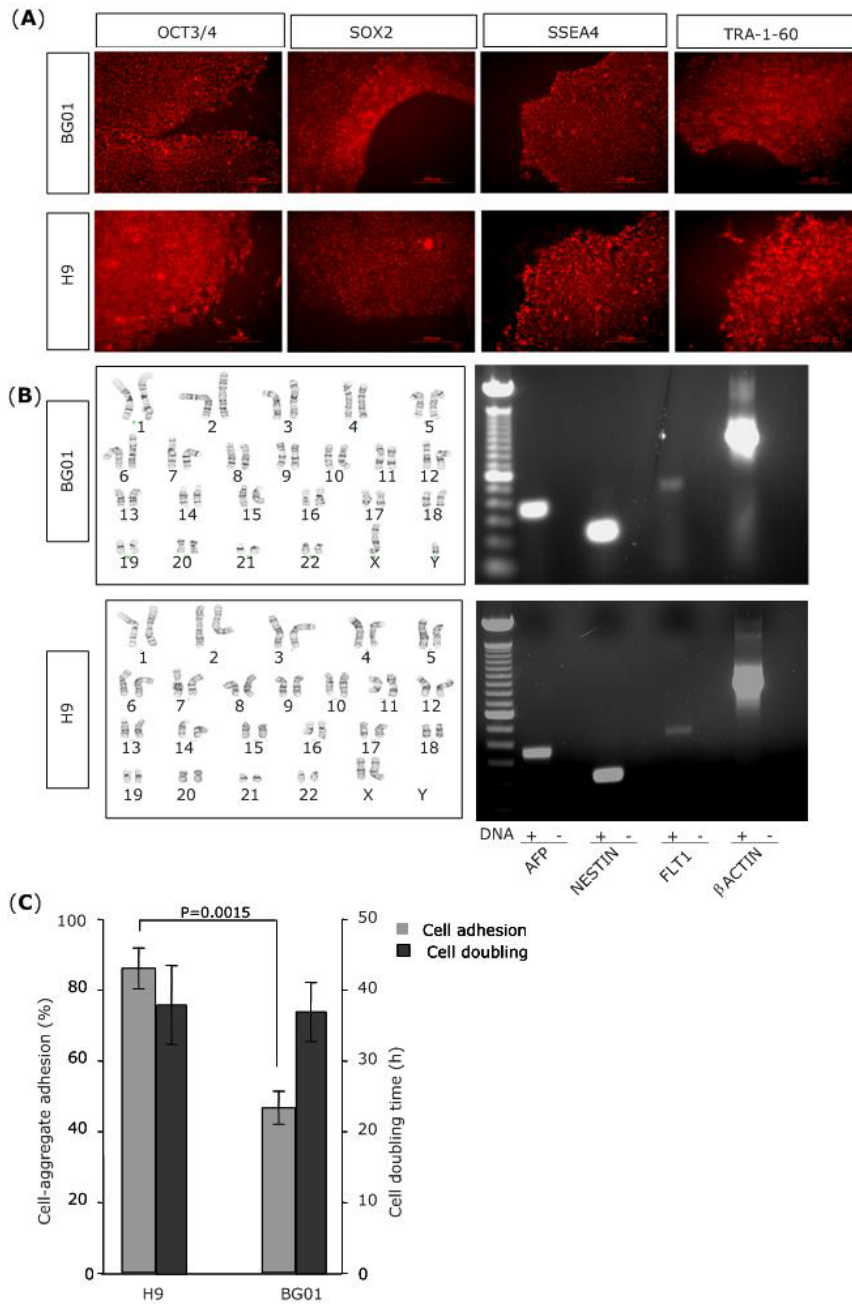
Figure 5.3: Characterization of BG01 and H9 hES cells on PMEDSAH in hCCM. (A) Fluorescence micrographs of colonies showing expression of undifferentiated markers: OCT3/4, SOX2, SSEA-4 and TRA-I-60. (B) Representative chromosomal spreads and RT-PCR analysis of embryoid bodies showing transcript expression of endoderm (AFP), ectoderm (NESTIN) and mesoderm (FLT-1). β-ACTIN was used as positive control and for each primer set tested, a reaction lacking RNA was assessed in parallel as a negative control. (C) Comparison of percentage of cell-aggregate adhesion and cell population-doubling time of both cell lines cultured on PMEDSAH in hCCM.
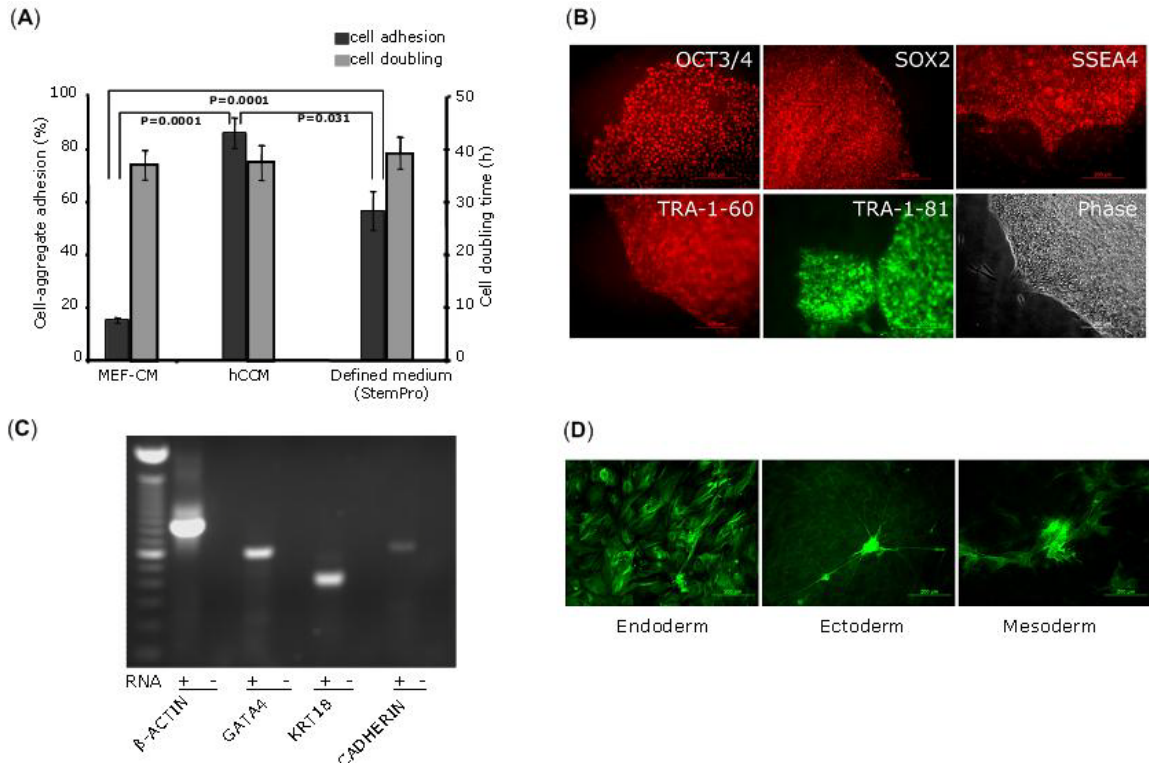
Figure 5.4: PMEDSAH supports culture of hES cells in defined medium. (A) Percentage of cell-aggregate adhesion (number of aggregates attached with respect to total aggregates passaged) and population doubling time (2-fold increase in colony area) for H9 hES cells cultured on PMEDSAH in MEF-CM, hCCM and defined medium. (B) Fluorescence micrographs of colonies of H9 cells cultured on PMEDSAH in StemPro medium showing expression of pluripotency markers: OCT3/4, SOX2, SSEA-4, TRA-I-60 and TRA-I-81; and phase-contrast image. (C) RT-PCR analysis of RNA from embryoid bodies showing expression of endoderm (GATA-4), ectoderm (KRT-18) and mesoderm derivatives (VE-CADHERIN). β-Actin was used as positive control and for each primer set tested, a reaction lacking RNA was assessed in parallel as a negative control. (D) Micrographs showing immunoreactivity for α-fetoprotein (endoderm), β-III tubulin (ectoderm) and smooth muscle actin (mesoderm) demonstrating the pluripotent state of H9 cells cultured on PMEDSAH in StemPro medium. Scale bars indicate 200 μm.
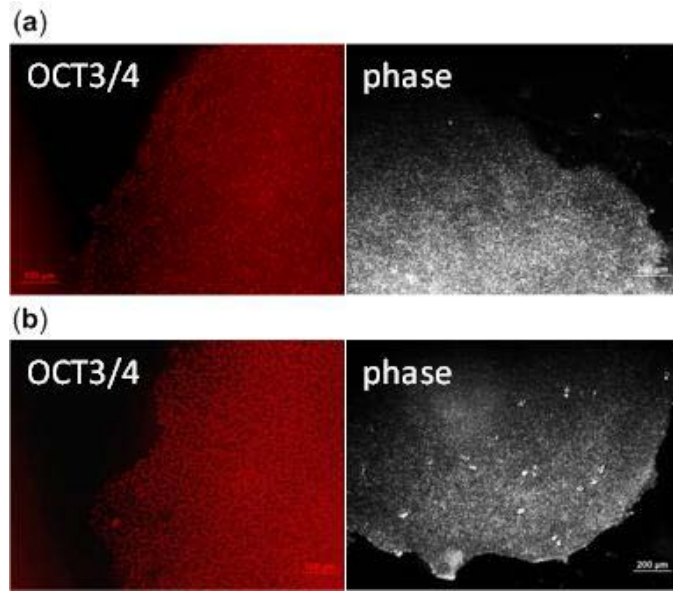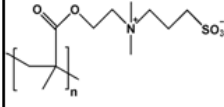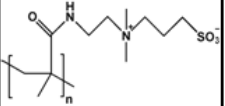
Figure 5.5: Characterization of hES cells cultured on PMAPDSAH in defined media (a) StemPro (b) mTeSR. Fluorescence micrographs of colonies of H9 cells cultured on PMAPDSAH showing expression of undifferentiated marker, OCT3/4 and phase-contrast image

Table 5.1: Elemental composition of PMAPDSAH attained using XPS. Relative composition of the elements was in agreement with the expected chemical composition of PMAPDSAH.

Element	XPS Peak position	% experimental	% theoretical
Carbon (C 1s)	285	75.4	61.1
Nitrogen (N 1s)	402	5	11.1
Oxygen (O 1s)	532	16.6	22.2
Sulfur (S 2p)	168	3	5.6

Table 5.2: Contact angle, reduced elastic modulus (GPa) for PMEDSAH and PMAPDSAH and initial hES cell-aggregate adhesion (%) in different media- MEF-CM, StemPro and mTeSR.

		PMEDSAH	PMAPDSAH
Contact angle		17.1±1.1	60.1±6.4
Reduced elastic modulus (GPa)		2.5±0.1	3.3±0.2
Cell-aggregate adhesion (%)	MEF-CM	15±1	50±1
	StemPro	56±7	70±2
	mTeSR	0	50±5

5.6 References

1.   Metallo, C.M. et al. Engineering the stem cell microenvironment. *Biotechnology Progress* **23**, 18-23 (2007).
2.   Hammer, D.A. & Tirrell, M. Biological adhesion at interfaces. *Annu. Rev. Mater. Sci.* **26**, 651-691 (1996).
3.   Nel, A.E. et al. Understanding biophysicochemical interactions at the nano-bio interface. *Nature Materials* **8**, 543-557 (2009).
4.   Guilak, F. et al. Control of stem cell fate by physical interactions with the extracellular matrix. *Cell Stem Cell* **5**, 17-26 (2009).
5.   Ross, A.M. & Jason, A.B. Controlling stem cell fate with material design. *Advanced Materials* (2009).
6.   Janmey, P.A. & McCulloch, C.A. Cell mechanics: Integrating cell responses to mechanical stimuli. *Annual Review of Biomedical Engineering* **9**, 1-34 (2007).
7.   Dawson, E., Mapili, G., Erickson, K., Taqvi, S. & Roy, K. Biomaterials for stem cell differentiation. *Advanced Drug Delivery Reviews* **60**, 215-228 (2008).
8.   Engler, A.J., Sen, S., Sweeney, H.L. & Discher, D.E. Matrix elasticity directs stem cell lineage specification. *Cell* **126**, 677-689 (2006).
9.   Abraham, S., Eroshenko, N. & Rao, R.R. Role of bioinspired polymers in determination of pluripotent stem cell fate. *Regenerative Medicine* **4**, 561-578 (2009).
10.   Azzaroni, O., Brown, A.A. & Huck, W.T.S. UCST wetting transitions of polyzwitterionic brushes driven by self-association. *Angewandte Chemie, International Edition* **45**, 1770-1774 (2006).
11.   Cheng, N., Brown, A.A., Azzaroni, O. & Huck, W.T.S. Thickness-dependent properties of polyzwitterionic brushes. *Macromolecules* **41**, 6317-6321 (2008).
12.   Ding, V., Choo, A.B.H. & Oh, S.K.W. Deciphering the importance of three key media components in human embryonic stem cell cultures. *Biotechnology Letters* **28**, 491-495 (2006).
13.   Rajala, K. et al. Testing of nine different xeno-free culture media for human embryonic stem cell cultures. *Human Reproduction* **22**, 1231-1238 (2007).
14.   Ludwig, T.E. et al. Derivation of human embryonic stem cells in defined conditions. *Nat Biotechnol* **24**, 185-187 (2006).
15.   Wang, L. et al. Self-renewal of human embryonic stem cells requires insulin-like growth factor-1 receptor and ERBB2 receptor signaling. *Blood* **110**, 4111-4119 (2007).
16.   Braam, S.R. et al. Recombinant vitronectin is a functionally defined substrate that supports human embryonic stem cell self-renewal via alpha V beta 5 integrin. *Stem Cells* **26**, 2257-2265 (2008).
17.   Brafman, D.A., Shah, K.D., Fellner, T., Chien, S., Williert, K. Defining long-term maintenance conditions of human embryonic stem cells with arrayed cellular microenvironment technology. *Stem Cells and Development* **18** (2009).
18.   Mallon, B.S., Park, K.Y., Chen, K.G., Hamilton, R.S., McKay, R.D. Toward xeno-free culture of human embryonic stem cells. *Int J Biochem Cell Biol* **38**, 1063-1075 (2006).

19. Martin, M.J., Muotri, A., Gage, F. & Varki, A. Human embryonic stem cells express an immunogenic nonhuman sialic acid. *Nat Med* **11**, 228-232 (2005).
20. Ludwig, T.E. et al. Feeder-independent culture of human embryonic stem cells. *Nature Methods* **3**, 637-646 (2006).
21. Prowse, A.B., Wilson, J., Osborne, G.W., Gray, P.P., Wolvetang, E.J. Multiplexed staining of live human embryonic stem cells for flow cytometry analysis of pluripotency markers. *Stem Cells and Development* (2009).
22. Wu, J.M. et al. A surface-modified sperm sorting device with long-term stability. *Biomedical Microdevices* **8**, 99-107 (2006).
23. Lahann, J. & Langer, R. Novel poly(p-xylylenes): Thin films with tailored chemical and optical properties. *Macromolecules* **35**, 4380-4386 (2002).
24. Gerberich, W.W. et al. Elastic loading and elastoplastic unloading from nanometer level indentations for modulus determinations. *J. Mater. Res.* **13**, 421-439 (1998).
25. Villa-Diaz, L.G. et al. Analysis of the factors that limit the ability of feeder-cells to maintain the undifferentiated state of human embryonic stem cells. *Stem Cells Dev* (2008).
26. Reubinoff, B.E., Pera, M.F., Vajta, G. & Trounson, A.O. Effective cryopreservation of human embryonic stem cells by the open pulled straw vitrification method. *Human reproduction (Oxford, England)* **16**, 2187-2194 (2001).
27. Engel, E., Michiardi, A., Navarro, M., Lacroix, D. & Planell, J.A. Nanotechnology in regenerative medicine: the materials side. *Trends in Biotechnology* **26**, 39-47 (2008).
28. Levenstein, M.E. et al. Basic fibroblast growth factor support of human embryonic stem cell self-renewal. *Stem Cells* **24**, 568-574 (2006).
29. Amit, M., Shariki, C., Margulets, V. & Itskovitz-Eldor, J. Feeder layer- and serum-free culture of human embryonic stem cells. *Biol Reprod* **70**, 837-845 (2004).
30. Kreuger, J., Spillmann, D., Li, J.P. & Lindahl, U. Interactions between heparan sulfate and proteins: the concept of specificity. *J. Cell Biol.* **174**, 323-327 (2006).
31. Levenstein, M.E. et al. Secreted Proteoglycans Directly Mediate Human Embryonic Stem Cell-Basic fibroblast growth factor 2 interactions critical for proliferation. *Stem Cells* **26**, 3099-3107 (2008).

CHAPTER 6

NITRIC OXIDE GENERATING STENT COATINGS

Abstract

This chapter describes a robust polymer coating that includes a novel nitric oxide generating chemistry. This coating was applied to intravascular stents such that the interface mimics the natural surface of endothelial cells (EC) that line all blood vessels with respect to NO generation. Briefly, chemical vapor deposition (CVD) was used to deposit functionalized coatings on the metallic stent surface. The functional groups were then used to attach catalytic sites that generate NO from endogenous plasma components (such as nitrosothiols). These coatings attempt to solve the problems of restenosis and thrombosis associated with the placement of coronary artery stents.

6.1 Introduction

Cardiovascular stents prompt a complex inflammatory healing reaction in the body as a result of interaction between the metallic stent surface and components in the blood. This includes processes such as protein adhesion, platelet activation, smooth muscle cell proliferation and thrombus formation over the stent surface.[1] In recent years, various surface coatings have been applied to stents in order to reduce in-stent restenosis (re-narrowing of a coronary artery after treatment with a stent) and thrombosis.[2-4]

Bioactive coatings containing restenosis-preventing drugs combined with a polymer-carrier, capable of releasing the drug, have been developed and marketed

123

extensively.[5, 6] These drug-eluting stents have become extremely popular because of their ability to deliver the drug locally as opposed to systemic drug delivery with high dosages. However, these systems are limited by the amount of drug loaded onto the stent and their success depends on the favorable interactions between the various components of the complex. Furthermore, the use of exogenous drugs to decrease the biological response to stents is based upon the assumption that interruption of one of the intermediate processes will be sufficient to prevent restenosis

An ideal stent coating would inhibit multiple pathways (both restenosis and thrombosis in addition to inflammation and infection) without causing systemic affects. Such a strategy, however, requires not only the identification of suitable therapeutic agent(s) with short biological half lives, but also advances in polymer technology to fabricate polymers that act as sophisticated drug carriers. An alternative for the development of blood-compatible materials is the creation of coatings which release naturally-occurring active agents such as nitric oxide. Nitric oxide has been recognized as anti-inflammatory, nonthrombogenic and a promoter of wound-healing, thus highly suitable for biomedical coatings.[7] NO is a naturally-occurring regulator in the human body, which plays a prominent role in the prevention of inflammation, thrombosis, atherosclerosis and promotes wound-healing.[8] NO is continuously released by vascular endothelial cells at an approximate flux of 1×10^{-10} mol/cm^2-min. Moreover, NO has an extremely short lifetime in blood (<1 sec) owing to rapid reaction with hemoglobin. Thus, the positive effects of nitric oxide can be exploited to enhance the properties of blood-contacting biomedical devices.

A number of coatings have been developed for catheters and sensors, which locally release NO from molecules acting as NO donors such as diazeniumdiolates.[9-15] However, long-term applicability of such coatings is limited by the amount of the NO-adducts loaded onto the stent.

It has been recently reported that blood contains a reservoir of NO precursors in the form of S-nitrosothiols (RSNO) and polymeric coatings containing lipophillic copper(II) complexes are capable of catalytically decomposing these endogenous RSNO species to NO in the presence of reducing molecules.[16] It was successfully demonstrated that films containing a Cu(II) ligated cyclen (1,4,7,10-tetraazacyclododecane) linked to a methacrylate polymer network can catalytically generate NO, both in buffer solution and in contact with fresh blood.[17] These coatings were capable of locally generating NO for extended periods of time. Cyclens are strong Cu(II) binders with binding constants approaching 10^{24} M^{-1}. In addition, the cyclen complex can be easily modified to contain functional groups, such as a methacrylate group, which allows for polymerization with other monomers.

In this chapter, the challenge of applying the abovementioned chemistry to a stent surface in a robust manner is addressed. Herein, the synthesis of polymer coatings which catalytically generate NO in physiological ranges, from endogenous RSNOs and nitrites present in the blood, is reported. This mechanically-stable coating was successfully applied to stents and NO generation was observed *in vitro* in buffer solution. The main advantages of such a NO-generating stent coating (as opposed to the drug-eluting stents) is that it generates a naturally-occurring agent and is not limited by the drug loading. The coatings were extensively characterized with respect to chemical composition, adhesion and stability.

6.2 Methods

Synthesis of cyclen methacrylate

Cyclen methacrylate was synthesized and characterized as previously described.[17]

Modification of stent surface with polymethacrylate/Cu(II)-cyclen coating

Stainless steel stents were coated with the photoreactive CVD polymer, poly[(4-benzoyl-*p*-xylylene)-co-(*p*-xylylene)] (PPX-CO-Ph), using standard CVD conditions.[18, 19] Starting material, 4-benzoyl[2.2]paracyclophane, was sublimed under vacuum (pressure of 0.5 mbar) and was converted by pyrolysis into reactive species, which polymerized after condensation on the substrate. Sublimation temperatures were kept between 110-130 °C, while pyrolysis temperature was 800 °C. Subsequently, polymerization occurred on a rotating, cooled sample holder placed inside a stainless steel chamber with a wall temperature of 130 °C. A carrier gas was used throughout the CVD polymerization with constant argon flow of 20 sccm.

A solution containing cyclen methacrylate (30%), 2-hydroxyethylmethacrylate (HEMA; Sigma-Aldrich, 60%) and polyethylene glycol dimethacrylate (PEG-dMA; Sigma-Aldrich, 10%) in methanol was spin-coated onto the stent. The stent was then exposed to broad-range UV radiation (~ 320 nm) for 30 min with constant rotation of the stent. The stent was then washed with DI-water and incubated in $CuCl_2$ solution (10 mM in DI-water) for 3 hours at 50 °C. Finally the coated stent was rigorously washed with DI-water to remove any non-specifically bound copper. For FTIR and ellipsometric analyses, flat stainless steel samples (Goodfellow, Cambridge, UK) were similarly coated.

Characterization of polymer coating

The elemental composition of the coatings was determined using Axis Ultra X-ray photoelectron spectrometer (Kratos Analyticals, UK) equipped with a monochromatized Al K_α X-ray source. Lens mode was in hybrid, pass energy was set to

160.0 eV with an X-ray power of 150 kW, and aperture was 600µm x 600µm.. Elemental maps of carbon (C1s), nitrogen (N1s) and copper (Cu2p) were performed at 285, 400 and 930 eV respectively with an X-ray power of 150 kW. Fourier transform infrared (FTIR) spectroscopy was performed on a Nicolet 6700 spectrometer utilizing the grazing angle accessory (Smart SAGA) at a grazing angle of 85°. Scanning electron microscopy (SEM; FEI Quanta 200 3D) was employed to observe the morphology of before and after coating.

In vitro nitric oxide measurements

The stent was placed in a vial and PBS buffer (1 ml) was added. The buffer was degassed by bubbling nitrogen gas through the system. GSNO and GSH were injected into the system. The nitric oxide generated was measured using chemiluminescence measurements. NO flux was measured in the presence of 18 µM GSNO, 53.4 µM GSH and 2.5 µM EDTA

Results and discussion

Fabrication of polymethacrylate/Cu(II)-cyclen coating

One of the main challenges is transferring the bioactive NO-generating polymeric coating onto the metallic stent surface. Thus a two-component approach was employed to apply the NO-generating polymer to the stent surface (Figure 6.1). The top-most layer was composed of the polymethacrylate part containing the active cyclen-Cu complex. To attach the polymethacrylate coating to the metallic stent surface, a thin vapor-based polymer film was used as an adhesive layer. This base anchoring layer was a

127

photoreactive polymer (Figure 6.1c) fabricated using chemical vapor deposition (CVD) polymerization, employing a CVD installation consisting of a sublimation zone, pyrolysis zone and deposition chamber.[18-20] For CVD polymerization, the precursor was slowly sublimed at a temperature of 110-130 ^{o}C and a low pressure of 0.5 mbar. The carrier gas-argon (flow rate of 20 sccm) carried the precursor into the pyrolysis zone which was at a temperature of 800 ^{o}C. The samples were placed on a cooled sample holder at 10 ^{o}C. The photoreactive CVD polymer contained active sites which initiated the polymerization of the methacrylate layer upon exposure to UV-radiation. The CVD polymer film possessed good adhesion to a variety of substrates and exhibited excellent mechanical properties.

The methacrylate monomer solution containing cyclen-derivatized methacrylate (31.5%), HEMA (66%) and polyethylene glycol dimethacrylate (PEG-dMA, 2.5%) was applied onto the photoreactive CVD-polymer coated stents for even distribution of the reactants. The stents were then UV-irradiated for 30 min with constant rotation to ensure uniform exposure of the complex stent surface, thus creating a crosslinked hydrogel on the CVD polymer. This coated stent was finally incubated in a solution containing copper(II) ions which conjugated to the cyclen sites present on the polymer coating. Non-specifically bound copper was removed by rinsing the coated stents with water.

Characterization of the polymer coating

Surface elemental composition of the coating was discerned using X-ray photoelectron spectroscopy (XPS). Imaging capabilities of the XPS instrument were utilized for spatially-resolved mapping of the distribution of individual elements on the surface (Figure 6.2). A uniform distribution of the elements was observed along the struts of the stents in the composition map. More specifically, in the compositional map of stents coated with the polymethacrylate layer, a homogeneous distribution of nitrogen

and copper was detected, indicating the presence of copper-conjugated cyclen moieties. Moreover, from the XPS survey spectrum, ratio of copper to nitrogen was estimated to be 0.2 which compares well with the theoretical value of 0.25. On the other hand, nitrogen and copper elements were not detected in the CVD-polymer coated stents which is consistent with the chemical composition of the CVD polymer.

Furthermore, morphological assessment of the coating on the stent surface using scanning electron microscopy (SEM) revealed the presence of a uniform polymer coating on the struts of the stent (Figure 6.3). Micrographs obtained from SEM analysis also show that the composite film was mechanically stable even after stent expansion.

Fourier transform infrared (FTIR) spectroscopy confirmed the presence of the carbonyl group characteristic of the methacrylates, as indicated by the strong signal at 1712 cm^{-1} (Figure 6.4b). The broad peak seen at 3397 cm^{-1} showed the hydroxyl groups present in 2-hydroxyethyl methacrylate (HEMA) which were absent in the CVD polymer (Figure 6.4a).

Taken together, these observations from imaging XPS, SEM and FTIR suggest that CVD polymerization combined with UV-polymerization not only produces a uniform coating on the stent surface, but the active component of the matrix, namely cyclen, is still present and conjugating copper.

Measurement of nitric oxide

Nitric oxide generated from cyclen-coated stents was measured in buffer solutions in vitro. The coated-stents were immersed in PBS buffer containing estimated physiological amounts of S-nitrosoglutathione (GSNO) and reducing agent glutathione (GSH). The NO generated from the stent was sent to a NO-analyzer which measured the NO using chemiluminescence techniques and the final NO-flux was reported based on

the stent surface area. As shown in figure 6.5, in two separate injections of GSNO, the CVD/polymethacrylate/Cu(II)-cyclen coated stents were able to convert the GSNO to NO under physiological conditions (37 ^{o}C, pH 7.4). NO generated from the cyclen-methacrylate coated stents was in the physiological range whereas the CVD polymer-coated stents demonstrated baseline fluxes.

6.4 Conclusions

Polymer coatings capable of catalytically generating nitric oxide from endogenous RSNOs and nitrites present in the blood, were fabricated. These robust coatings were applied to stainless steel stents and were extensively characterized to confirm the chemical composition, adhesion and stability of the coatings. Finally, NO flux measured from the coated stents was found to be in the physiological range. This novel polymer system can be used to improve the biocompatibility of implantable medical devices, specifically vascular grafts and stents

6.5 Figures and Tables
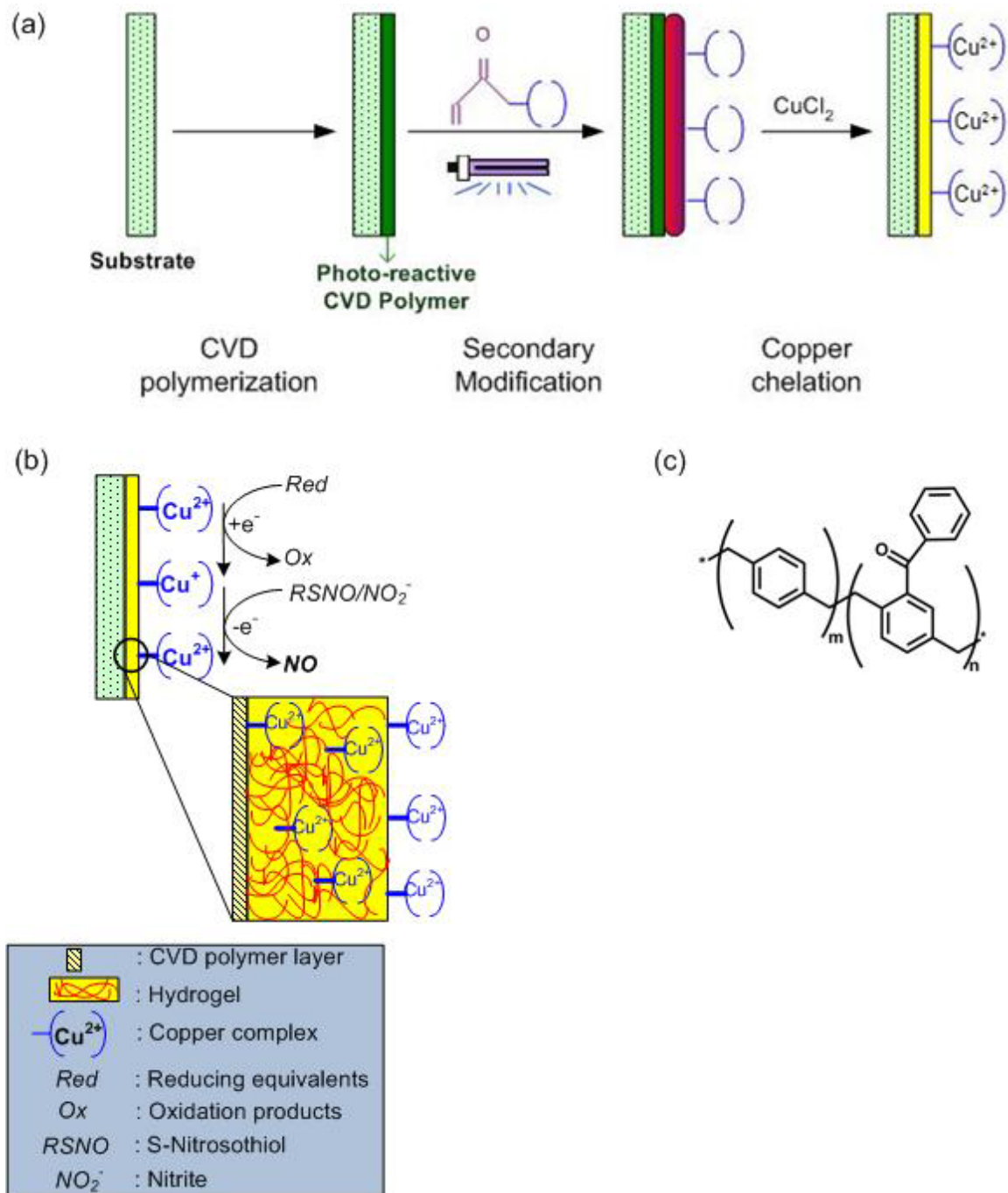
Figure 6.1: (a) Scheme depicting the synthesis of polymethacrylate hydrogel coatings containing copper-conjugating cyclen complexes covalently linked to photoactivable CVD polymer. (b) Schematic showing the NO generation activity of the polymethacrylate/Cu(II)-cyclen coating. (c) Chemical structure of photo-reactive CVD polymer, poly[(4-benzoyl-p-xylylene)-co-(p-xylylene).
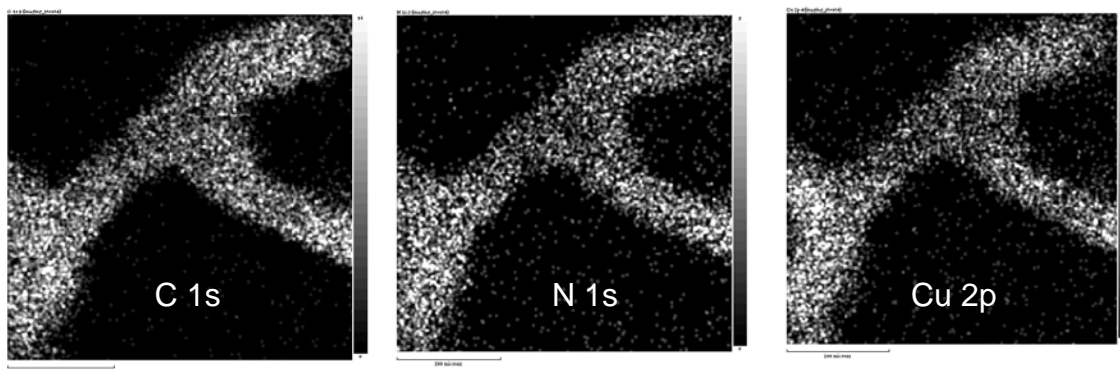
Figure 6.2: XPS mapping (C1s: 285 eV, N1s: 400 eV and Cu2p: 930 eV) of polymethacrylate/Cu(II)-cyclen on CVD coatings on the stainless steel stents.

Figure 6.3: Micrographs obtained using SEM showing the morphology of the polymethacrylate/Cu(II)-cyclen on CVD coatings on the stainless steel stents after expansion. No defects in the coating were observed even after mechanical expansion of the stent.
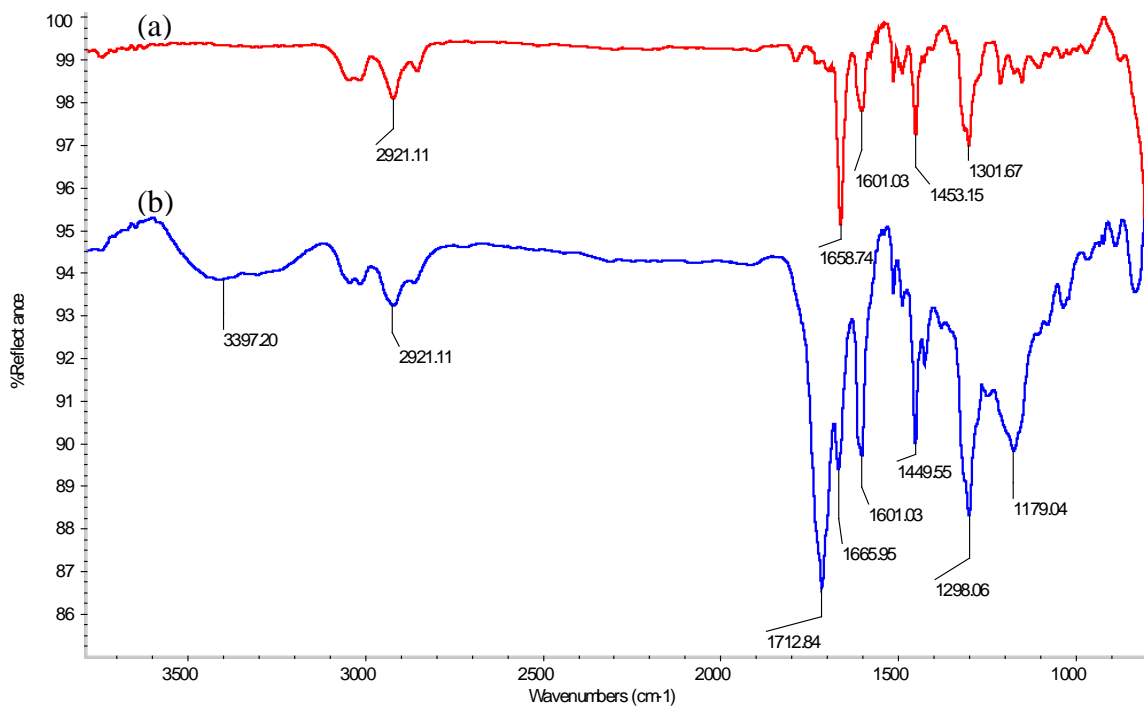
Figure 6.4: Comparison of the infrared spectra of (a) CVD coating (b) polymethacrylate/Cu(II)-cyclen on CVD coatings on the stainless steel substrates

Figure 6.5: (a) NO flux from the stents coated with polymethacrylate/Cu(II)-cyclen on CVD coatings in the presence of 18 µM GSNO, 53.4 µM GSH and 2.5 µM EDTA. (b) NO flux measured from CVD polymer coated stents. Each arrow indicates a new injection of GSNO.

6.6 References

1. Serruys, P.W., Kutryk, M.J.B. & Ong, A.T.L. Drug therapy - Coronary-artery stents. *New England Journal of Medicine* **354**, 483-495 (2006).
2. Ratner, B.D. & Bryant, S.J. Biomaterials: Where we have been and where we are going. *Annual Review Of Biomedical Engineering* **6**, 41-75 (2004).
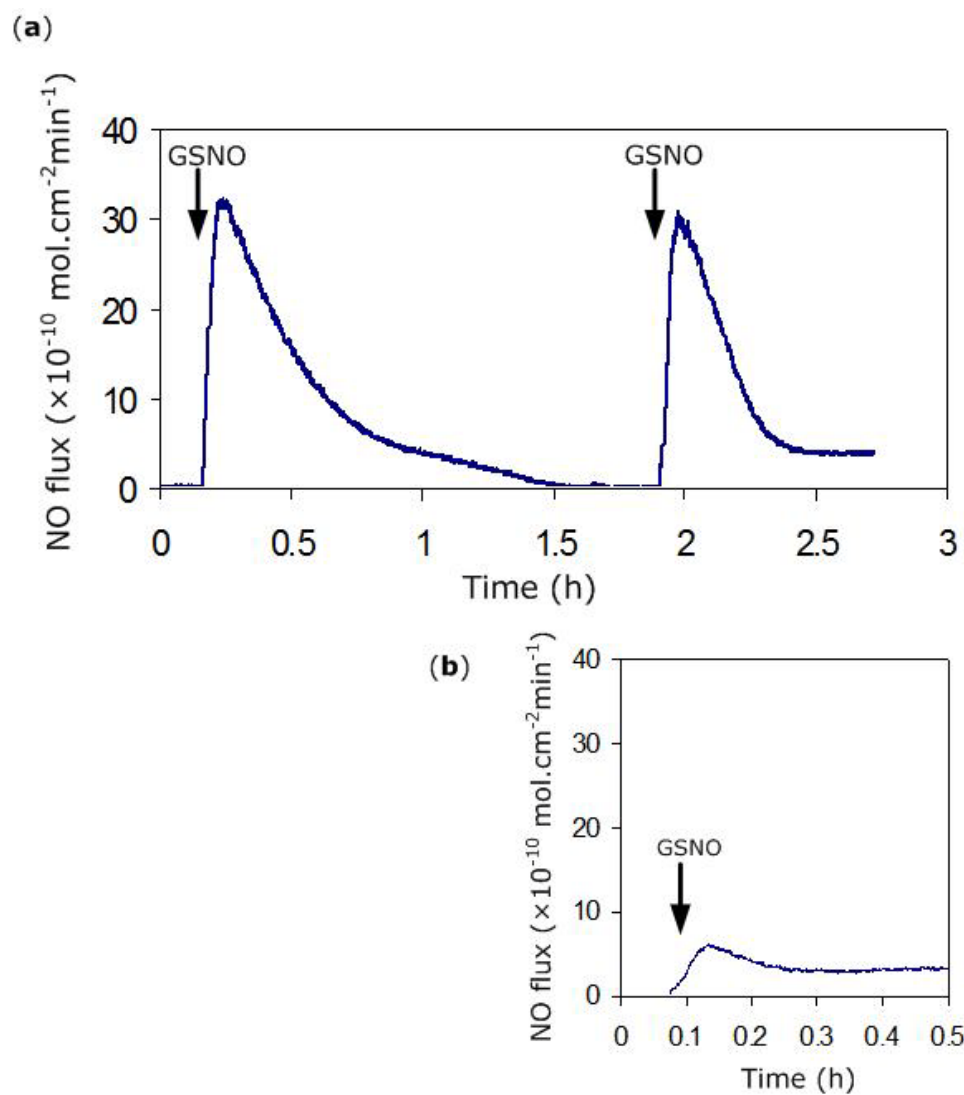3. Jagur-Grodzinski, J. Polymers for tissue engineering, medical devices, and regenerative medicine. Concise general review of recent studies. *Polymers for Advanced Technologies* **17**, 395-418 (2006).
4. Burt, H.M. & Hunter, W.L. Drug-eluting stents: A multidisciplinary success story. *Advanced Drug Delivery Reviews* **58**, 350-357 (2006).
5. van der Hoeven, B.L. et al. Drug-eluting stents: results, promises and problems. *International journal of cardiology* **99**, 9-17 (2005).
6. Bhargava, B., Karthikeyan, G., Abizaid, A.S. & Mehran, R. New approaches to preventing restenosis. *Br. Med. J.* **327**, 274-279 (2003).
7. Keefer, L.K. Biomaterials - Thwarting thrombus. *Nature Materials* **2**, 357-358 (2003).
8. Verma, S. & Marsden, P.A. Nitric oxide-eluting polyurethanes - Vascular grafts of the future? *New England Journal of Medicine* **353**, 730-731 (2005).
9. Frost, M.C., Reynolds, M.M. & Meyerhoff, M.E. Polymers incorporating nitric oxide releasing/generating substances for improved biocompatibility of blood-contactincy medical devices. *Biomaterials* **26**, 1685-1693 (2005).
10. Lipke, E.A. & West, J.L. Localized delivery of nitric oxide from hydrogels inhibits neointima formation in a rat carotid balloon injury model. *Acta Biomaterialia* **1**, 597-606 (2005).
11. Jun, H.W., Taite, L.J. & West, J.L. Nitric oxide-producing polyurethanes. *Biomacromolecules* **6**, 838-844 (2005).
12. Bohl, K.S. & West, J.L. Nitric oxide-generating polymers reduce platelet adhesion and smooth muscle cell proliferation. *Biomaterials* **21**, 2273-2278 (2000).
13. Reynolds, M.M. et al. Nitric oxide releasing polyurethanes with covalently linked diazeniumdiolated secondary amines. *Biomacromolecules* **7**, 987-994 (2006).
14. Frost, M. & Meyerhoff, M.E. In vivo chemical sensors: Tackling biocompatibility. *Analytical Chemistry* **78**, 7370-7377 (2006).
15. Keefer, L.K. Progress toward clinical application of the nitric oxide-releasing diazeniumdiolates. *Annual Review of Pharmacology and Toxicology* **43**, 585-607 (2003).
16. Oh, B.K. & Meyerhoff, M.E. Spontaneous catalytic generation of nitric oxide from S-nitrosothiols at the surface of polymer films doped with lipophilic copper(II) complex. *Journal of the American Chemical Society* **125**, 9552-9553 (2003).
17. Hwang, S., Cha, W. & Meyerhoff, M.E. Polymethacrylates with a covalently linked Cu-II-cyclen complex for the in situ generation of nitric oxide from nitrosothiols in blood. *Angewandte Chemie-International Edition* **45**, 2745-2748 (2006).

18. Suh, K.Y., Langer, R. & Lahann, J. A novel photoderinable reactive polymer coating and its use for microfabrication of hydrogel elements. *Advanced Materials* **16**, 1401-+ (2004).

19. Chen, H.Y. & Lahann, J. Fabrication of discontinuous surface patterns within microfluidic channels using photodefinable vapor-based polymer coatings. *Analytical Chemistry* **77**, 6909-6914 (2005).

20. Chen, H.Y., Elkasabi, Y. & Lahann, J. Surface modification of confined microgeometries via vapor-deposited polymer coatings. *Journal of the American Chemical Society* **128**, 374-380 (2006).

CHAPTER 7

CONCLUSIONS AND FUTURE DIRECTIONS

7.1 Conclusions

In this dissertation, a range of different biointerfaces were designed by integrating structural motifs from biology into materials to create biofunctional materials, which can control the interactions between materials and biology.

In **Chapter 2**, two carbonyl-functionalized polymer coatings were synthesized using chemical vapor deposition (CVD) polymerization and characterized using surface analysis techniques such as X-ray photoelectron spectroscopy (XPS) and Fourier transform infrared spectroscopy (FTIR). The polymer was stable in a range of organic solvents. The availability and reactivity of aldehyde groups was assessed using hydrazone formation by spatio-selective binding of hydrazide-functionalized biotin and sugars. On the other hand, polymer containing a perfluorinated side chain was employed to create superhydrophobic reactive coatings by combining the low energy coating with complex surface architecture. The self-assembly of biotinylated biphasic microparticles was also demonstrated by creating micropatterns of streptavidin on the surface of the perfluorinated polymer.

In **Chapter 3**, alkyne-functionalized vapor-based polymer coating was fabricated and characterized using XPS and FTIR. The alkyne-functionalized polymer was amenable towards copper-catalyzed "click" reaction. Various azide-conjugated biomolecules such as proteins, saccharides and cell-adhesive peptides were covalently linked to the alkyne-functionalized surface in a spatio-selective manner. More

specifically, surfaces micropatterned with azide-functionalized laminin-derived peptide sequences was used to direct endothelial cell attachment.

In **Chapter 4**, the issue of developing clinically-relevant defined microenvironments for human embryonic stem (hES) cell cultures was addressed. Towards this goal, a group of polymer coatings with different side chain chemistries were fabricated and tested for initial hES cell attachment and proliferation. Only, zwitterionic polymer, PMEDSAH, supported long-term self-renewal and pluripotency of hES cells in mouse embryonic fibroblast conditioned medium (MEF-CM). This represents a significant advance towards clinically-applicable culture systems.

In **Chapter 5**, the effect of zwitterionic sulfobetaine containing polymers on hES cells was further extended to include serum-free defined culture media. PMEDSAH sustained the culture of hES cells for 15 passages in xeno-free human cell conditioned medium and for 10 passages in defined medium StemPro. Furthermore, another sulfobetaine-containing polymer, PMAPDSAH supported the proliferation of hES cells in both StemPro and mTeSR. This is a substantial improvement over PMEDSAH which was unable to support hES cell culture in the presence of mTeSR medium.

In **Chapter 6**, a nitric oxide generating polymer coating was fabricated for cardiovascular stents. This coating consisted of a copper-conjugating ligand which was capable of generating NO using endogenous components of the blood. The polymer coating was extensively characterized using XPS, FTIR and SEM. Polymer coated stents generated NO in the physiological range, in the presence of nitrosothiols in buffer.

To summarize, the observations and results detailed in this dissertation provide a toolbox of specialized interfaces, that improve the bioresponse towards materials and can be utilized in a variety of applications such as microfluidics, tissue engineering, biomedical devices and understanding basic biology

7.2 Future Directions

Understanding the interaction between PMEDSAH and hES cells

The ability of biointerfaces to modulate the behavior of human embryonic stem (hES) cells opens several avenues to study basic hES cell biology and applications towards lineage-specific differentiation. In order to determine the factors important for the hES cell attachment to PMEDSAH and PMAPDSAH, growth factor binding studies should be performed using basic fibroblast growth factor (bFGF) ELISA, comparing all the polymer coatings (described in Chapter 4). This can be achieved by incubating the polymer-coated dishes with the different cell culture media and measuring the bFGF bound to the surface using ELISA. A general protein analysis should be performed using techniques such as SDS Page or Western blotting.

Human ES cells growing on PMEDSAH and PMAPDSAH in the presence of StemPro can be compared directly by quantifying the amount of RNA extracted for RT-PCR. The cells should be mechanically passaged onto PMEDSAH and PMAPDSAH coated dishes and cultured until passage point is reached. Amount of RNA extracted can be correlated to the number of undifferentiated hES cells growing on each coating.

To gain better control of PMEDSAH polymerization process, surface-initiated atom transfer radical polymerization (ATRP) can be utilized.[1] Surface-initiated ATRP has garnered considerable attention because of its compatibility with a range of monomers and tolerance of water and excellent control of reaction kinetics. It has been successfully used to fabricate films for applications such as biomaterials, biosensors, and nano/micro-fabrication.[2-7] To create the initiator coatings for ATRP, CVD polymerization can be used to fabricate poly(*p*-xylylene-4-methyl-2-bromoisobutyrate-co-*p*-xylylene) coatings.[8] Preliminary experiments have shown that this process can be used to grow PMEDSAH films with different thicknesses by varying the concentrations of the catalyst

and the reaction time (Figure 7.1a). Chemical composition of the PMEDSAH-modified surfaces was confirmed using XPS and FTIR. Table 1 summarizes the XPS survey spectra of substrates after different time-points of surface-initiated ATRP for a catalyst concentration of 40 mM, which compared well with the theoretical composition of PMEDSAH. Contact angles of the films grown with different catalyst concentrations were compared with initiator-coated samples (Figure 7.1b).

Human ES cells can be cultured on PMEDSAH films with varying thicknesses in the presence of different defined culture media to assess the importance of various physicochemical properties of PMEDSAH on hES cell propagation.. For instance, hydrophilicity and protein adsorption have been shown to be dependent on the thickness of the PMEDSAH coatings.[9-11] Furthermore, thickness of the PMEDSAH films would determine the mechanical properties such as stiffness and modulus of the films, which influence the differentiation lineage of stem cells.[12] The elastic moduli of PMEDSAH coatings synthesized using ATRP should be measured using nanoindentation and correlated to any observable differences in the cellular behavior.

Adsorption of basic fibroblast growth factor (bFGF) can be assessed using ELISA experiments. In addition, surface plasmon resonance (SPR) spectroscopy can be utililized to study the kinetics of biomolecular interactions in real time, monitoring the unlabeled analyte molecule adsorption. This technique has a high degree of surface sensitivity that allows weakly bound interactions to be monitored in the presence of excess solution species. Furthermore, molecular structures of polymer surfaces and interfacial proteins can be investigated using a nonlinear optical spectroscopy, sum frequency generation (SFG) vibrational spectroscopy. This will enable understanding the interplay between the inter- or intrachain behavior of the zwitterionic PMEDSAH and orientation of the adsorbed proteins. Orientation and conformation of adsorbed proteins in turn determines the behavior of hES cells and can elucidate the unique behavior of PMEDSAH in supporting the growth of undifferentiated hES cells as compared to other polymers.

Exploration of the physico-chemical properties of the PMEDSAH platform may pave the way for exciting studies in basic biology and specific differentiation. Removal of unknown and undefined components from hES cell microenvironment will propel research towards a detailed analysis of hES cell-substrate interactions. More importantly, varying the physical properties of the surface independent of the chemical structure is a powerful means for studying the specific parameters influencing cell behavior.

Towards multifaceted biointerfaces

CVD polymerization has also been extended to create multifunctional polymer coatings containing two or more reactive groups which can be utilized for orthogonal surface reactions.[13] [14, 15] Gradients of biological ligands can also be fabricated using multifunctional CVD polymerization.[15]

This is especially attractive for combining the different approaches mentioned in this dissertation in order to create sophisticated multifunctional biointerfaces. For instance, a copolymer containing ATRP initiator and alkyne functional groups can be used to immobilize azide-derivatized biomolecules together with controlled radical polymerization of PMEDSAH. The properties of such a multipotent coating will depend on the biomolecule conjugated with the surface, which could include enhanced adhesion, migration or lineage-specific differentiation of hES cells. The alkyne group can be used for the immobilization of azide-functionalized laminin-derived peptides, which have been used to promote attachment of undifferentiated human embryonic stem cells.[16]

Furthermore, the multifunctional reactive CVD coatings can be used for covalent immobilization of growth factors such as fibroblast growth factor (bFGF) in conjuction with PMEDSAH polymerized using ATRP. In addition, bFGF can also be conjugated to the surface through non-covalent albeit specific interaction between surface-immobilized

heparin and growth factor molecules. These surfaces can be compared to culture systems containing soluble growth factors.

Polyzwitterionic PMEDSAH, supported hES cell proliferation, whereas other polymers with the same backbone but differing side chain chemistries did not. The presence of both negative and positively charged groups on PMEDSAH can be investigated by using model surfaces that can systematically alter the surface charge balances to study their role in protein adsorption and cell culture in defined media. The CVD co-polymerization can be utilized to create surfaces with either sulfonate or ammonium groups as well as homogeneous surfaces with various ratios (CVD co-polymerization) and gradients (two source CVD polymerization) of the 2 functional groups.

For demonstration of the utility of reactive copolymer coatings for dual-surface immobilization, r-hirudin and heparin were used.[14] Immobilization of r-hirudin, a recombinant protein which deactivates thrombin, may be one remediation approach for blood-contacting devices, such as cardiovascular stents. In addition, heparin is a highly-sulfated glycosaminoglycan anticoagulant. Hirudin and heparin were immobilized onto co-polymer coating of PPX-CH$_2$NH$_2$/-COCF$_3$ through aminomethyl group via a diisocyanate linker and carbonyl groups via adipic acid dihydrazide, respectively (Figure 7.2).[14] Moreover, co-immobilization of anticoagulant moieties together with the Cu(II)-cyclen ligand would enhance the performance of blood-contacting devices.

Finally, integration of the different strategies mentioned in this dissertation for the creation of stimuli-responsive materials, which have the ability to dynamically modulate surface properties would be a tremendous step for numerous biomedical applications, such as cell culture, tissue engineering, biosensors, biofouling and microfluidics. Dynamic remodeling of materials and interfaces is a widely observed phenomenon in nature, however examples of synthetic systems that can be switched on-demand are

scarce. Development of stimuli-responsive biomimetic interfaces will be the ultimate

future direction for this dissertation.
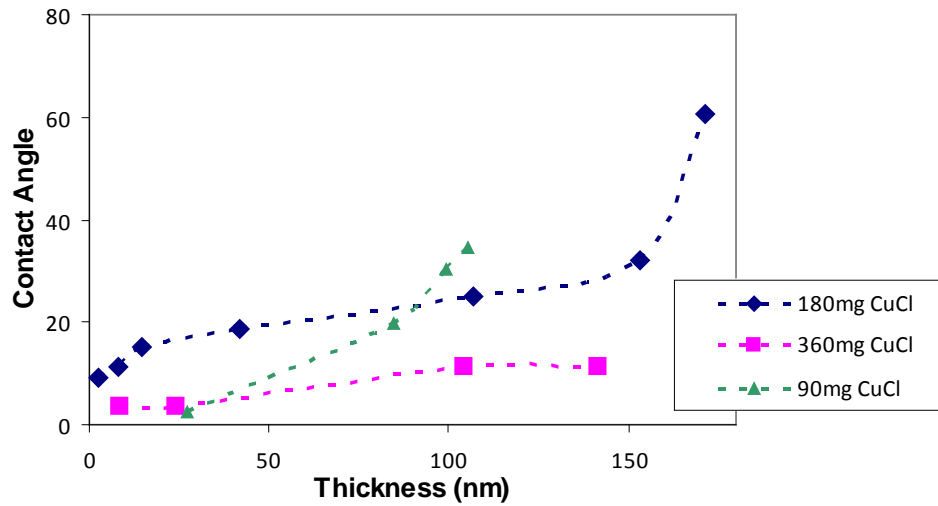
7.3 Figures and tables

(**a**)
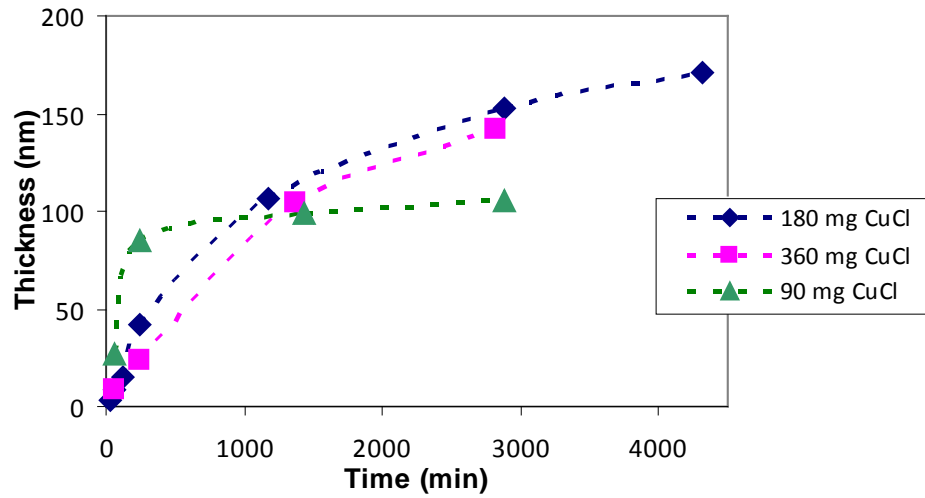
(**b**)

Figure 7.1: (a) Thickness of PMEDSAH films obtained by varying the concentration of CuCl and (b) the corresponding contact angle measurements obtained from those films.
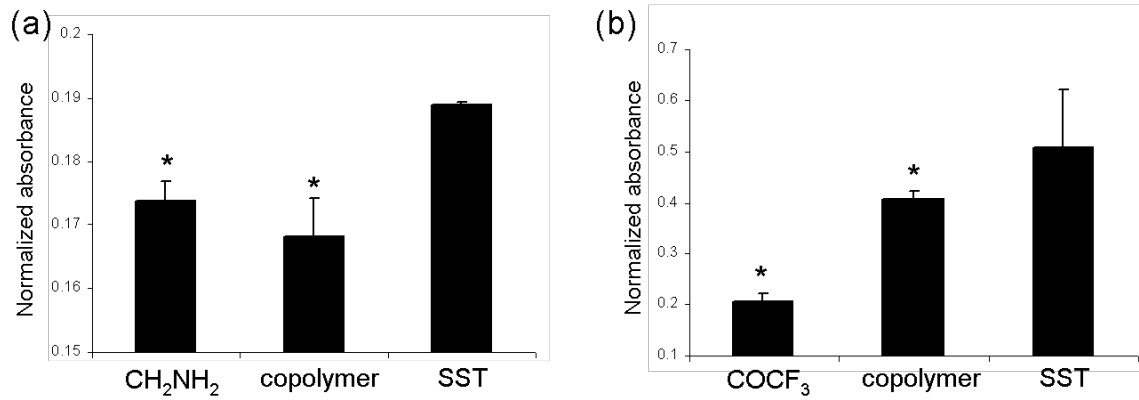
Figure 7.2: Immobilization of hirudin and heparin onto vapor-based copolymer coatings. (a) Hirudin binding as measured by chromogenic assay. Normalized absorbance at 405 nm are reported. n=3, *: $p < 0.05$ compared to stainless steel. (b) Heparin binding as measured by toluidine blue absorbance. Normalized absorbance at 631 nm are reported. n=3, *: $p < 0.05$ compared to stainless steel.

Table 7.1: Preliminary data from XPS elemental analysis of the PMEDSAH films grown using ATRP for 30 min, 1 h, 2 h and 19.5 h compared to theoretical composition.

Element	% experimental				% theoretical
	30 min	1 h	2 h	19.5 h	
C	69.3	67.5	67.5	65.16	64
O	22.3	23.3	24.1	24.95	28
N	3.3	4.0	3.6	4.46	4
S	5.1	5.2	4.8	5.45	4

7.4 References

1. Chen, H., Yuan, L., Song, W., Wu, Z.K. & Li, D. Biocompatible polymer materials: Role of protein-surface interactions. *Progress in Polymer Science* **33**, 1059-1087 (2008).
2. Xu, F.J., Neoh, K.G. & Kang, E.T. Bioactive surfaces and biomaterials via atom transfer radical polymerization. *Progress in Polymer Science* **34**, 719-761 (2009).
3. Cho, W.K., Kong, B.Y. & Choi, I.S. Highly efficient non-biofouling coating of zwitterionic polymers: Poly((3-(methacryloylamino)propyl)-dimethyl(3-sulfopropyl)ammonium hydroxide). *Langmuir* **23**, 5678-5682 (2007).
4. Huang, J.Y., Murata, H., Koepsel, R.R., Russell, A.J. & Matyjaszewski, K. Antibacterial polypropylene via surface-initiated atom transfer radical polymerization. *Biomacromolecules* **8**, 1396-1399 (2007).
5. Fan, X.W., Lin, L.J., Dalsin, J.L. & Messersmith, P.B. Biomimetic anchor for surface-initiated polymerization from metal substrates. *Journal of the American Chemical Society* **127**, 15843-15847 (2005).
6. Hucknall, A., Rangarajan, S. & Chilkoti, A. In Pursuit of Zero: Polymer brushes that resist the adsorption of proteins. *Advanced Materials* **21**, 2441-2446 (2009).
7. Lokuge, I., Wang, X. & Bohn, P.W. Temperature-controlled flow switching in nanocapillary array membranes mediated by poly(N-isopropylacrylamide) polymer brushes grafted by atom transfer radical polymerization. *Langmuir* **23**, 305-311 (2007).
8. Jiang, X.W., Chen, H.Y., Galvan, G., Yoshida, M. & Lahann, J. Vapor-based initiator coatings for atom transfer radical polymerization. *Adv. Funct. Mater.* **18**, 27-35 (2008).
9. Cheng, N., Brown, A.A., Azzaroni, O. & Huck, W.T.S. Thickness-dependent properties of polyzwitterionic brushes. *Macromolecules* **41**, 6317-6321 (2008).
10. Yang, W. et al. Film thickness dependence of protein adsorption from blood serum and plasma onto poly(sulfobetaine)-grafted surfaces. *Langmuir* **24**, 9211-9214 (2008).
11. Azzaroni, O., Brown, A.A. & Huck, W.T.S. UCST wetting transitions of polyzwitterionic brushes driven by self-association. *Angewandte Chemie, International Edition* **45**, 1770-1774 (2006).
12. Engler, A.J., Sen, S., Sweeney, H.L. & Discher, D.E. Matrix elasticity directs stem cell lineage specification. *Cell* **126**, 677-689 (2006).
13. Elkasabi, Y., Chen, H.Y. & Lahann, J. Multipotent polymer coatings based on chemical vapor deposition copolymerization. *Advanced Materials* **18**, 1521-+ (2006).
14. Elkasabi, Y., Yoshida, M., Nandivada, H., Chen, H.Y. & Lahann, J. Towards multipotent coatings: Chemical vapor deposition and biofunctionalization of carbonyl-substituted copolymers. *Macromolecular Rapid Communications* **29**, 855-870 (2008).
15. Elkasabi, Y. & Lahann, J. Vapor-based polymer gradients. *Macromolecular Rapid Communications* **30**, 57-63 (2009).

16.	Derda, R., Li, L., Orner, B.P., Lewis, R.L., Thomson, J.A., Kiessling, L.L. Defined substrates for human embryonic stem cell growth identified from surfaces arrays. *ACS Chemical Biology* **2**, 347-355 (2007).